CHAPTER 1

INTRODUCTION

1.1 Project Background

A study of lightning-overvoltage behavior is important to designing insulation of electric power system. This is because insulation design of power equipment is based on frequent occurrence of a specific event, distribution of the overvoltage probability corresponding to the event and to failure probability of the insulation (J.A. Martinez and F. Castro-Aranda, IEEE, 2003). Hence, the lightning overvoltage is a significant factor for the protection of power plant and substation equipment (Takamitsu Ito et al., IEEE, 2003). Lightning overvoltage is caused mainly by lightning discharging on transmission line towers, from strikes to shield-wire or to phase-conductor.

Generally, lightning strikes mostly the top of a transmission tower (shield-wire) rather than the power transmission line (phase-conductor). When lightning current hits the top of a transmission tower, it flows to the bottom of the tower and out onto ground wire. This causes voltage to develop across line insulation. If the voltage equals or exceeds the line's critical flashover voltage (CFO), flashover occurs (Andrew R. Hileman, 1999), known as back-flashover. This dissertation concentrates on back-flashover studies as they are important to evaluation of lightning performance.

In Malaysia, lightning-overvoltage is a major concern for 132kV/275kV transmission line systems, whereas for 500kV and more, switching-overvoltage is considered. The randomness of lightning makes observation of lightning-overvoltage in an experiment difficult. Numerical simulation such as modelling the overhead transmission-line by using appropriate software is thus the better approach. One of the more famous tools for modelling transmission-line systems is the ATP-EMTP software.

Recently, many researchers have modelled transmission lines and towers by using ATP-EMTP software. It is widely used in power system transient analysis studies.

The most well-known modelling of transmission tower via ATP-EMTP is the multistory tower model by Masaru Ishii who based his design on 500kV transmission line (M. Ishii et al., IEEE, 1991). The model, however, is inaccurate and not applicable to investigation of lightning studies for lower-voltage overhead transmission-lines. According to Takamitsu Ito et al., (IEEE, 2003), simple distributed line model is sufficient to model lower-voltage transmission-line systems such as Malaysia's 132kV overhead transmission-line system. The main objective of this dissertation is thus to model a 132kV overhead transmission-line by using ATP-EMTP software, for back-flashover pattern recognition.

1.2 Project Objective

The objectives of this project are:

a) The study and modelling of 132kV overhead transmission-line by using ATP-EMTP software.
b) The investigation of back-flashover voltage pattern when four lightning-current magnitudes are injected into a transmission-tower top.
c) The study of tower-footing resistance effects on back-flashover voltage obtained across insulator strings at each phase.

1.3 Project Scope

This project is focused on modelling 132kV overhead transmission-line, for back-flashover pattern recognition. The model was developed by using ATP-EMTP software. Four magnitudes of lightning currents (positive polarity) were injected into a transmission-tower top, to study back-flashover voltage pattern at each phase. Effects of

tower-footing resistance on back-flashover voltage were investigated through ATP-EMTP simulation, for four magnitudes of lightning current.

1.4 Outline of Dissertation

Chapter 1 summarizes project background and elaborates on project objectives and scope. The dissertation is introduced in this chapter.

Chapter 2 reviews literatures, including description of lightning strike/flash phenomenon, problems of lightning in power system, back flashover, and travelling-wave in transmission lines. Transmission line and tower, line-insulator flashover, lightning source, tower surge impedance, and tower-footing resistance of transmission line are also included.

Chapter 3 describes the methodology of the dissertation. ATP-EMTP software is introduced and described. Methodology flow chart is presented in this chapter as well.

Chapter 4 elaborates on ATP-EMTP modelling guidelines for 132kV overhead transmission-line. Modelling of transmission line and tower, cross-arms, insulator strings, tower surge impedance, lightning source, and AC voltage source are explained briefly in this chapter.

Chapter 5 presents results of simulations, together with necessary analysis and appropriate discussion of them.

Finally, Chapter 6 discusses the conclusions of the dissertation, and recommends possible future research.

CHAPTER 2

LITERATURE REVIEW

2.1 Introduction

Lightning is considered a major source of disturbance to transmission-line system in Malaysia as it generates huge surge current and voltage in system. Malaysia ranks one of the countries with highest lightning activities in the world; average thunder-days for Kuala Lumpur are 180-300 per annum. Eighty percent of lightning-discharge currents to ground in Malaysia exceed 20 kA, potentially approaching 50-100 million volts (Lightning in Malaysia, Online, 2008).

Studies in lightning strikes to power lines show that lightning strikes the same structure repeatedly. This is a serious problem for power lines, typically the highest structures in high-incidence lightning regions (M.A. Uman, Toronto: Dover, 1986). Any structure, whatever its size, may be struck by lightning, but the probability of a structure being struck raises with its height.

2.2 Lightning Phenomenon

2.2.1 Mechanism of Lightning

Lightning is basically an electric discharge in the form of a spark or a flash originating from a charged cloud. Generally, a cloud consists of a positive-charge centre and a negative-charge centre. Lower part of the cloud is negative-charge centre with temperature of -5°C, whereas the main positive-charge centre is located several kilometers higher up, with temperature typically below -20°C. In the majority of storm clouds, there is also a localized positively charged region near the base of the cloud, with 0°C temperature. Figure 2.1 shows a cloud located above an overhead transmission line (J. Rohan Lucas, 2001).

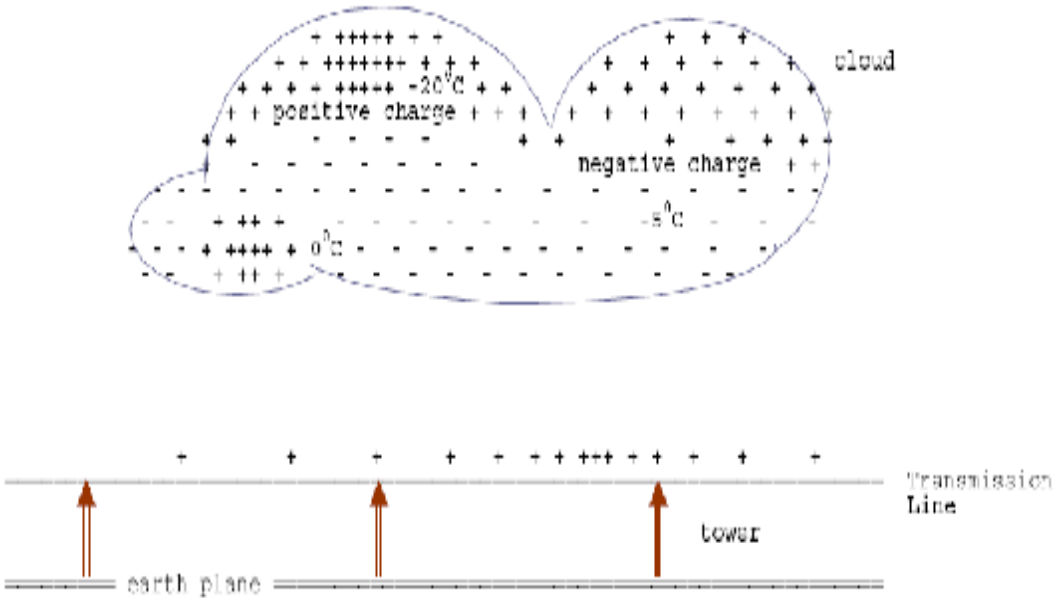

Figure 2.1: Charges induced on transmission line

2.2.2 Breakdown Process

Lightning occurs when clouds acquire charge or become polarized. Electric fields of considerable strength are then created within the clouds and between the clouds and nearby masses such as earth and other clouds. When the fields become excessive, to the extent that dielectric (air) in the intervening space can no longer support electrical stress, a breakdown or a lightning flash occurs, which usually is a high-current discharge (D. Rodriguez-Sanabria, C. Ramos-Robles, L. Orama-Exclusa, Lightning and Lightning Arrester Simulation in Electrical Power Distribution Systems, Online).

2.2.3 Lightning Problems in Power System

Generally, lightning is the main factor leading to outage in transmission and distribution lines. The problem of lightning can be classified a transient event. When

lightning strikes a power line, it is like closing a “big switch” between a large current source and power-line circuit. Sudden closing of the “big switch” causes sudden change in circuit conditions, creating a transient. There is also the case where lightning strikes power-line vicinity, and large magnetic field generated by lightning current causes mutual coupling between the power line and the lightning (D. Rodriguez-Sanabria et al., Lightning and Lightning Arrester Simulation in Electrical Power Distribution Systems, Online). The event alters conditions of the power-line circuit, producing an electrical transient.

Three possible discharge paths that can cause surges on line (J. Rohan Lucas, 2001) are:

a) The first discharge path is from leader core of lightning strike, to earth. Capacitance between the leader and earth is discharged promptly, and capacitances from leader head to earth wire and to phase-conductor are ultimately discharged by travelling-wave action, developing voltage across insulator string, known as induced voltage (due to lightning-strike to nearby ground); not a significant factor in lightning performance of systems above about 66 kV, but causes considerable trouble on lower-voltage systems.

b) The second discharge path is between lightning head and earth conductor, discharging capacitance between the two. The resulting travelling-wave comes down the tower and acts through its effective impedance, raising potential of tower top to a point where difference in voltage across insulation is sufficient to cause flashover from tower back to conductor. This type of strike is called back flashover.

c) The third type of discharge is between leader core and phase conductor, where capacitance is discharged between the two, the main discharge

current injected into the phase conductor, developing surge-impedance voltage across insulator string. At relatively low current, insulation strength is exceeded, and discharge path to earth is completed through tower. This type of strike is known as shielding failure (or, direct strike to phase-conductor).

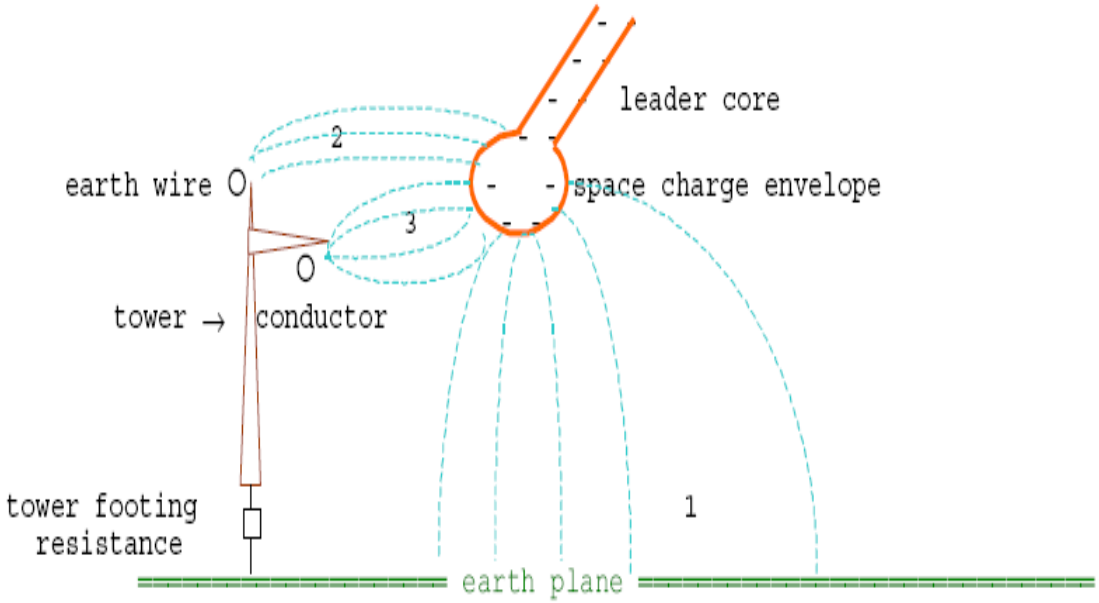

Figure 2.2: Lightning leader strike and transmission line

2.3 Back Flashover

Back-flashover pattern recognition will be conducted in this work. Back flashover is a phenomenon that occurs when lightning strike terminates at overhead ground wire or tower. A strike that terminates forces currents to flow down tower and out onto ground wires. Voltages thus build up across line insulation. Back flashover thus occurs across insulator string if the voltages equal or exceed the line's critical flashover voltage (CFO) (Andrew R. Hileman, 1999). Back-flashover analysis is extremely important in evaluating lightning performance, as most lightning strikes terminate on shield wire rather than on phase wire.

2.4 Travelling Wave

Disturbance such as sudden opening or closing of a circuit breaker, short circuit, or fault in transmission line/system develops over-voltages or over-currents at the disturbance point. This disturbance propagates as a travelling wave, to the ends of the line or to a termination such as a substation, in high frequency. During the period of propagation, they may be reflected, transmitted, attenuated, or distorted, until energy is absorbed (M.S. Naidu, V. Kamaraja, 2006). Any transient disturbances can usually be analyzed by travelling-wave method.

2.5 Transmission Line System

The transmission line has to be represented by means of several multi-phase un-transposed distributed-parameter line spans on both sides of impact point. The representation can be obtained by using either a frequency-dependent, or a constant-parameter, model (Juan A. Martinez-Velasco, Ferley Castro-Aranda, IPST'05, June 19-23, 2005). ATP-EMTP offers a few models that have been used for transmission-line system:

a) Bergeron: constant-parameter K.C. Lee or Clark models
b) PI: nominal PI-equivalent (short lines)
c) J. Marti: Frequency-dependent model with constant transformation matrix
d) Noda: frequency-dependent model
e) Semlyen: frequency-dependent simple fitted model.

The most commonly used transmission line and tower models are the Bergeron model, the PI model, and the J. Marti model. Here, the Bergeron model is used, to represent overhead transmission lines and cables, as most of transmission lines in

Malaysia are Bergeron type. The grounding wire is represented like phase wire connected to tower top.

The Bergeron model basically is based on distributed LC-parameter travelling wave line model with lumped resistance. This time-domain Bergeron model is commonly used in power system transient fault analyses (Bin Li et al., APPEEC 2009**).** It represents in distributed manner, the L and the C elements of a PI section. It also is approximate equivalent by means of an infinite number of PI Sections, except that the resistance is lumped [1/2 in the middle of the line, 1/4 at each end].

The Bergeron Model has a lossless distributed parameters' line as described by the following two values:

Surge Impedance, $Z_c = \sqrt{\frac{L}{C}}$ [1]

Phase Velocity, $v = \frac{1}{\sqrt{LC}}$ [2]

Similar to PI Sections Model, Bergeron Model accurately represents only fundamental frequency (50Hz); therefore the surge impedance is constant. It also represents impedances at other frequencies, for as long as losses do not change. Figure 2.3 shows an actual model of a Bergeron tower for 132kV transmission line in Malaysia, courtesy of TNB.

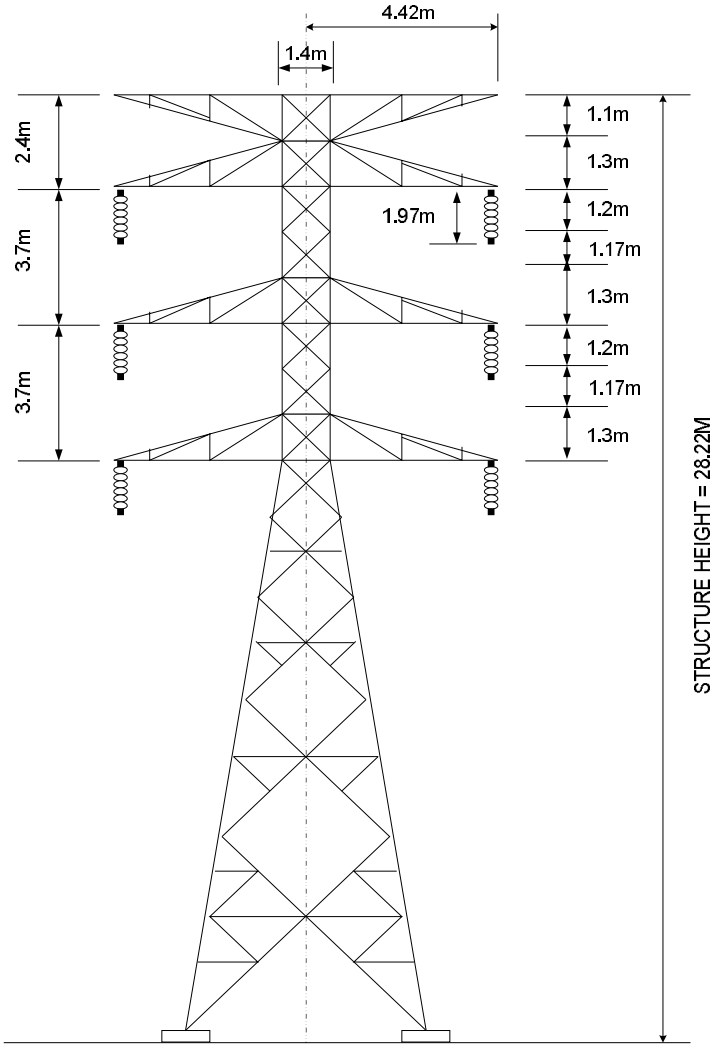

Figure 2.3: Bergeron Model

2.6 Transmission Tower

In recent years, theories proposed by researchers abound, on modeling of transmission tower. One of the more well-known models is the multistory model designed by Masaru Ishii (M. Ishii et al., IEEE, 1991). A multistory tower model basically is composed of distributed parameter lines with parallel RL circuits and has been recommended by the Japanese Guideline of insulation design/coordination against lightning (Takamitsu Ito et al., IEEE, 2003). This model is widely used for lightning-surge analysis in Japan. Figure 2.4 shows the multistory tower model.

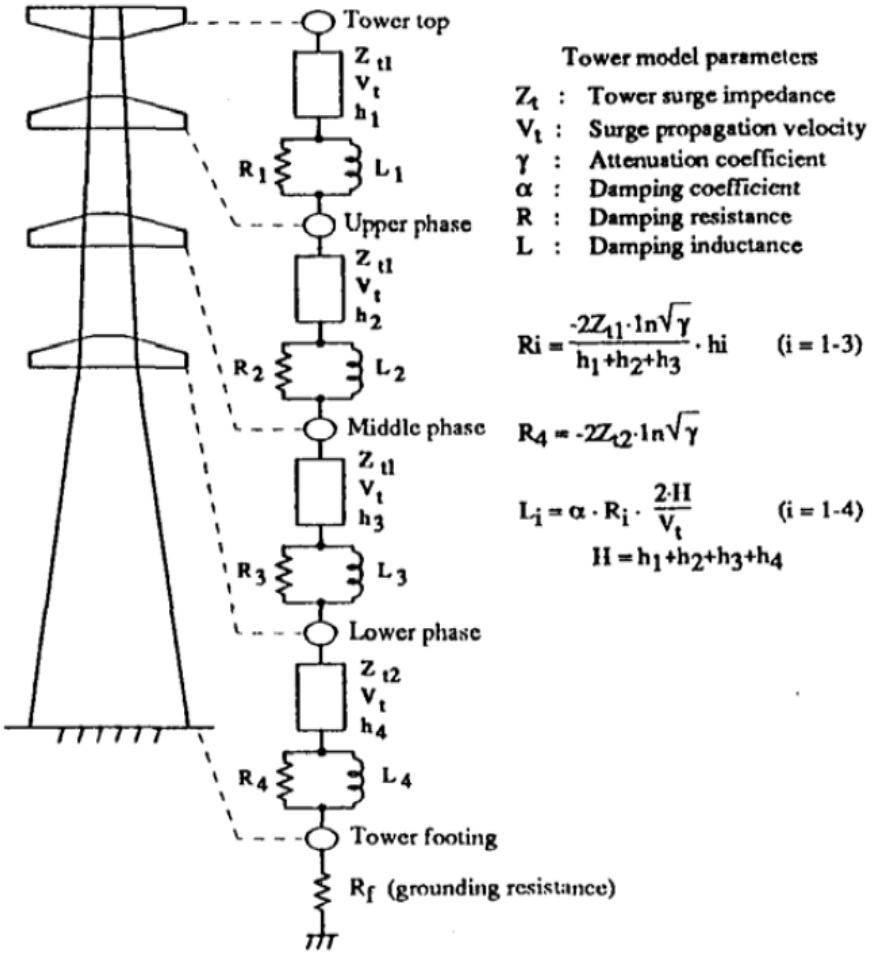

Figure 2.4: Multistory Tower Model

However, design of the multistory tower model was based on 500kV transmission line. Hence, multistory tower model is not applicable to Malaysia's lower-voltage (such as 132kV and 275kV) transmission line system. According to the investigation by Takamitsu Ito et al., (IEEE, 2003), a Simple Distributed Line Model is sufficient representation of a low-voltage transmission line system model in ATP-EMTP software, thus this model will be used to design this work's transmission tower. To represent a real transmission tower, a cross-arms model and an insulator-strings model need also be included. Figure 2.5 shows a simple distributed line model without cross-arms and insulator strings.

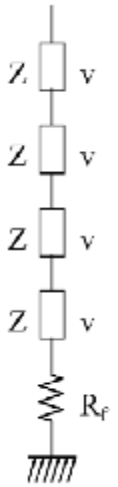

Figure 2.5: Simple Distributed Line Model

2.7 Cross-arms

In Malaysia, most cross-arms for 132kV and 275kV transmission lines are made of hard wood (especially the Chengal species). Usually, cross-arms are used as transmission-line supports for 132kV and 275kV towers (K. Khalid et al., Online, 2004).

In ATP- EMTP software, transmission-line system cross-arms are represented by distributed constant lines branched at junction point, their surge impedance given by:

$$Z_{AK} = 60 \ln\left(\frac{2h}{r_A}\right) \qquad [3]$$

where h is height of the cross- arms,

r_A is radius of the cross- arms.

According to research investigations, equation [3] proves applicable to cylindrical arms and to scale-model arms when equivalent radius is chosen as ¼ of arms' width at junction point (T. Hara, O. Yamamoto, IEE Proceedings on Generation, Transmission and Distribution, 1996).

2.8 Line-Insulator Flashover

The traditional model for insulator flashover uses measured volt-time curve specifically determined for a gap or insulator string that has the standard 1.2/50 μs wave shape. However, as insulator string is subject to non-standard impulse wave shapes, empirical volt-time curves bear little resemblance to physical breakdown process. Thus, a better line-insulation model is leader progression model (CIGRE Working Group 33.01, Technical Brochure 63, 1991).

2.8.1 Leader Progression Model

Leader progression model is the best model for designing insulator strings in transmission line. It can be used for non-standard lightning voltages (Juan A. Martinez and Ferley Castro-Aranda, Power Engineering Society General Meeting, IEEE, 2006). According to it, the flashover mechanism comprises three steps which are corona inception, streamer propagation, and leader propagation. Streamers propagate along insulator string when applied voltage exceeds corona inception voltage. If this voltage remains very high, the streamers become leader channel. When the leader crosses the gap between cross-arm and conductor, a flashover occurs. Time-to-flashover total can thus be expressed as:

$$t_t = t_c + t_s + t_1 \qquad [4]$$

where t_c is corona inception time.

t_s is streamer propagation time.

t_1 is leader propagation time.

t_c is neglected, as it is very short compared with the other two times.

According to Juan A. Martinez-Velasco, Ferley Castro-Aranda, (IPST'05, June 19-23, 2005), t_s can be calculated as follows:

$$t_s = \frac{E_{50}}{1.25E - 0.95E_{50}} \quad [5]$$

where E_{50} is average gradient at critical flashover-voltage

E is maximum gradient in the gap before breakdown.

Leader propagation time, t_1 can be obtained from the following equation:

$$\frac{dl}{dt} = K_1 V(t)\left[\frac{v(t)}{g-1} - E_{10}\right] \quad [6]$$

where $V(t)$ is voltage across gap,

g is gap length,

l is leader length,

E_{10} is critical leader-inception gradient,

K_1 is leader coefficient.

Leader propagation stops if gradient in un-bridged part of the gap falls below E_{10}.

2.9 Lightning Source

Impulse-current magnitude due to lightning charge is a probability function. Low (about 5-22 kA) discharge levels of lightning current may increase the tendency for lightning-strike to pass by shield wires (ground wires), instead striking a phase-conductor. Lightning impulse currents of large magnitudes will strike a tower top or overhead ground wire, causing back flashover across insulator string (B. Marungsri et al., International Journal of Energy and Power Engineering 2, 2009).

In ATP- EMTP software, lightning-strike model is represented by a current source with parallel resistance. The parallel resistance is actually lightning-path

impedance. The model used in this study is the Heidler current model, where four characteristics of lightning current quantities at striking point must be considered: lightning-current peak, maximum of current-steepness, rise time, and decay time (F. Heidler et al., IEEE Transactions on Power Delivery, 1999). Figure 2.6 shows the Heidler model in ATP- EMTP. Figure 2.7 below shows the lightning-strike waveform for the Heidler model.

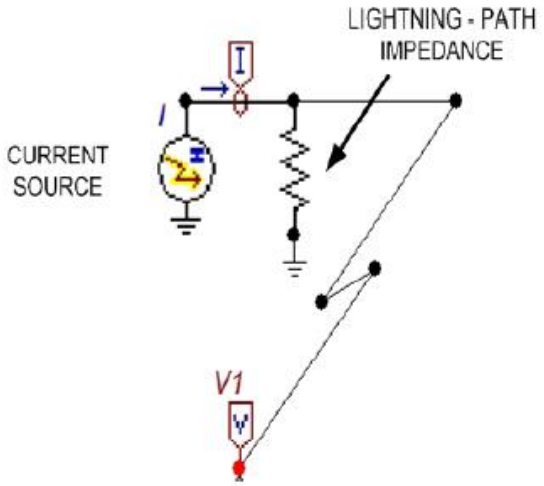

Figure 2.6: Lightning Strike, Heidler Model

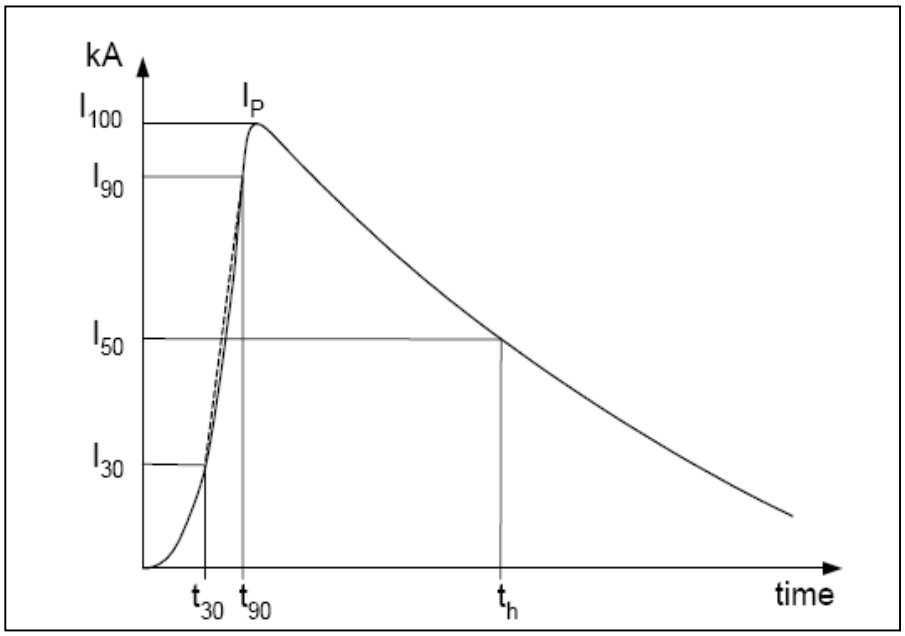

Figure 2.7: Lightning-Strike Waveform

Heidler's function that represents lightning-current waveform is (K. Fekete et al., MELECON 2010- 2010 15th IEEE Mediterranean Electrotechnical Conference, 2010):

$$i(t) = \frac{I_0}{h} \cdot \frac{\left[\frac{t}{t_1}\right]^n}{\left[\frac{t}{t_1}\right]^n + 1} \cdot e^{\left[\frac{-t}{t_2}\right]} \quad [7]$$

where

$$h = e^{\left[-\left[\frac{t_1}{t_2}\right]\left[\frac{ht_2}{t_1}\right]^{\frac{1}{n}}\right]} \quad [8]$$

and

I_0 : lightning current peak,

τ_1 : time constant determining current rise-time;

τ_2 : time constant determining current decay-time;

n : current steepness factor

2.10 Tower Surge-Impedance

In this work, surge impedance was determined from surge-impedance formula for cylindrical tower. M.A. Sargent and M. Darveniza in IEEE Transactions on Power Apparatus and Systems, May 1969 stated that surge impedance of a cylindrical tower varies with waveshape of the current impressed. Tower surge impedance for a cylindrical tower is approximated by:

$$Z = 60 \ln\left[\sqrt{2}\left(\frac{2h}{r}\right) - 1\right] \quad [9]$$

where h is tower height and r the tower radius. Equation [9], however, is an approximation, as surge impedance is a time-varying quantity.

2.11 Tower-Footing Resistance

An accurate footing-impedance model is important for decreased resistance value when discharge current value increases. Resistance value is agreed to be greater when lightning currents are small. Its variation to low current and low frequency values is only significant for large soil resistivities (Juan A. Martinez-Velasco, Ferley Castro-Aranda, IPST'05, June 19-23, 2005). A footing-impedance model incorporating soil ionization effect can be approximated as follows:

$$R_T = \frac{R_o}{\sqrt{1+\left(\frac{I}{I_g}\right)}} \qquad [10]$$

where Ro is footing resistance at low current and low frequency, Ig the limiting current to initiate sufficient soil ionization, and I the strike current through resistance. The limiting current is given by

$$I_g = \frac{E_0 r}{2pR_o^{\,2}} \qquad [11]$$

where ρ is soil resistivity (ohm-m), and E_0 is soil ionization gradient (400kV/m).

CHAPTER 3

METHODOLOGY

3.1 Introduction

Generally, project methodology defines methods/steps necessary for successful completion of a project. This chapter describes the software used in this project, and presents the project's methodology flow chart.

3.2 Alternative Transient Program (ATP)

3.2.1 Introduction

The software used for modeling of the overhead transmission-line system was ATP-EMTP. ATP is the royalty-free version of Electromagnetic Transients Program (EMTP) widely used for power system transient simulation. It can simulate phenomena such as lightning occurring in electric power. It is a full-feature transient analysis program initially developed for electrical power systems simulation. It appeared in early 1984. Drs. W. Scott Meyer and Tsu-Huei Liu (both Co-Chairmen of the Canadian/American EMTP User Group) contributing to its development (Alternative Transient Program Online, February 2010).

ATP is one of the more widely-used programs in digital simulation of transient electromagnetic and electromechanical phenomena in electric power systems. Complex networks and control systems of arbitrary structure can be simulated with it. It has powerful modelling capabilities and additional important features besides computation of transient analysis.

The ATP-EMTP simulation package comprises separate programs communicating with each other through disk files. Output of pre-processors, for example, is used as input to the main program (TPBIG.EXE), while the simulation

product can be used as input to program plotting. The main program itself is frequently used as pre-processor (e.g., for LINE CONSTANTS, CABLE CONSTANTS, BCTRAN, or DATABASE MODULE runs); the punch-file products thus can be re-used as input, in subsequent $Include run-through. Structure of the program components is quite difficult, so a user shell that supervises execution of separate programs and input/output flows has great advantage (Høidalen, H. K., ATPDRAW Version 3.0 User Manual, 1996).

3.2.2 Operating Principle of ATP

ATP simulation calculates variables of interest within electric power networks as functions of time, usually initiated by disturbance. Trapezoidal rule of integration usually solves in time domain, the differential equations of system components. Non-zero initial conditions can be determined automatically by steady-state phasor solution, or user-entered for simpler components (Høidalen, H. K., ATPDRAW Version 3.0 User Manual, 1996).

A few models introduced by ATP software are rotating machines, transformers, surge arresters, transmission lines, and cables. Ability to interface program's TACS (Transient Analysis of Control Systems) modules and MODELS (a simulation language) enables modelling of control systems and components with nonlinear characteristics such as arcs and coronas. TACS and MODELS control system modelling can also simulate dynamic systems, without use of electrical network.

The model in the ATP-program library presently comprises the following components (Alternative Transient Program Online, February 2010):

a) Uncoupled and coupled linear, lumped R, L, C elements.
b) Transmission lines and cables with distributed and frequency-dependent parameters.

c) Nonlinear resistances and inductances, hysteretic inductor, and time-varying resistance.

d) Elements with nonlinearity: transformers including saturation and hysteresis, surge arresters, and arcs.

e) Ordinary switches, time-dependent and voltage-dependent switches, and statistical switching.

f) Valves [diodes, thyristors, triacs].

g) Rotating machines: 3-phase synchronous machines and universal machines.

h) MODELS and TACS [Transient Analysis of Control Systems] components.

3.2.3 ATPDraw

ATPDraw for Windows application is a graphical pre-processor to the ATP version of the Electromagnetic Transients Program (EMTP). ATPDraw allows the user to create the electrical circuit to be simulated, through a mouse and selection of predefined components from an extensive palette. It will generate the input file for ATP simulation in the appropriate simulation-format. Usually, ATPDraw controls the naming process for the circuit node. The user thus needs to give a name to the nodes of special interest (Alternative Transient Program, Online, February 2010).

About 70 standard components and 28 TACS objects are available in ATP. Users can also create their own circuit objects by using MODELS or $INCLUDE (Data Base Module). ATPDraw has a standard Windows layout, supports multiple documents, and offers a large Windows help file system that explains basic rules (which helps users use ATPDraw). Generally, it provides standard component that can be used to create both single-phase and three-phase systems. Other facilities of ATPDraw are (Alternative Transient Program, Online, 2000):

a) Built-in editor for ATP-file editing.

b) Support of Windows clipboard for bitmap/metafile.

c) New module for use of Line/Cable Constant punch files in ATPDraw.

d) Tool-bar below main menu, containing the most-used selections together with the last 9 selected components.

e) An extensive Undo/Redo handling with more than 100 steps.

Line/Cable modeling including KCLee, PI-equivalent, Semlyen, JMarti and Noda is also available in ATPDraw; the user can specify selected geometry and material data. There is an option for the user to view the cross section graphically and verify the model in the frequency domain. Objects for Harmonic Frequency Scan (HFS) are also included. There are also special objects that help the user in machine and transformer modeling, including the powerful UNIVERSAL MACHINE and BCTRAN features of ATP (Høidalen, H. K., ATPDRAW Version 3.0 User Manual, 1996).

ATPDraw supports hierarchical modeling, replacing with a single icon, a selected group of objects in unlimited numbers of layers. The $PARAMETER feature of ATP is also implemented, allowing user to specify a text string as input in a components' data field and to assign numerical values to the texts strings. The circuit is stored on disk in a single project file which includes all the simulation objects and options needed to simulate the program. The project file is in zip-compressed format, facilitating file sharing.

ATPDraw is thus most valued by new users of ATP-EMTP. It is also an excellent educational tool. Possibility of multi-layer modelling makes ATPDraw a powerful front-end processor for professionals in their analysis of electric power system transients.

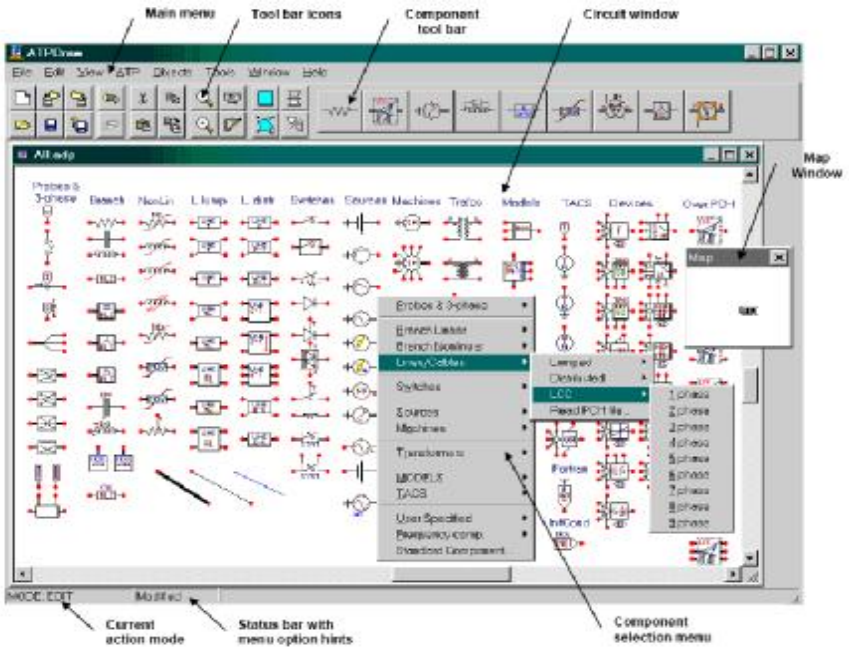

Figure 3.1: Main components of ATPDraw

3.2.4 Plotting on ATP

ATP is interfaced with these post-processors by the disk files. Their main function is to display simulation results in time-domain or frequency-domain. Data from ATP simulation are stored in a file having extension .pl4. Processing can be off-line or on-line. The latter displays results while simulation is proceeding, and is available only if the operating system provides concurrent PL4-file access for ATP and the post-processor program.

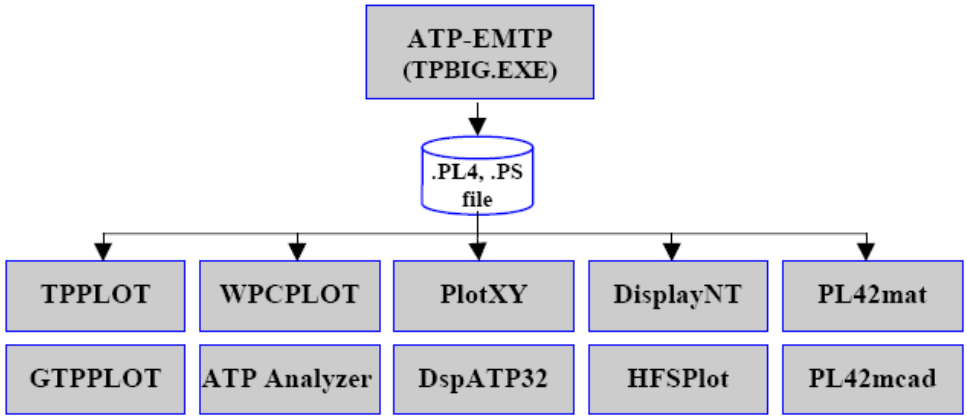

Figure 3.2: Plotting program in ATP

In ATP, two most widely-used plotting programs are PLOTXY and GTPPLOT. PlotXY is a WIN32 plotting program originally designed for ATP-EMTP software. It is mainly designed to make, as easy and fast as possible for line plots in Microsoft Windows environments. It can post-process plotted curves; algebraic operation, computation of Fourier series coefficients, etc. It has an easy-to-use graphical user interface, and its 32-bit code provides very fast operation. Up to 3 PL4 or ADF files can be simultaneously held in memory for easy comparison of various data, and up to 8 curves per plots versus time or X-Y plots are allowed. It has automatic axis-scaling, can plot with two independent vertical axes, and provides easy tools for factors, offsets, and zoom support, and a graphical cursor to see values in numerical format. It also can export screen plots as Windows Metafile via win32 clipboard. Figures 3.3 and 3.4 below are examples for plotting via PLOTXY (Alternative Transient Program, Online, February 2010).

Figure 3.3: Two main windows for PLOTXY

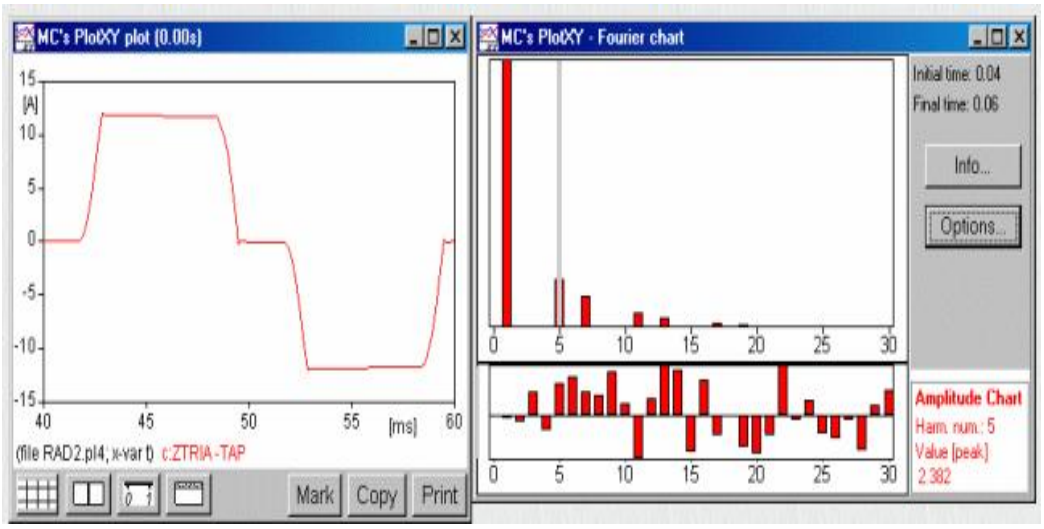

Figure 3.4: Fourier Chart

GTPPLOT is a plotting program for ATP output, compiled with GNU FORTRAN, and makes use of DISLIN graphical package. The program is available for DOS-djgpp extender, Windows 32, and Linux. Figures 3.5 and 3.6 below are examples of plotting via GTPPLOT.

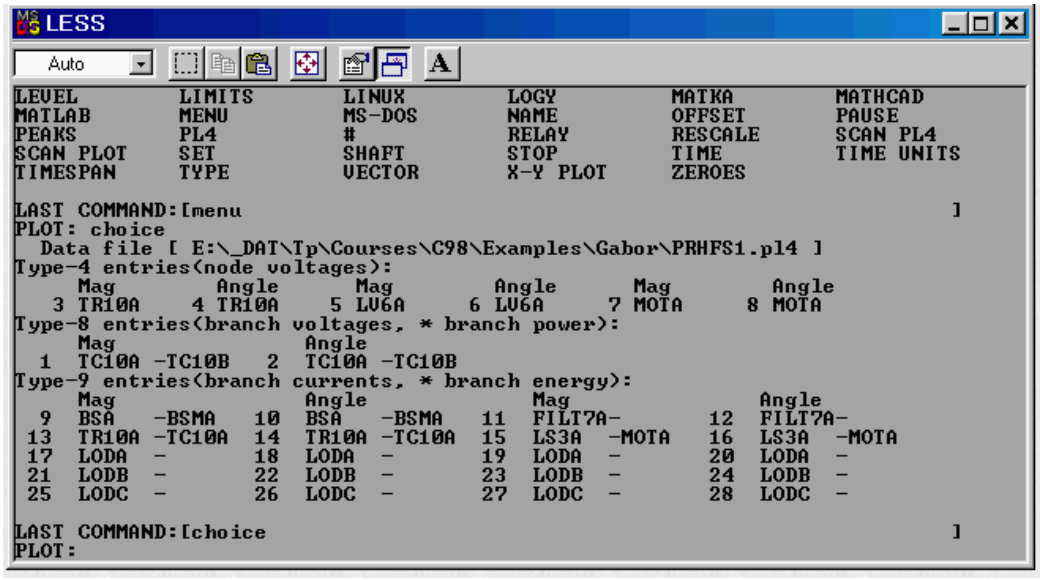

Figure 3.5: Execution in DOS Window

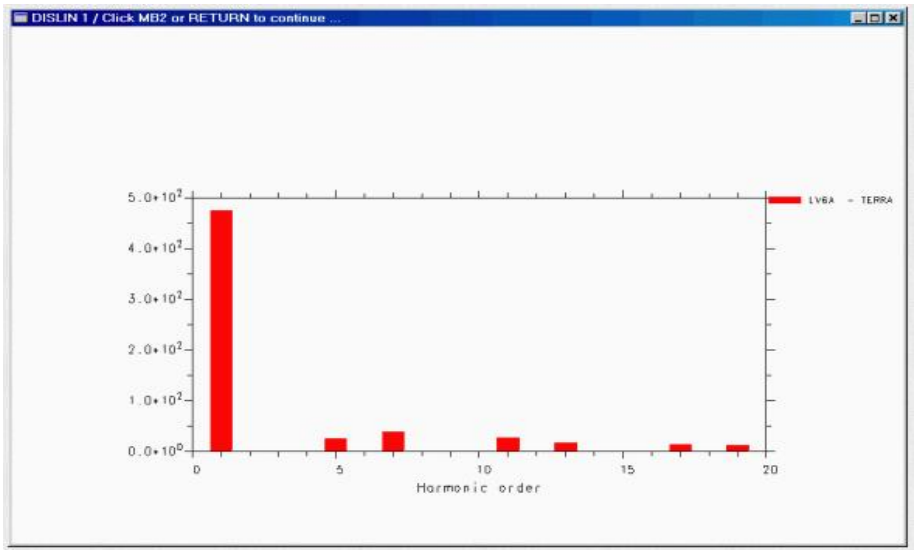

Figure 3.6: Harmonic Analysis via DISLIN

GTPPLOT has the following capabilities and limitations:

a) It can read *widenn*, formatted graphics files (FMTPL4 = 10Fnn.), both with nn arbitrary and C-like binary files including the new format obtained with NEWPL4=2 (called PISA) with normal or double precision. It also can read FORTRAN (DOS-djgpp, Mingw32, Linux, and SALFORD) unformatted files. The program automatically detects file format. COMTRADE files (both ASCII and binary) and ADF (ASCII Data Files) can be read by GTPPLOT, too.

b) GTPPLOT can process graphics files up to 1000000 points and up to 1000 variables; sufficient for the usual application.

c) The program is capable of plotting graphics with 1-20 curves. The plotted curves can be distinguished by color, line-type, symbol, or any combination of the three. For FS and HFS, the plot can be bar charts.

d) The program does not sense the mouse. Hence, the user must use a keyboard for all input operations.

e) The program can generate graphics files in nine formats: HP-GL (Hewlett-Packard Graphic Language), CGM (Computer Graphics Metafile), WMF

(Windows Meta File), PCX, PostScript, PNG (Portable Network Graphics), WMF (Windows MetaFiles), JAVA, and GNUPLOT. Some options are limited in GNUPLOT format.

f) The data can be exported as *widenn* pl4, COMTRADE (ASCII and binary), Matlab, MathCad and Mathematica files.

g) The screen plot can be in any of these formats: color, black, or white. Screen resolutions supported are 640*480, 800*600, and 1024*768. The Mingw32 and Linux versions use O/S-defined screen resolution.

h) The program calculates from data, a lot of PQI; as FOURIER analysis, turbine-shaft loss-of-life estimation, Bode plots, plot of ARMAFIT output, impedance calculation, generation of sources for HFS, and various simple math operations with variables, as integration, derivation, RMS, power, energy, I2T. The program searches for extrema, zeroes, and peaks, of the variables. The GTPPLOT can help to generate KIZILCAY F-DEPENDENT elements from FREQUENCY SCAN pl4 files.

i) The GTPPLOT can produce plots with different pl4 files or create a pl4 file with variables of different pl4 files.

j) The program can copy all the files in the same directory, easily included in PATH definition.

3.2.5 ATP-EMTP Domain Solution Method

In any transient analysis, the most popular solution methods are the “Frequency Domain” and “Time Domain” methods. Use of the two in ATP-EMTP will be elaborated in the following subtopic (Alternative Transient Program, Online, February 2010).

3.2.5.1 Frequency-Domain Solution Method

Its implementation in ATP-EMTP is based on Alternating Current [AC] steady-state solution of linear network. Nodal equations are written by using complex phasor quantities for currents and node voltages (Mohd Khairi Bin Mohd Zambri, Master Degree Thesis, Universiti Malaya, 2010). For any type of network with n-nodes, the system's equations can be explained as:

$$[Y][V] = [I] \quad [12]$$

With [Y]: symmetric nodal admittance matrix with complex elements,

[V]: vector of n node voltages (complex phasor values)

[I]: vector of n current sources (complex phasor values).

Equation [12] above is divided into set-A nodes of unknown voltages and set-B nodes of known voltages (Mohd Khairi Bin Mohd Zambri, Master Degree Thesis, Universiti Malaya, 2010). Unknown voltages are then obtained by solving the equations below:

$$[Y_{AA}][V_A] = [I_A] - [Y_{AB}][V_B] \quad [13]$$

The terms $[Y_{AB}]$ $[V_B]$ changed from the left-hand side in equation [12] to the right-hand side of equation [13] (generalization of converting Thevenin equivalent circuits [voltage vector $[V_B]$ behind admittance matrix $[Y_{AB}]$] into Norton equivalent circuits [current vector $[Y_{AB}][V_B]$ parallel with admittance matrix $[Y_{AB}]$]) (Mohd Khairi Bin Mohd Zambri, Master Degree Thesis, Universiti Malaya, 2010).

3.2.5.2 Time-Domain Solution Method

Each element is performed via time-step discretization. Values of all the power system's variables are supposed to be known at $t - \Delta t$, the values to be determined at time t. Time-step Δt is assumed so small that the differential equations are approximated by difference equations (Mohd Khairi Bin Mohd Zambri, Master Degree

Thesis, Universiti Malaya, 2010). As example, a simple algebraic relationship is obtained by replacing with differential equation for inductance; equation [14]:

$$V = L\frac{di}{dt} \qquad [14]$$

Central difference equations equivalent to numerical integration of current via trapezoidal rule for one time-step are shown in equations [15] and [16] below:

$$\frac{v(t) + V(t - \Delta t)}{2} = L\frac{i(t) - i(t - \Delta t)}{\Delta t} \qquad [15]$$

$$i(t) = G.v(t) + I_{hist}(t - \Delta t) \qquad [16]$$

$$G = \frac{\Delta t}{2L} \qquad [17]$$

With;

G : Equivalent conductance remaining constant when Δt of the computation is constant,

I_{hist}(t-Δt) : History term composed of known quantities from preceding Ampere-unit time-step.

This type of formulation can also be written for capacitor and resistors. The multi-phase coupled element is the basic formulation still being used, and the equations for multiphase coupled elements are incorporated into nodal admittance matrix of the electrical network (Mohd Khairi Bin Mohd Zambri, Master Degree Thesis, Universiti Malaya, 2010).

For any type of network with multiple n-nodes, a system's equations can be explained as follows:

$$[G][v(t)] = [i(t)] - [I_{hist}] \qquad [18]$$

With;

[G]: n x n (symmetric) nodal conductance matrix,

[v(t)]: vector of n node voltages,

[i(t)]: vector of n current sources,

[I_{hist}]: vector of "n" known "history" term.

Usually, there are nodes of known voltages owing to connected voltage sources or grounded node. Equation [18] is thus partitioned into set-A nodes of unknown voltages and set-B nodes of known voltages (Mohd Khairi Bin Mohd Zambri, Master Degree Thesis, Universiti Malaya, 2010). Unknown voltages are determined by solving for [$V_A(t)$] via equation [19]:

$$[G_{AA}][v_A(t)] = [i_A(t)] - [I_{hist_A}] - [G_{AB}][v_B(t)] \quad [19]$$

Actual computation in ATP-EMTP is Matrices [G_{AA}] and [G_{AB}]; [G_{AA}] is triangularized with ordered elimination and explitation of sparsity. For each time-step, vector on the right-hand side of equation [19] is updated from known history terms and known current and voltage sources. Next, system of linear equations is solved for $[v_A(t)]$ by using the information contained in the triangularized conductance matrix (Mohd Khairi Bin Mohd Zambri, Master Degree Thesis, Universiti Malaya, 2010).

During "repeat solution" process, symmetry of the matrix is exploited with the assumption that the triangular matrix used for downward operations is also used in back-substitution. Before proceeding to the next time step, the history terms included in [I_{histA}] are updated for use in the next following time-step (Mohd Khairi Bin Mohd Zambri, Master Degree Thesis, Universiti Malaya, 2010). Transient simulation can start from:

a) Zero initial conditions

b) AC steady-state initial conditions at a given frequency [one source] or superimposed through more sources with different frequencies.

3.2.6 Typical ATP-EMTP Applications

ATP-EMTP is widely used for switching and lightning surge analysis, insulation coordination, shaft torsional oscillation studies, protective relay modelling, harmonic and power quality studies, and modeling of HVDC and FACTS. Its typical applications are (Høidalen, H. K., ATPDRAW Version 3.0 User Manual, 1996):

a) Lightning overvoltage studies
b) Switching transients and faults studies
c) Statistical and systematic overvoltage studies
d) Very fast transients in GIS and groundings studies
e) Machine modelling system
f) Transient stability and motor startup
g) Shaft torsional oscillations
h) Transformer and shunt reactor/capacitor switching
i) Ferroresonance analysis
j) Power electronic applications
k) Circuit breaker duty (electric arc) and current chopping
l) FACTS devices: STATCOM, SVC, UPFC, TCSC modelling
m) Harmonic analysis and network resonances
n) Protection device testing

3.3 Flow Chart of Project Methodology

The flow chart describes activities or tasks to be done in each stage of the project's planning, important to ensuring successful completion of the project. Figure 3.7 presents the flow chart:

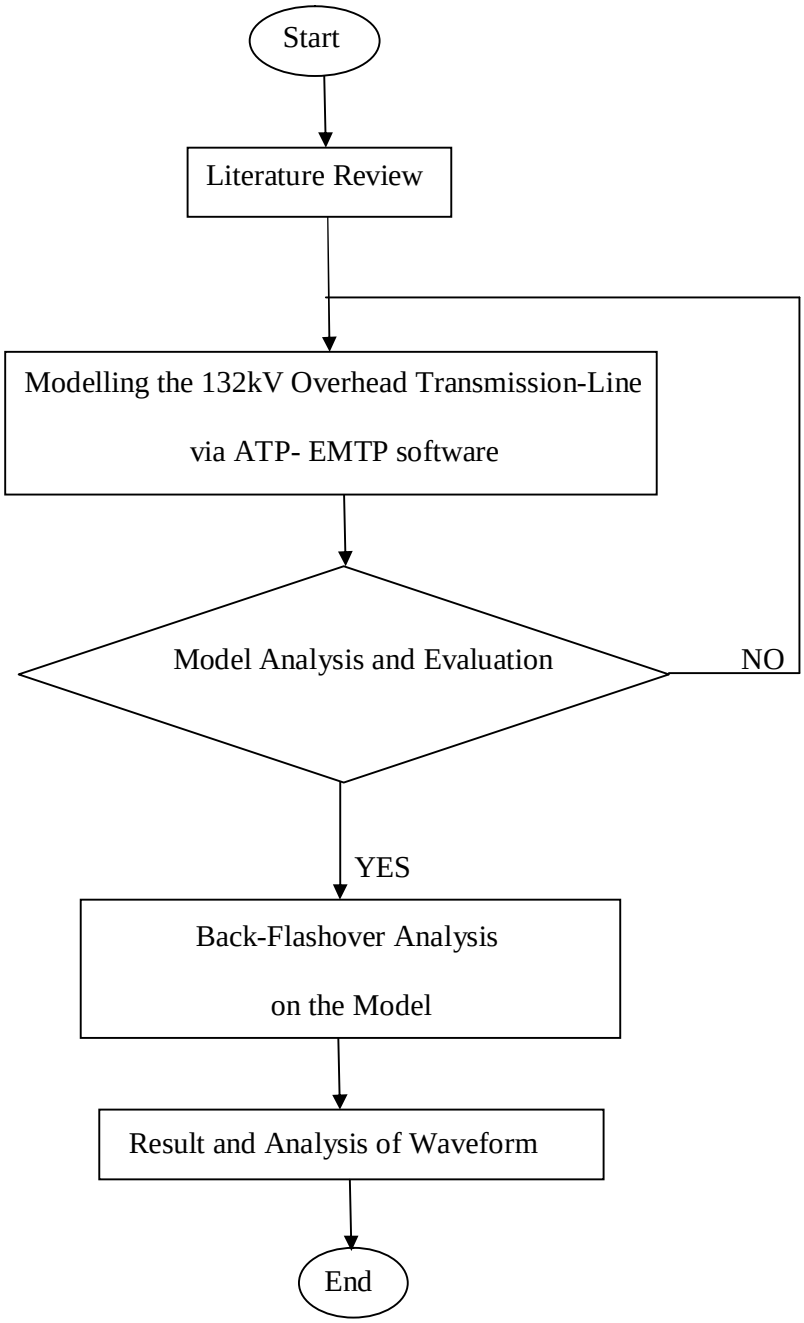

Figure 3.7: Methodology Flow Chart

(a) Literature Review

Literature review was via fact-finding research through internet, reference books, IEEE papers and journals, etc. It is vital to better understanding of the project.

(b) Modelling the 132kV Overhead Transmission-Line via ATP-EMTP software

The next step is modelling the 132kV overhead transmission line. ATP-EMTP software is the most powerful tool commonly used in power system transient analysis such as lightning analysis. This study modeled five spans of transmission towers. The full transmission-line model includes wires (shield wires and phase conductors), towers, insulator strings, cross- arms, tower surge impedance, and tower-footing resistance. Modeling guidelines will be explained in the next chapter.

(c) Model Analysis and Evaluation

The modeling will have been referred to IEEE journals/papers whose proposed methods proved compliant to field results. Most of the methods are not specified for 132kV transmission-line system. Modifications are thus necessary, for the correct model to be produced. Correctly-designed model producing correct output will be re-used in future/further investigations.

(d) Perform Back Flashover Analysis on the Model

Once the model for the 132kV overhead transmission-line system is assumed correct, back-flashover analysis will be conducted on it. Four magnitudes of lightning current will be injected into the top tower of one of the transmission

lines. Back-flashover-voltage pattern across line insulation will be observed for all three phases, as well as its response to tower-footing resistance.

(e) Result and Analysis of the Waveform

This part analyses the waveform obtained from simulation results, and discusses the results.

CHAPTER 4

MODELLING OF 132kV OVERHEAD TRANSMISSION LINES

4.1 Introduction

ATP-EMTP software has been used for modeling of 132kV overhead transmission line to simulate back flashover pattern recognition. The software is known to be one of the best tools for analysis of power-system transient problems. However, modeling the real 132kV overhead transmission line in ATP-EMTP software for back-flashover simulation is not so easy, as past researchers were more interested on modeling higher-voltage (above 275kV) transmission-line system rather than lower-voltage transmission-line system (below 275kV). References from IEEE papers, journals, and theses have been used as guidelines to designing the model. The modeling method is detailed in this chapter.

4.2 Transmission Line and Tower Model

This work modeled a 132kV double circuit with two overhead ground wire transmission towers. The phase conductor and ground wire are explicitly modelled between the towers; five tower spans were used. Line termination at each side of the model was to avoid any reflection that might affect the simulated over-voltages around the point of impact (Juan A. Martinez-Velasco, Ferley Castro-Aranda, IPST'05, June 19-23, 2005). This was done by terminating the phase conductor with AC operation voltages, and by grounding the shield wire. Figure 4.1 shows the span of five towers, with line termination at each side of the model.

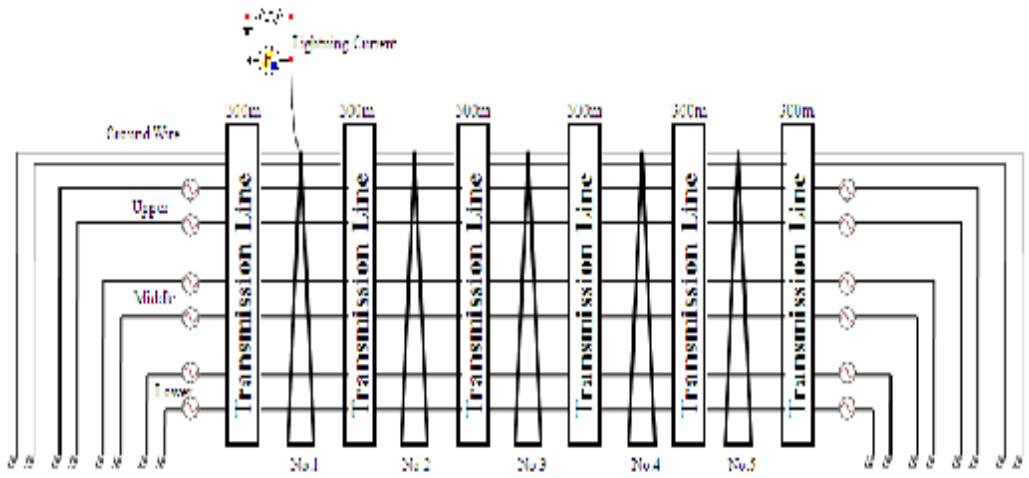

Figure 4.1: Span of five towers

The Bergeron overhead line model was used for modeling in ATP-EMTP software as it is the common type of transmission line used for 132kV overhead transmission-line system. Height of the transmission-line tower was 28.22m. The tower is represented basically by simple distributed line between cross-arms and insulator strings. Figure 4.2 shows line/cable data for transmission line used in this study. Figure 4.3 shows data features of the model.

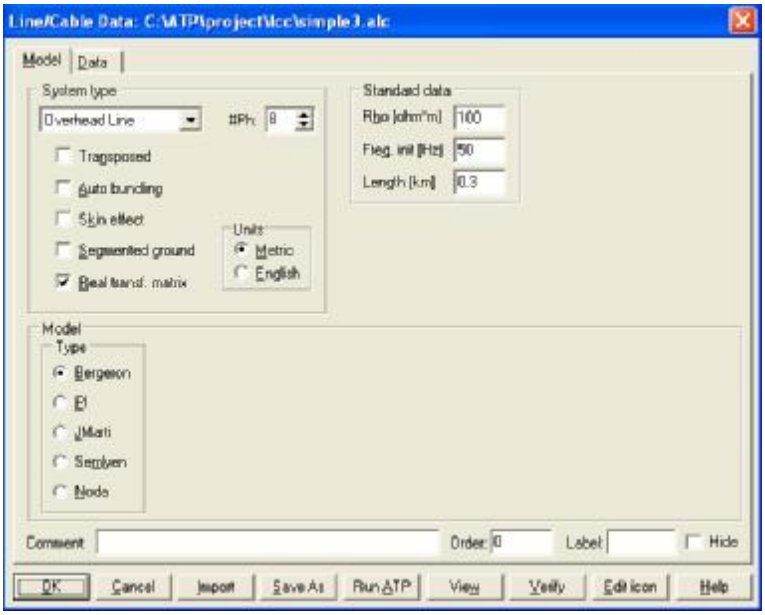

Figure 4.2: Model for Line/Cable data

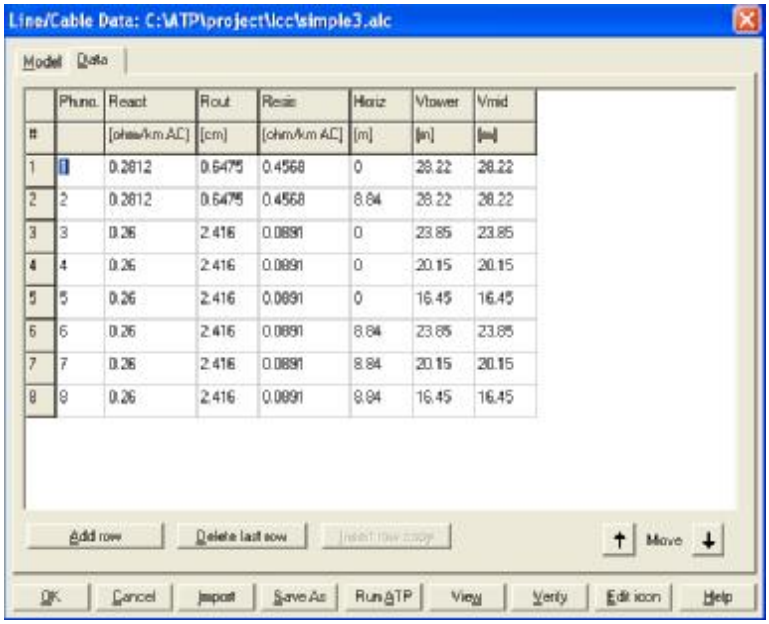

Figure 4.3: Line/Cable data

According to Figure 4.2, 'Overhead Line' was selected for the system type in LCC module. This type considers real transfer matrix of the conductor. The transformation matrix is assumed to be real because the imaginary part is neglected. On the other hand, the selected Bergeron model is based on constant parameter of K.C. Lee, or Clark, model. Standard data for this system type includes:

a) **Rho** - ground resistivity (ohmm) of homogeneous earth [Carson's theory].

b) **Freq. init** - frequency at which line parameters are calculated [Bergeron and PI models], or lower-frequency point [J. Marti, Noda, and Semlyen model].

c) **Length** is length of overhead line [m/km/miles].

In this project, the value selected for Rho was 100 ohm, for freq. init, 50 Hz [base frequency], and for distance or length, 300m (span between the towers).

Figure 4.3 shows a data parameter of the 132kV transmission-line structure. The system line has 8 phases including 2 shield wires (known as ground wire in ATP-

EMTP). All the input data are based on actual data taken from reliable sources. Details of the input data are as follows;

a) **Phase no. -** Phase number; 0 = ground wire [eliminated].

b) **RESIS -** Conductor resistance at DC [with skin effect] or at Freq. Init. [no skin effect]

c) **REACT -** Frequency-independent reactance for one-unit spacing [meter/foot]; available only without skin effect.

d) **Rout -** Outer radius [cm or inch] of one conductor.

e) **Rin -** Inner radius of one conductor; available only with skin effect.

f) **Horiz:** Horizontal distance [m or foot] from the center of bundle to a user selectable reference line.

g) **VTower:** Vertical bundle height at tower [m or foot].

h) **VMid:** Vertical bundle height at mid-span [m or foot]. **[**The height h= 2/3* VMid + 1/#*VTower is used in the calculations.]

4.3 Cross-Arms Model

Cross-arms model in ATP-EMTP is expressed basically by wave impedance and calculated via the formula described in Chapter 2. Width of the arms at junction point, for upper, middle, and lower, phases of conductor, is the same, and the three conductors have the same wave-impedance value. Width of the arms at junction point for shield wire is different from conductor's width, resulting in a different wave-impedance value. Calculations for wave impedance of shield wire and phase conductor are:

a) Upper, middle, and lower phases of conductor

$$Z_{AK} = 60ln\left(\frac{2h}{r_A}\right)$$

$$Z_{AK} = 60ln\left(\frac{2x28.22}{\frac{1}{4}x1.3}\right)$$

$$Z_{AK} = 309.426\Omega$$

b) Shield wire

$$Z_{AK} = 60ln\left(\frac{2h}{r_A}\right)$$

$$Z_{AK} = 60ln\left(\frac{2x28.22}{\frac{1}{4}x1.1}\right)$$

$$Z_{AK} = 319.45\ \Omega$$

Figure 4.4 shows the data for cross-arms model of the upper-phase conductor.

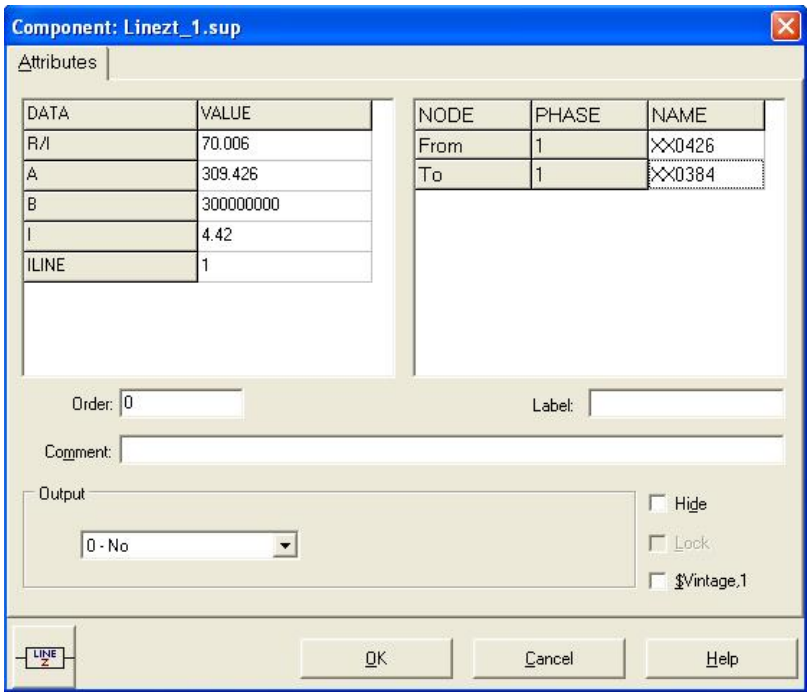

Figure 4.4: Data for the cross-arms impedance

The details of the data for the cross arms model are explained as follows:

a) R/l= Resistance per length in [Ohm/length]

b) ILINE=1: A=Modal surge impedance in [ohm]

c) ILINE=1: B=propagation velocity in [length/sec.]

d) l= length of line (>0 for transposed lines)

4.4 Insulator-Strings Model

In ATP-EMTP software, the insulator strings are modelled by capacitors parallel with voltage-dependent flashover switches connected between phases and tower (Ali F. Imece et al., IEEE Transactions on Power Delivery, 1996). Capacitor value (for pin insulators) in this work is 10pF. Figure 4.5 is a model of the insulator strings.

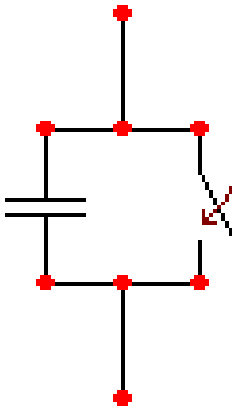

Figure 4.5: Model of the insulator strings

4.5 Lightning Source Model

The lightning source model selected for this study is the Heidler type. Heidler lightning source model can be used as a current-type or voltage-type surge source. Here the source is modeled as an impulse current parallel with lightning-path impedance; see

Figure 4.6. The resistance value selected is 400Ω (L. V. Bewley, Transactions of the American Institute of Electrical Engineers, 1931).

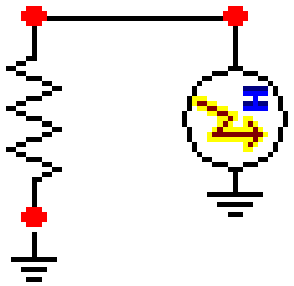

Figure 4.6: Heidler type of lightning source

Four different values of current magnitudes, front time and tail time are used in this lightning simulation. Figure 4.7 shows one of the data for the Heidler model used in the ATP-EMTP software. Figure 4.8 shows the lightning-strike waveform.

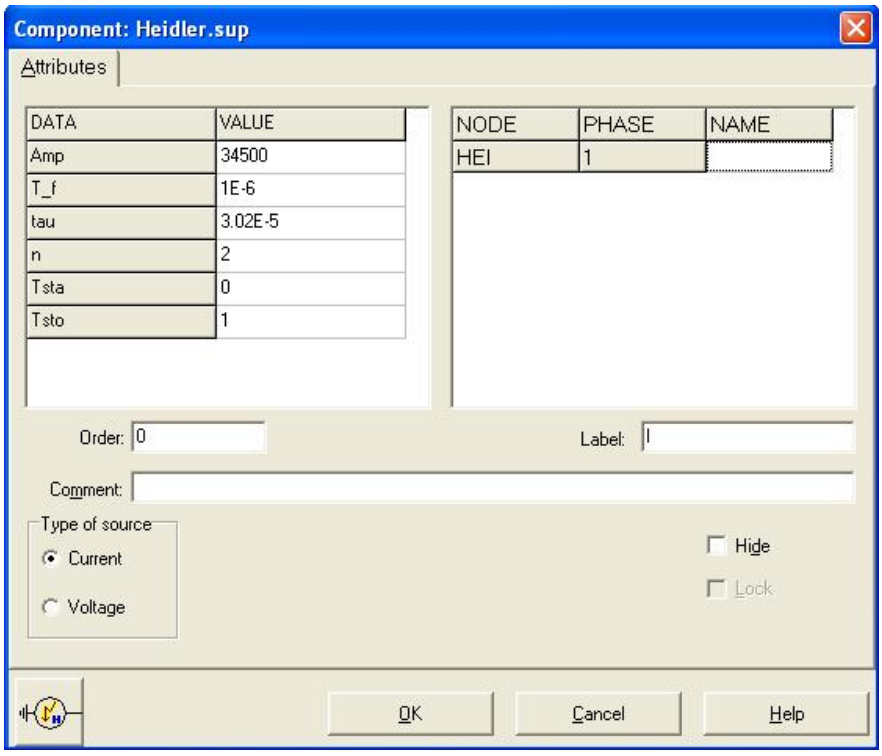

Figure 4.7: Data for the Heidler Surge Model

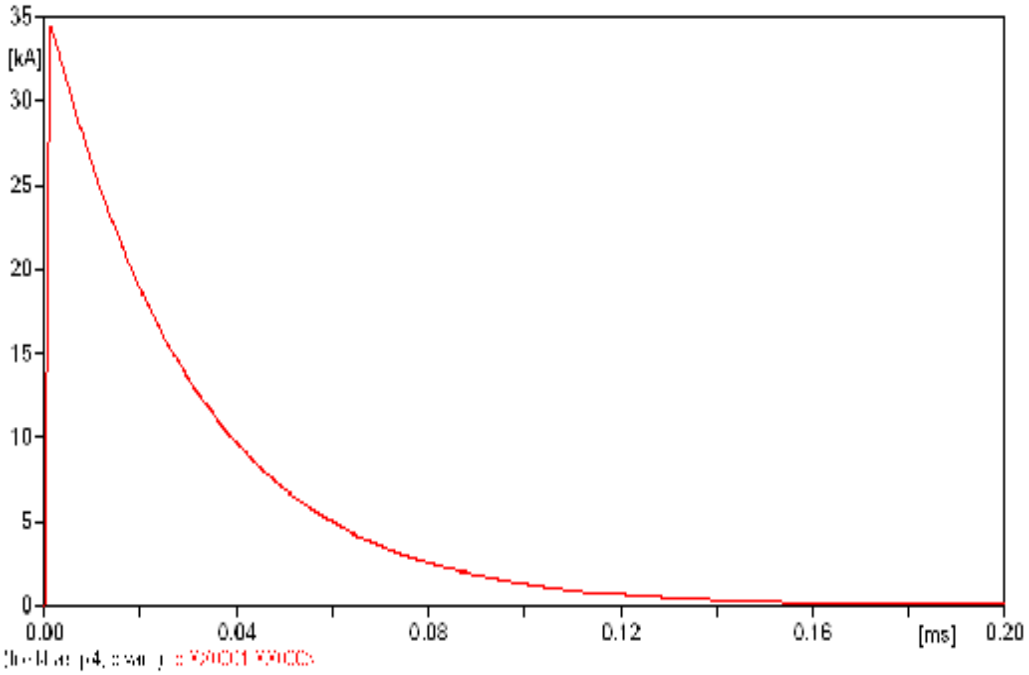

Figure 4.8: Output waveform for lightning strike at 34.5kA peak;

1.0μs front duration, 30.2μs strike duration

Details of input parameters of the Heidler-type lightning source:

a) U/I = 0: Voltage source, -1: Current source.

b) Amp = multiplicative number [A] or [V] of the function; does not represent peak value of surge.

c) T_f = front duration [seconds]; interval between t=0 and time at function peak.

d) Tau = strike duration [seconds]; interval between t=0 and point on tail where function amplitude fell to 37% of its peak value.

e) n = factor influencing rate of rise of function; increased n increases maximum steepness.

f) Tsta = start time [seconds]; source value zero for T<Tsta.

g) Tsto = end time [seconds]; source value zero for T>Tsto.

4.6 Tower Surge-Impedance Model

Tower surge impedance model in ATP-EMTP is expressed by wave impedance. Figure 4.8 shows the model's data, which are the same as those of the cross-arms model except the difference in impedance value (a different formula was used to calculate surge impedance, as elaborated in Chapter 2). Calculations for tower surge impedance of both shield wire and phase conductor are as below:

$$Z_{AK} = 60\left[ln\sqrt{2}\frac{2h}{r_A} - 1\right]$$

$$Z_{AK} = 60\left[ln\sqrt{2}\frac{2 \times 28.22}{4.42} - 1\right]$$

$$Z_{AK} = 113.62\ \Omega$$

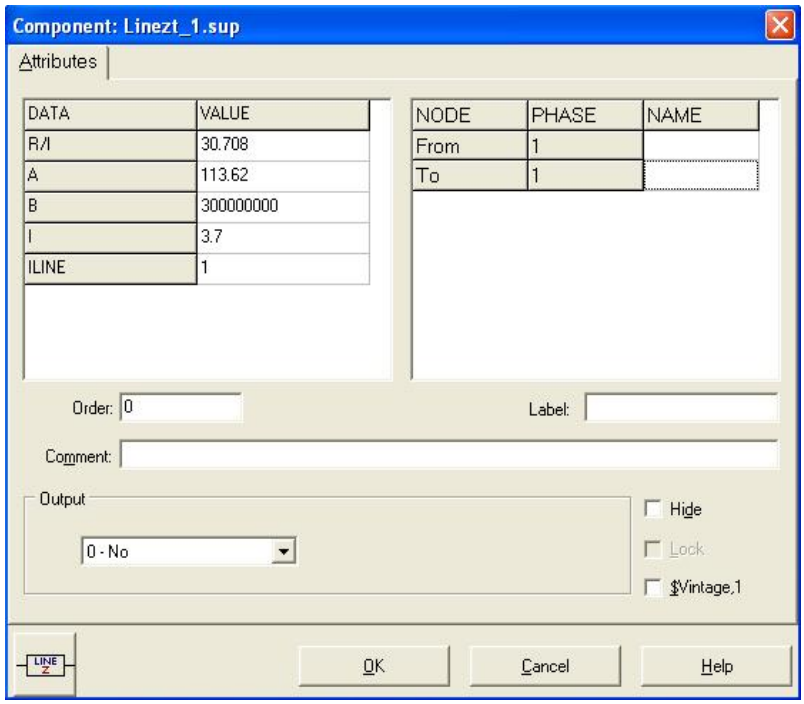

Figure 4.9: Model of the Tower Surge Impedance

4.7 Tower-Footing Resistance Model

Tower footing resistance model in ATP-EMTP is expressed by a resistor. To determine line performance for footing resistance, R_o of 10Ω or less can be used

(Electrical Transmission and Distribution Reference Book, 1964). Thus, R_o of 10Ω is used in the simulation. Figure 4.10 shows the model's data.

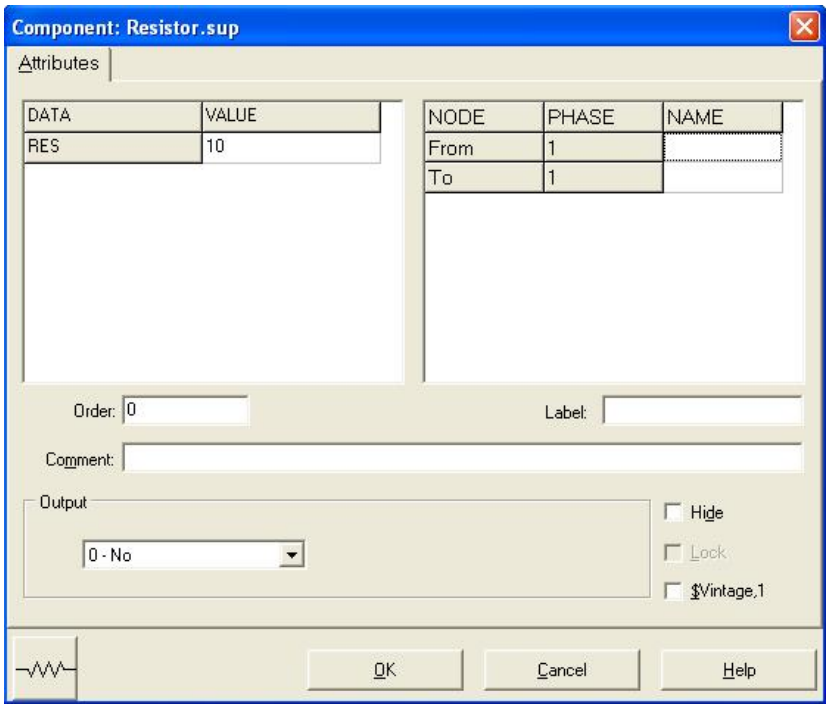

Figure 4.10: Model of the Tower-Footing Resistance

4.8 AC Voltage Source Model

AC voltage source in the ATP- EMTP software used peak amplitude of system voltage for the simulation process. Modeling of AC voltage source can thus be done by converting system voltage of $132kV_{L\text{-}L(RMS)}$ to peak voltage, via the following equation:

$$V_{peak} = \frac{\sqrt{2}}{\sqrt{3}} V_{L-L(RMS)}$$

$$V_{peak} = \frac{\sqrt{2}}{\sqrt{3}} \times 132kV$$

$$V_{peak} = 107777.5V$$

Figure 4.11 shows input data for the AC voltage source while Figure 4.12 shows the three phase AC voltage source used for this simulation.

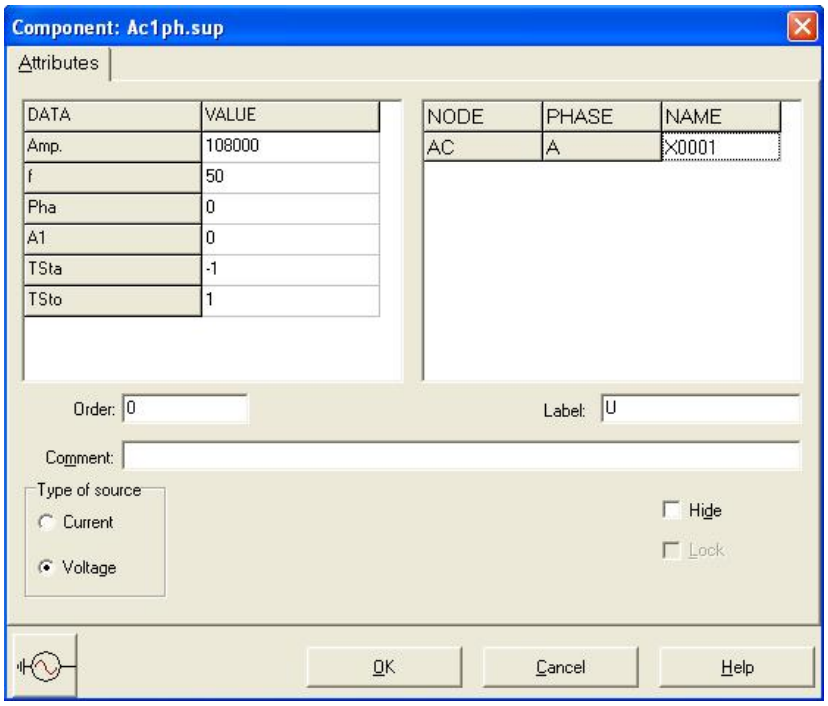

Figure 4.11: Model of the AC Voltage Source in ATP- EMTP software

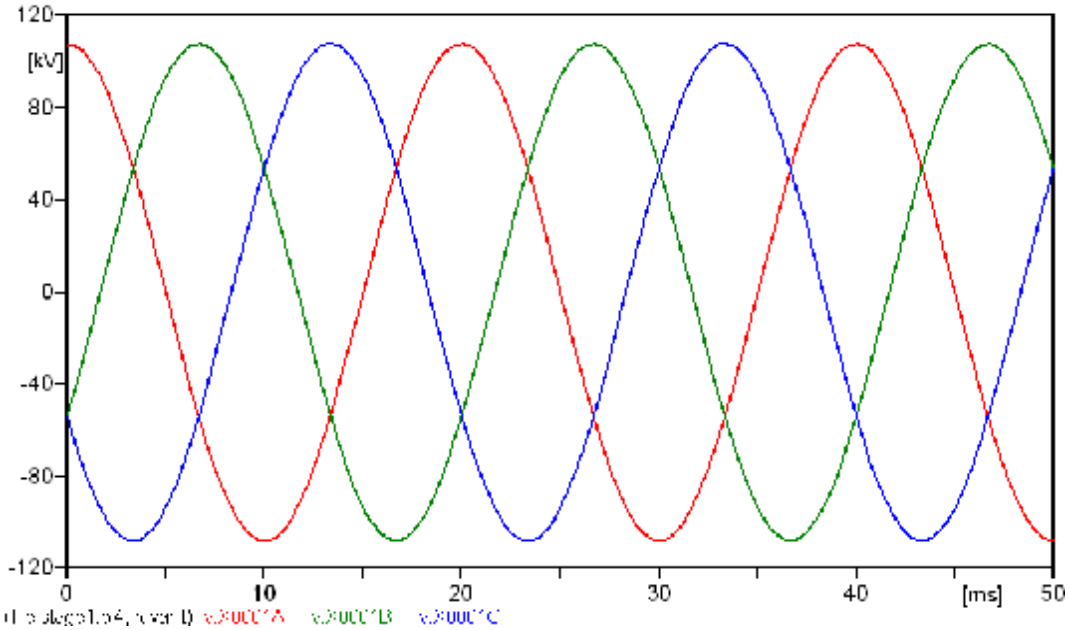

Figure 4.12: Three-Phase AC Voltage Source in ATP- EMTP software

Details of the AC-voltage-source input parameters:

a) U/I= 0: Voltage source, -1: Current source.

b) Amp = peak value [V] of the function.

c) f = frequency [Hz]; in Malaysia, 50Hz ±2%.

d) Pha = phase-shift (in degrees).

e) Tsta = start time [seconds]; source value zero for T<Tsta.

f) Tsto = end time [seconds]; source value zero for T>Tsto.

CHAPTER 5

RESULTS AND DISCUSSIONS

5.1 Introduction

This chapter presents simulation results obtained from ATP-EMTP simulation. They are based on back-flashover analysis of the 132kV overhead transmission-line modeled. The first part of this chapter mainly discusses and analyses simulation results obtained from four magnitudes of lightning current injected into the top tower of the transmission line. Back-flashover voltage occurring across insulator strings at each phase is studied. The second part describes effects of tower-footing resistance on back-flashover voltage obtained from simulation. Complete analysis and discussion on waveforms obtained from simulation results are presented in this chapter.

5.2 Part 1: Lightning Surge Simulation on 132kV Overhead Transmission Line

The modeled 132kV overhead transmission line with five towers was used for lightning-surge simulation. The towers were modeled in Simple Distributed Line Model (see previous chapter). Figure 5.1 shows the model for a part of the simulation circuit. Appendix A is a full diagram of the model.

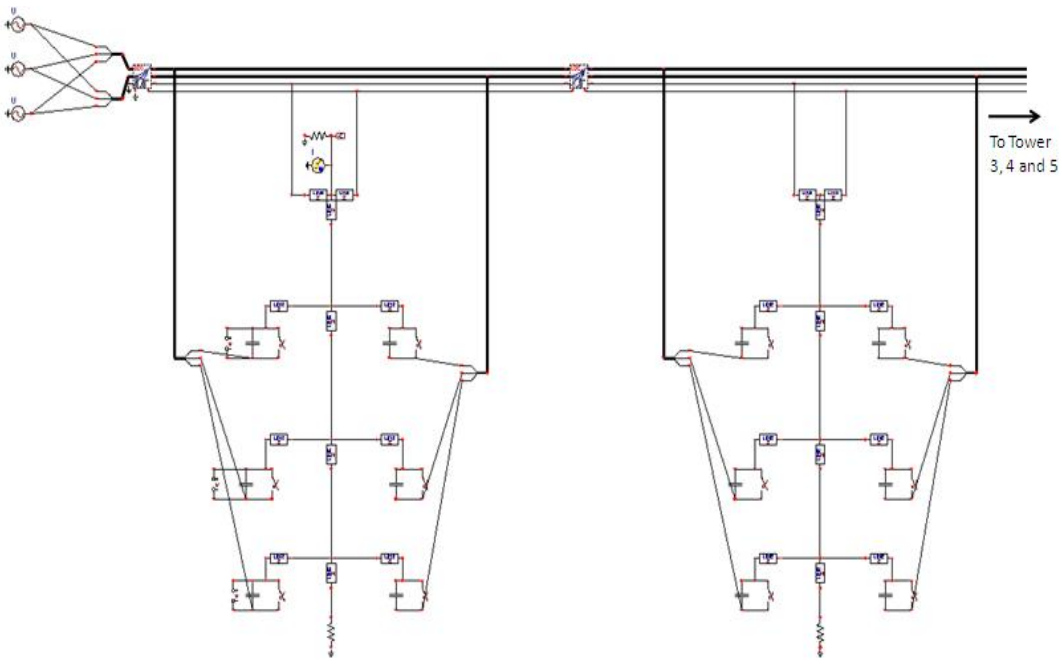

Figure 5.1: Part of the ATP-EMTP model for 132kV double circuit transmission lines

In this study, four amplitudes of lightning current (positive polarity) were used to perform back-flashover analysis on the modelled circuit. The simulation is based basically on lightning behavior in Malaysia, which has an average 34.5kA lightning-strike current. Minimum lightning-strike current for back flashover is 20kA. Simulations are thus conducted with 4 levels of lightning-strike current: 20kA, 34.5kA, 50kA and100kA.

For the simulation, lightning-surge current was injected into the top tower of the first tower; see Figure 5.1. Back-flashover voltage across insulator string was measured at each phase, for single-circuit line, by using probe branch voltage. As has been explained, back flashover occurs when voltage across line insulation is equal to or greater than Critical Flashover Voltage (CFO), which is determined from Basic Insulation Level (BIL) calculated via the equation below (Andrew R. Hileman, 1999):

$$BIL = CFO\left(1 - 1.28\frac{s_f}{CFO}\right) \qquad [20]$$

where σ_f is coefficient of the variation, known as sigma. For lightning, the sigma is 2% to 3 % (Andrew R. Hileman, 1999). According to ANSI C92 IEEE1313.1 (Ab Halim Ab Bakar et al., 2007), the suggested BIL for 150kV is 650kV, so, with this BIL value and 2% sigma, the CFO is approximately 650kV; this value will be used throughout the analysis.

Table 5.1 gives lightning-current amplitudes, front times, and tail times, of the lightning waveform used in the analysis.

Table 5.1: Lightning Amplitudes, Front Times, and Tail Times

Lightning Current Amplitude	Front Time and Tail Time
20kA	1/30.2 µs
34.5kA	1/30.2 µs
50kA	1.2/50 µs
100kA	2/77.5 µs

a) Lightning current = 20kA, front/tail time = 1/30.2µs

Lightning-strike current of 20kA was injected into the top tower. Figure 5.2(a) shows the waveforms for voltages obtained across insulator strings at each phase. Figure 5.2(b) is a close-up of the waveforms.

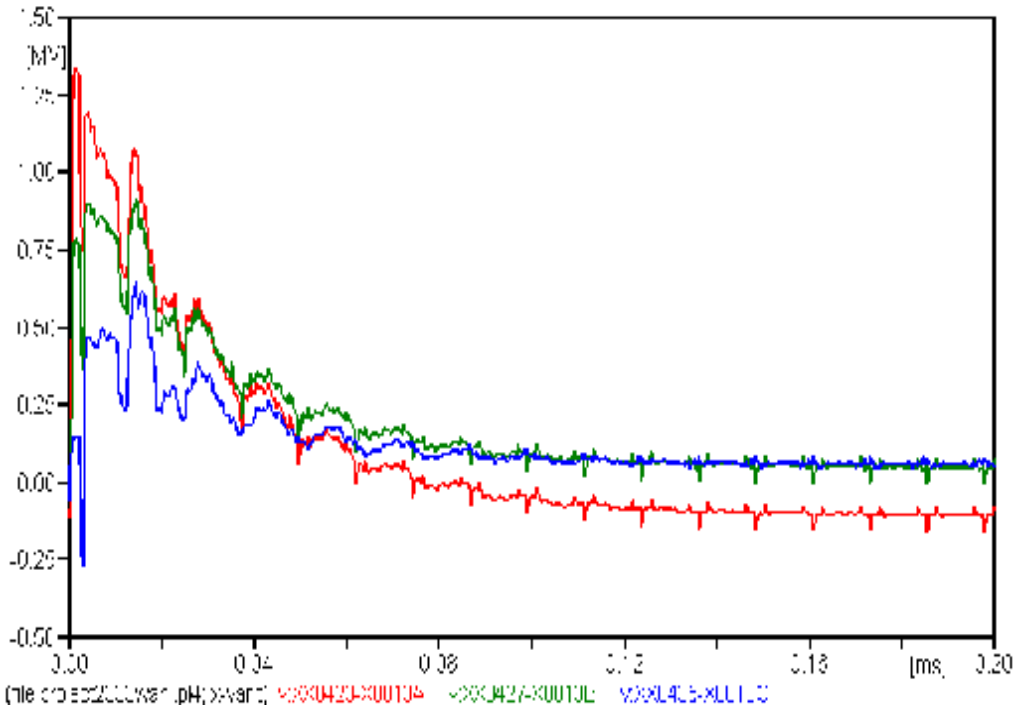

Figure 5.2(a): Voltage across insulator strings, for 20kA lightning-strike current

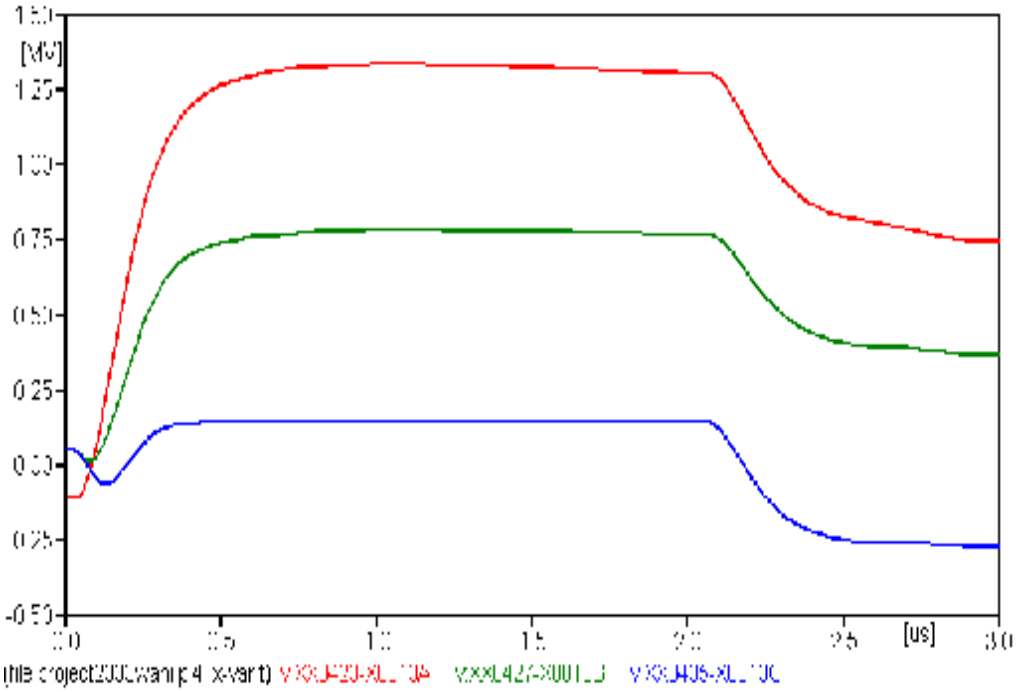

Figure 5.2(b): Close-up of 20kA waveform

b) Lightning current = 34.5kA, front/tail time = 1/30.2µs

Lightning-strike current of 34.5kA was injected into the top tower. Figure 5.3(a) shows the waveforms for voltages obtained across insulator strings at each phase. Figure 5.3(b) is a close-up of the waveforms.

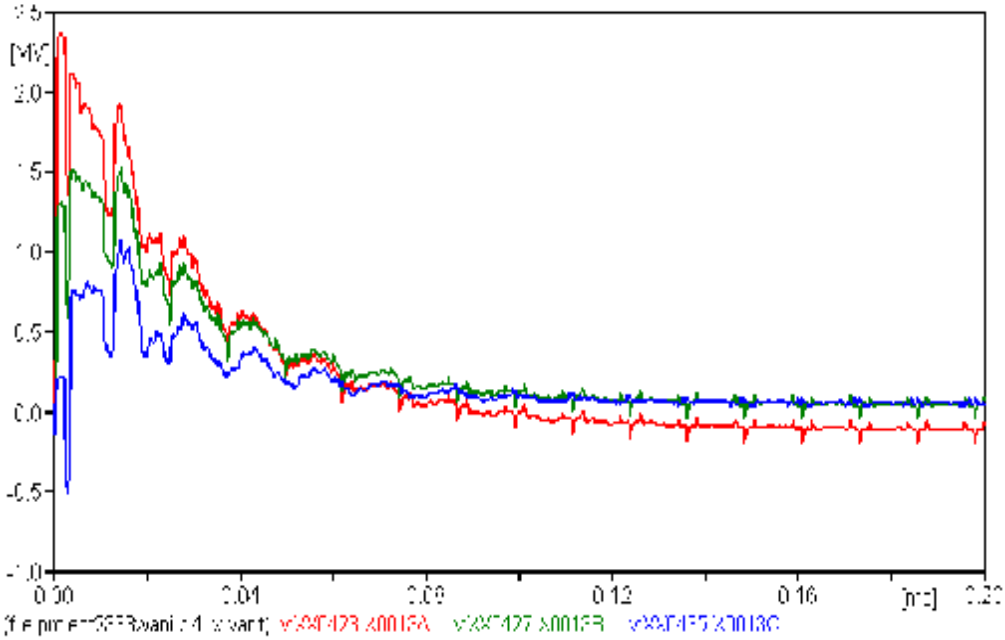

Figure 5.3(a): Voltage across insulator strings, for 34.5kA lightning-strike current

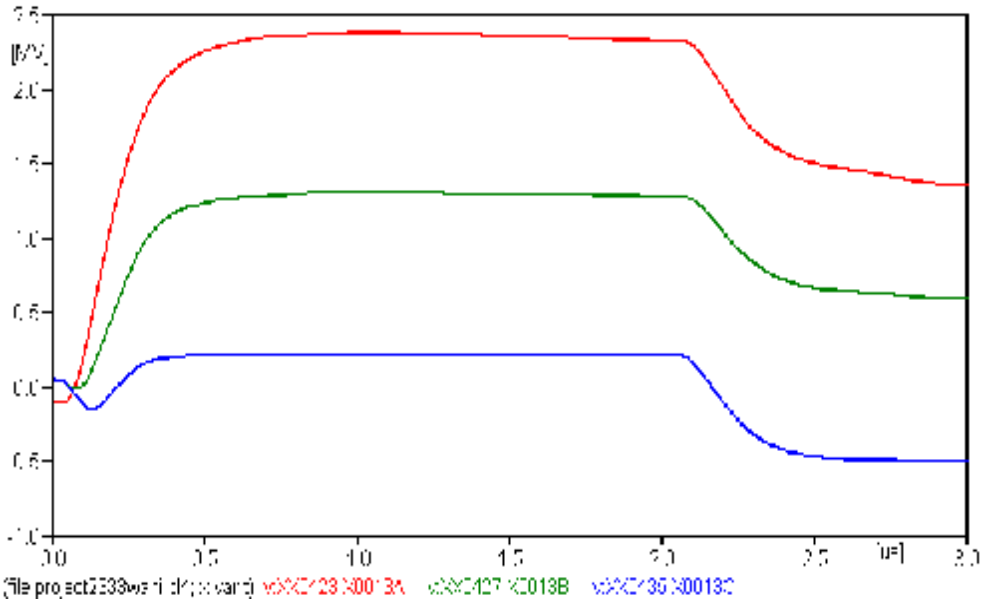

Figure 5.3(b): Close-up of 34.5kA waveform

c) Lightning current = 50kA, front/tail time = 1.2/50μs

Lightning-strike current of 50kA was injected into the top tower. Figure 5.4(a) shows the waveforms for voltages obtained across insulator strings at each phase. Figure 5.4(b) is a close-up of the waveforms.

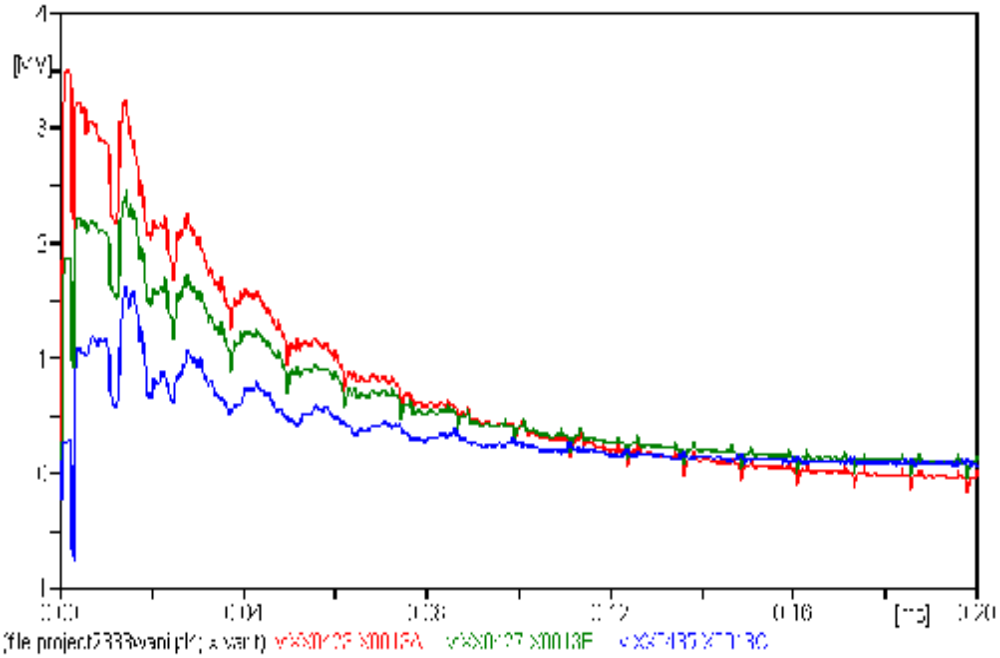

Figure 5.4(a): Voltage across insulator strings, for 50kA lightning-strike current

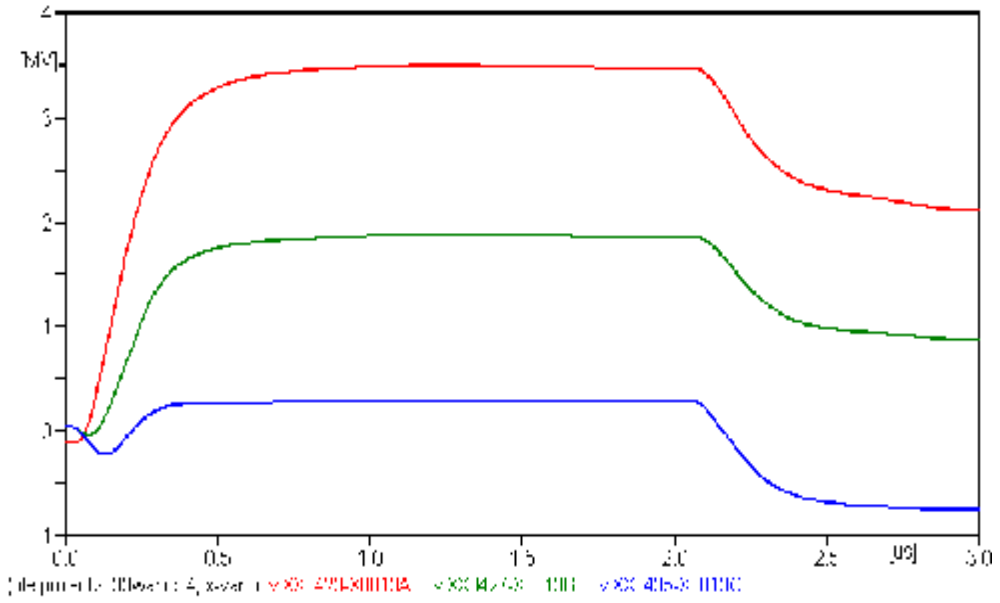

Figure 5.4(b): Close-up of 50kA waveform

d) Lightning current = 100kA, front/tail time = 2/77.5μs

Lightning-strike current of 100kA was injected into the top tower. Figure 5.5(a) shows the waveforms for voltages obtained across insulator strings at each phase. Figure 5.5(b) is a close-up of the waveforms.

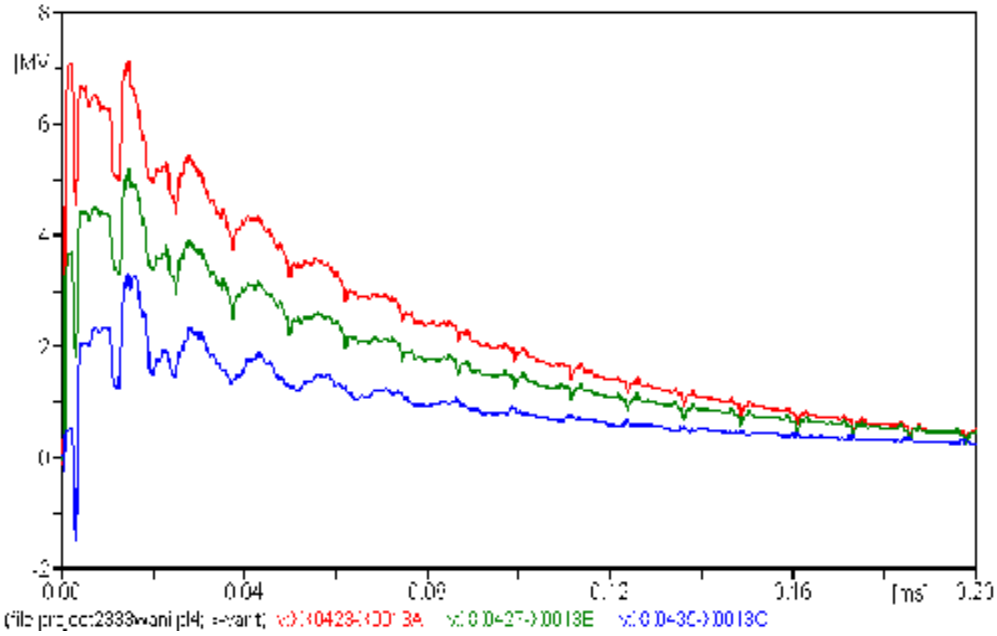

Figure 5.5(a): Voltage across insulator strings, for 100kA lightning-strike current

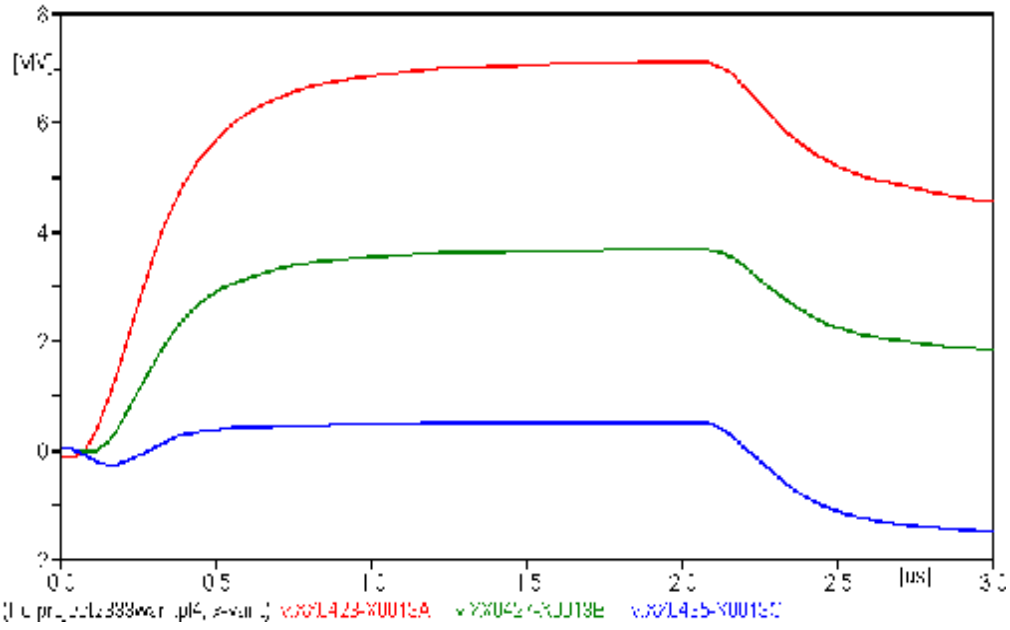

Figure 5.5(b): Close-up of 100kA waveform

Figures 5.2 (a) and (b) to 5.5 (a) and (b) show amplitudes of induced voltage across insulator strings when lightning-strike current is injected into the top of the first transmission-tower.

According to Figures 5.2 (a) and (b), maximum voltage induced across the insulator string is observed in the upper phase, followed by in the middle phase, and then in the lower phase, at 1.5μs average time. According to the CFO determined for this analysis (650kV), voltage at only the upper and the middle phases exceeds 650kV; back-flashover thus occurred only in the two phases.

The same phenomena occurred when 34.5kA, 50kA and 100kA lightning-strike currents were injected into the top tower of the transmission line. Figures 5.3(a) and (b) to 5.5 (a) and (b) show maximum induced voltage across insulator string, in the upper, then in the middle, and finally in the lower, phases. As voltages at upper phase and middle phase are greater than the defined CFO voltage, back-flashover occurred in those phases. In all cases, flashover did not occur in the lower phase. However, as magnitude of lightning-strike current was increased from 20kA to 100kA, maximum voltage induced across insulator string in each phase also increased, showing possibility of all phases to flashover increasing when magnitude of lightning-strike current increases. The analyses were done with 10Ω tower-footing resistance.

5.3 Part 2: Effect of Tower-Footing Resistance on Back-Flashover Voltage

In this part, simulation on the modelled 132kV overhead transmission line with five towers is done with varying tower-footing resistance R_o from 5Ω to 50Ω. The same four different magnitudes of lightning-strike current as applied in Part 1 will be used in the simulation. Effect of varying tower-footing resistance on back-flashover voltage across insulator strings at each phase is the concern in this analysis.

Maximum voltage induced across insulator strings at each phase when tower-footing resistance is varied was recorded. Graphs of maximum voltage induced across insulator strings versus tower-footing resistance were plotted for all four magnitudes of lightning-strike current. Tables show phases that flashover when tower-footing resistance increases.

a) Lightning current = 20kA, front/tail time = 1/30.2µs

Lightning-strike current of 20kA was injected into the top tower. Figure 5.6(a) – (j) show the waveforms for voltages obtained across insulator strings at each phase when the tower-footing resistance varied from 5Ω to 50Ω. Figure 5.7 shows the graph of maximum voltage induced across insulator strings versus tower-footing resistance. Table 5.2 show phases that flashover when tower-footing resistance increases.

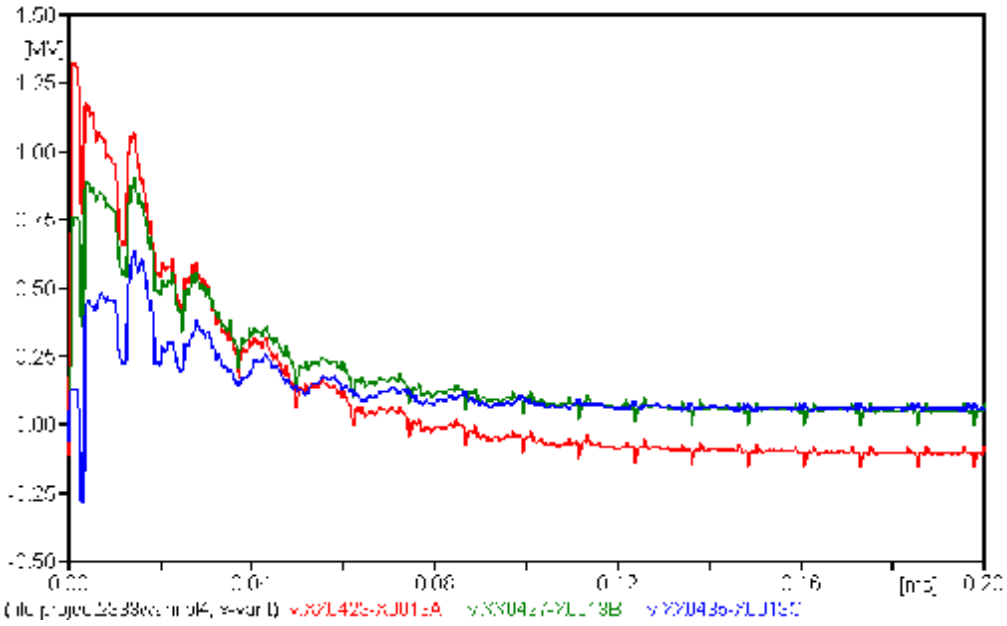

(a)

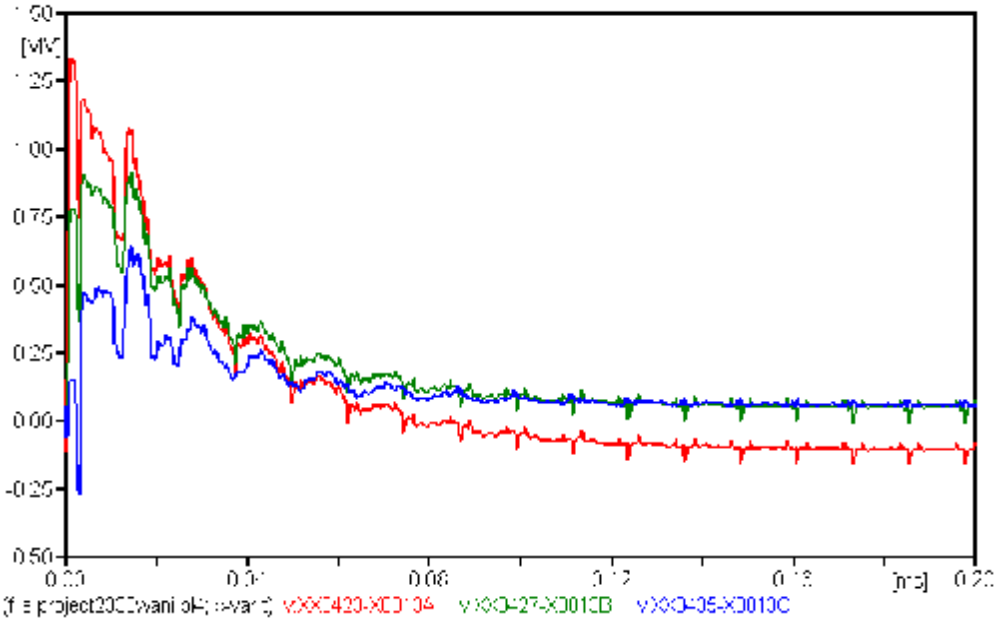

(b)

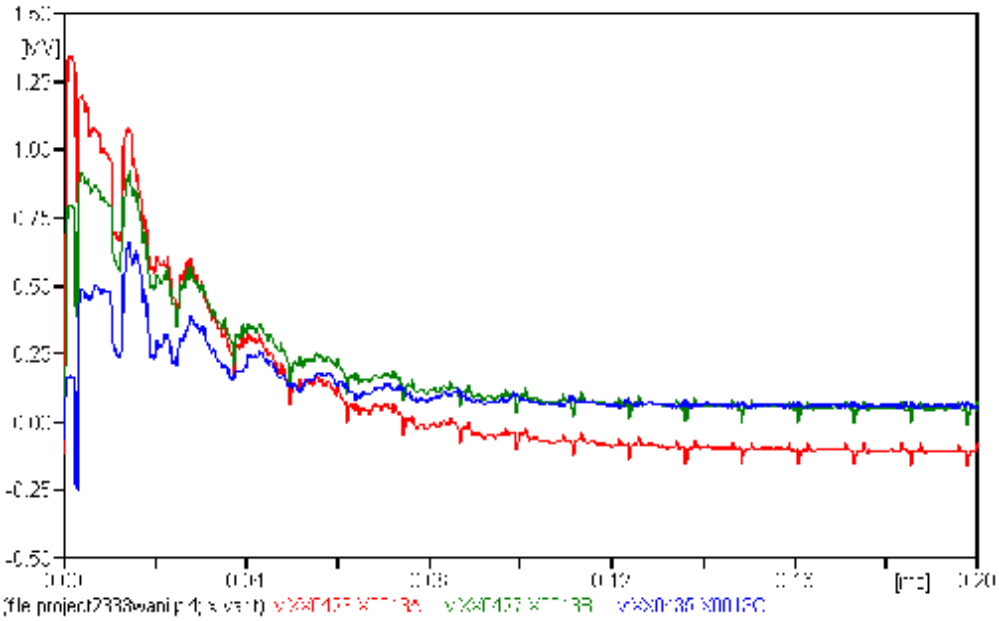

(c)

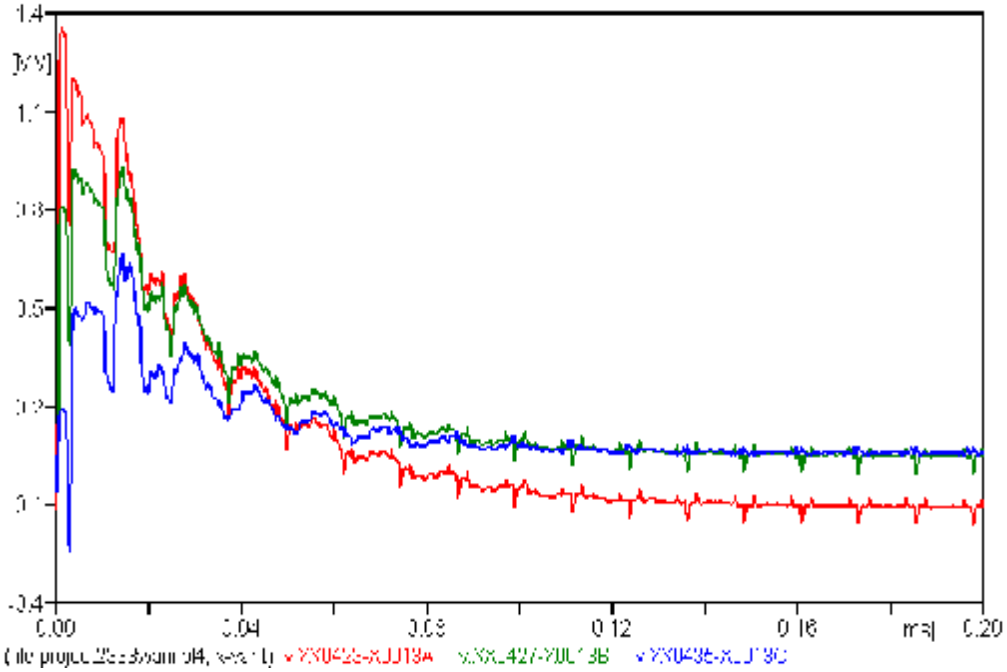

(d)

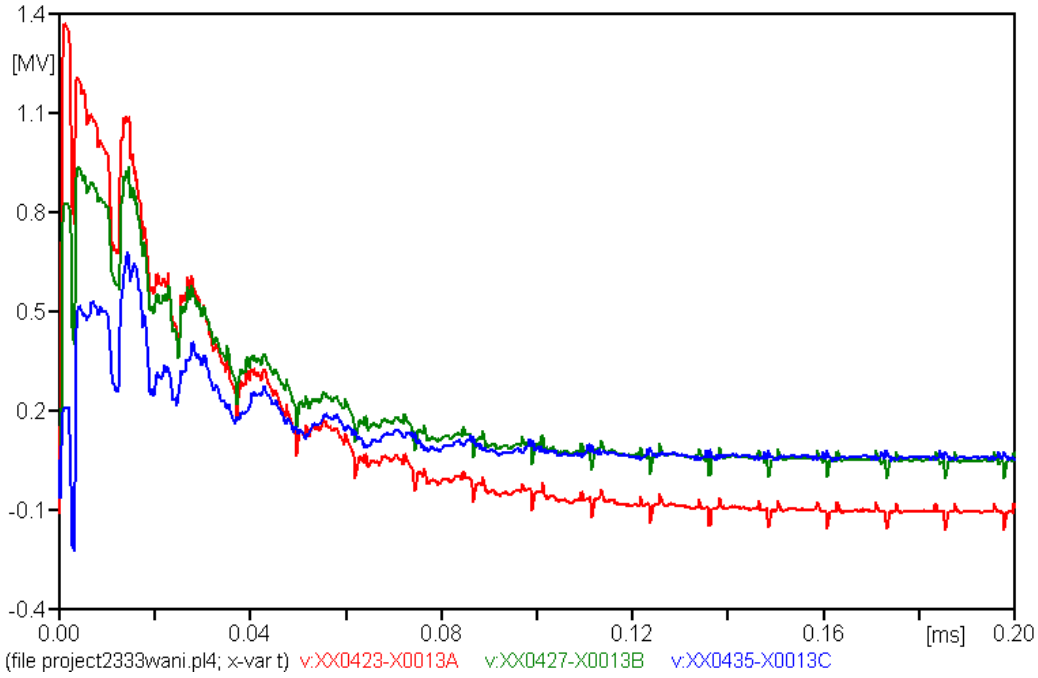
1.4
[MV]
1.1
0.8
0.5
0.2
-0.1
-0.4
0.00
0.04
0.08
0.12
0.16
[ms]
0.20
(file project2333wani.pl4; x-var t) v:XX0423-X0013A v:XX0427-X0013B v:XX0435-X0013C

(e)

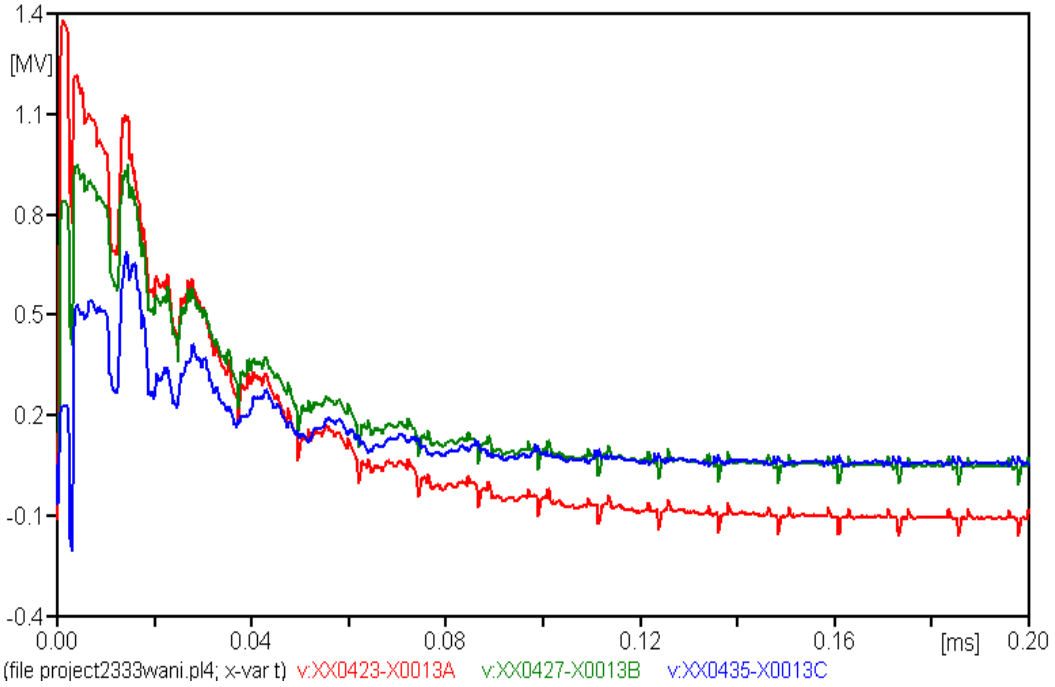
1.4
[MV]
1.1
0.8
0.5
0.2
-0.1
-0.4
0.00
0.04
0.08
0.12
0.16
[ms]
0.20
(file project2333wani.pl4; x-var t) v:XX0423-X0013A v:XX0427-X0013B v:XX0435-X0013C

(f)

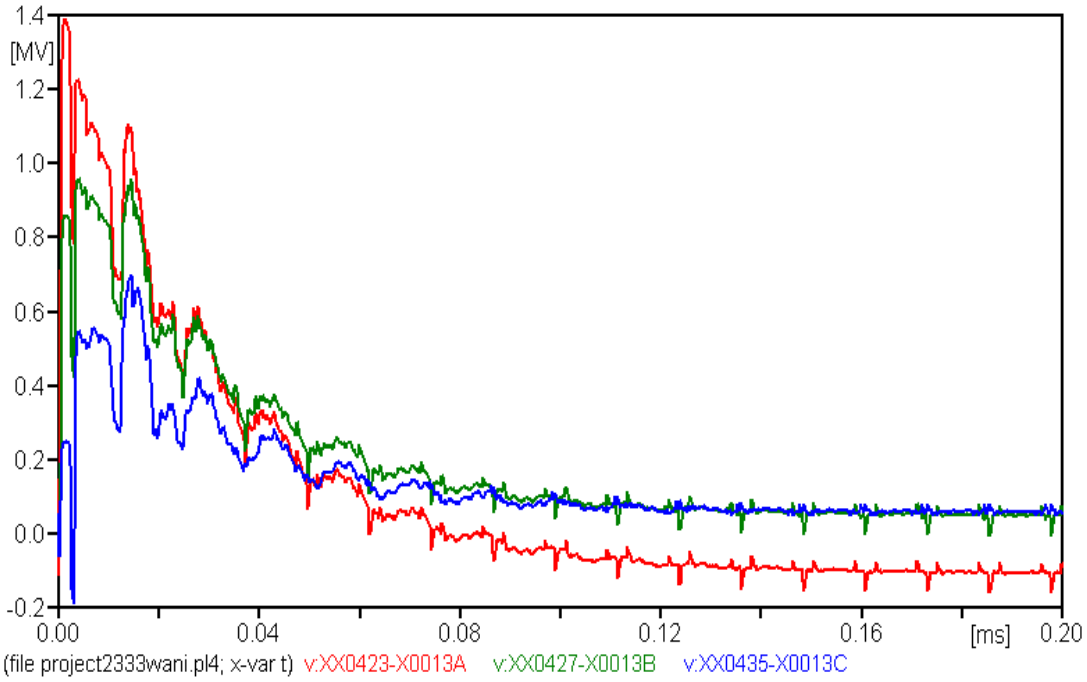
1.4
[MV]
1.2
1.0
0.8
0.6
0.4
0.2
0.0
-0.2
0.00
0.04
0.08
0.12
0.16
[ms]
0.20
(file project2333wani.pl4; x-var t) v:XX0423-X0013A v:XX0427-X0013B v:XX0435-X0013C

(g)

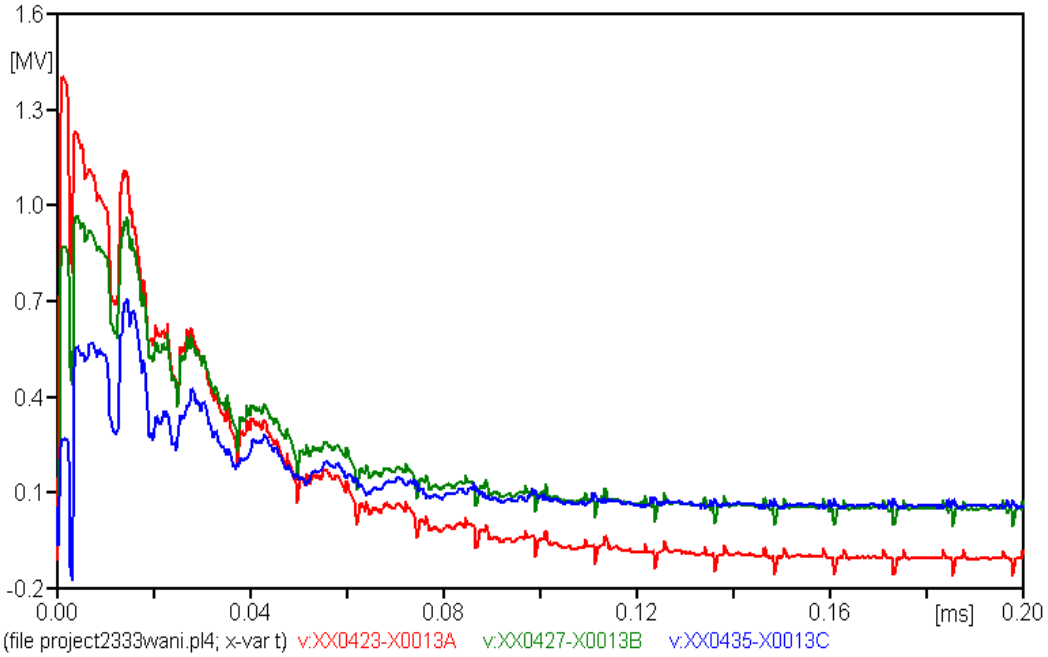
1.6
[MV]
1.3
1.0
0.7
0.4
0.1
-0.2
0.00
0.04
0.08
0.12
0.16
[ms]
0.20
(file project2333wani.pl4; x-var t) v:XX0423-X0013A v:XX0427-X0013B v:XX0435-X0013C

(h)

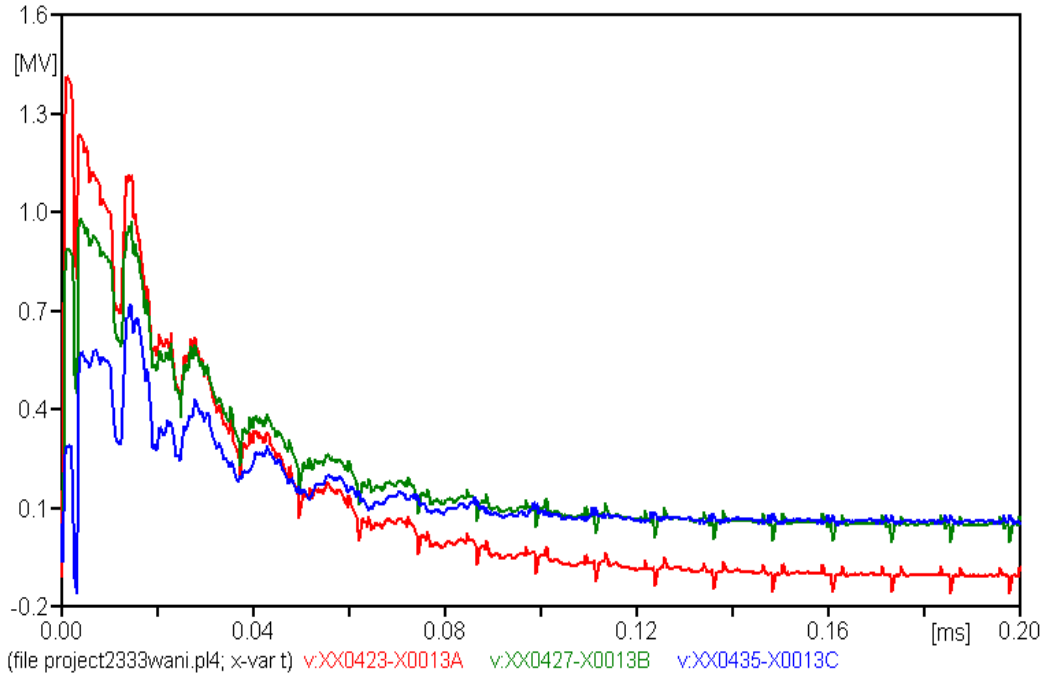
1.6
[MV]
1.3
1.0
0.7
0.4
0.1
-0.2
0.00
0.04
0.08
0.12
0.16
[ms]
0.20
(file project2333wani.pl4; x-var t) v:XX0423-X0013A v:XX0427-X0013B v:XX0435-X0013C

(i)

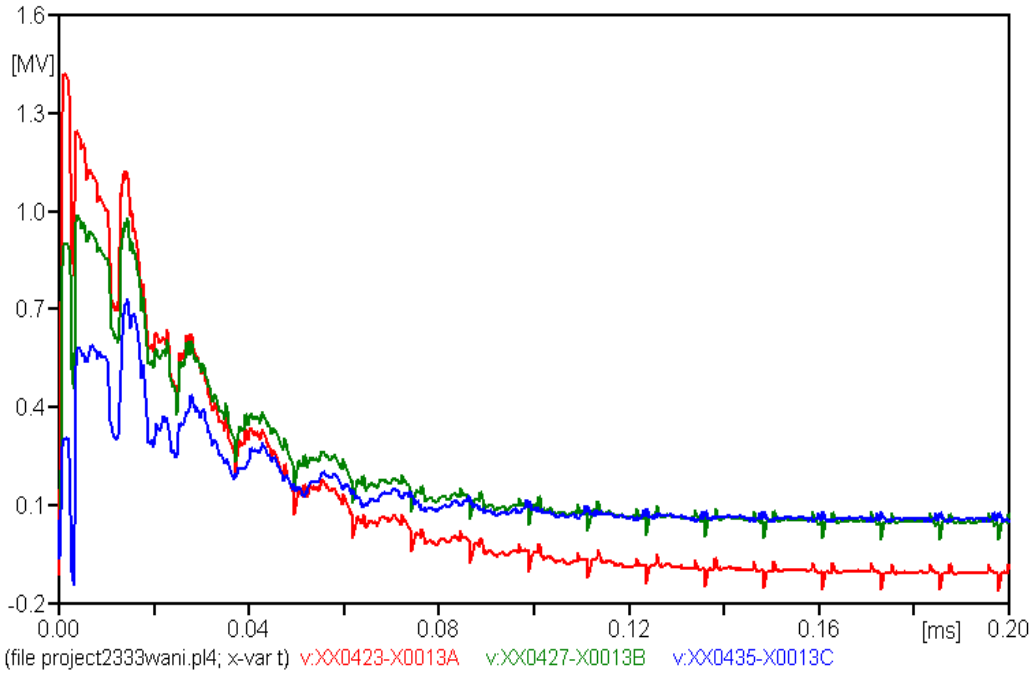

(j)

Figure 5.6: Voltage across insulator strings, for 20kA lightning-strike current (a) 5Ω, (b) 10Ω, (c)15Ω, (d) 20Ω, (e) 25Ω, (f) 30Ω, (g) 35Ω, (h) 40Ω, (i) 45Ω, (j) 50Ω.

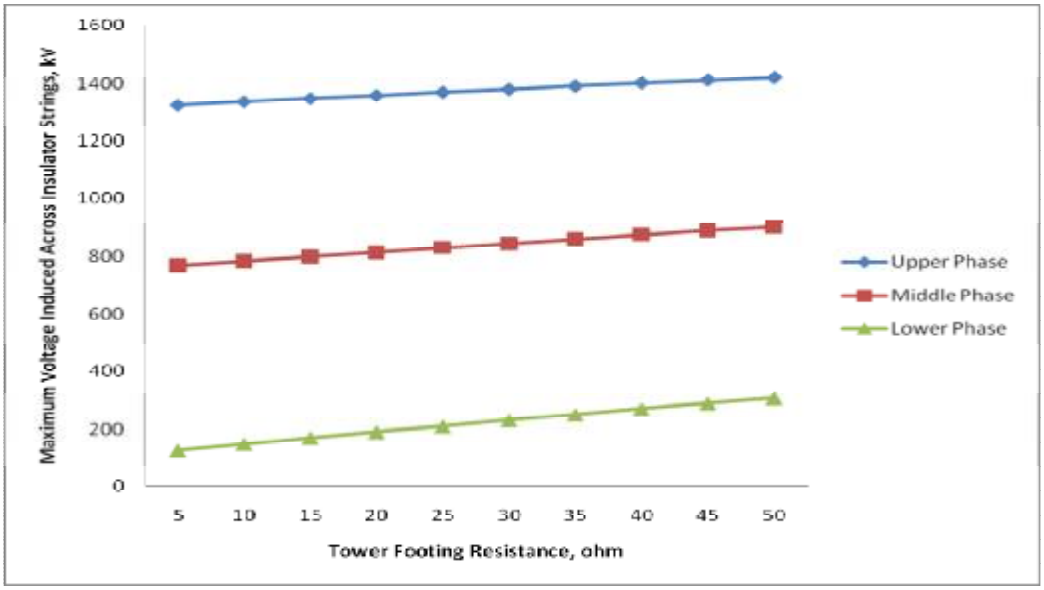

Figure 5.7: Graph of maximum voltage across insulator strings versus tower-footing resistance, for 20kA lightning-strike current

Table 5.2: Back flashover across insulator strings at each phase, for 20kA lightning-strike current

Tower Footing Resistance (Ω)	20kA		
	Upper	Middle	Lower
5	Y	Y	N
10	Y	Y	N
15	Y	Y	N
20	Y	Y	N
25	Y	Y	N
30	Y	Y	N
35	Y	Y	N
40	Y	Y	N
45	Y	Y	N
50	Y	Y	N

Y : Flashover
N : No Flashover

b) Lightning current = 34.5kA, front/tail time = 1/30.2μs

Lightning-strike current of 34.5kA was injected into the top tower. Figure 5.8(a) – (j) show the waveforms for voltages obtained across insulator strings at each phase when the tower-footing resistance varied from 5Ω to 50Ω. Figure 5.9 shows the graph of maximum voltage induced across insulator strings versus tower-footing resistance. Table 5.3 show phases that flashover when tower-footing resistance increases.

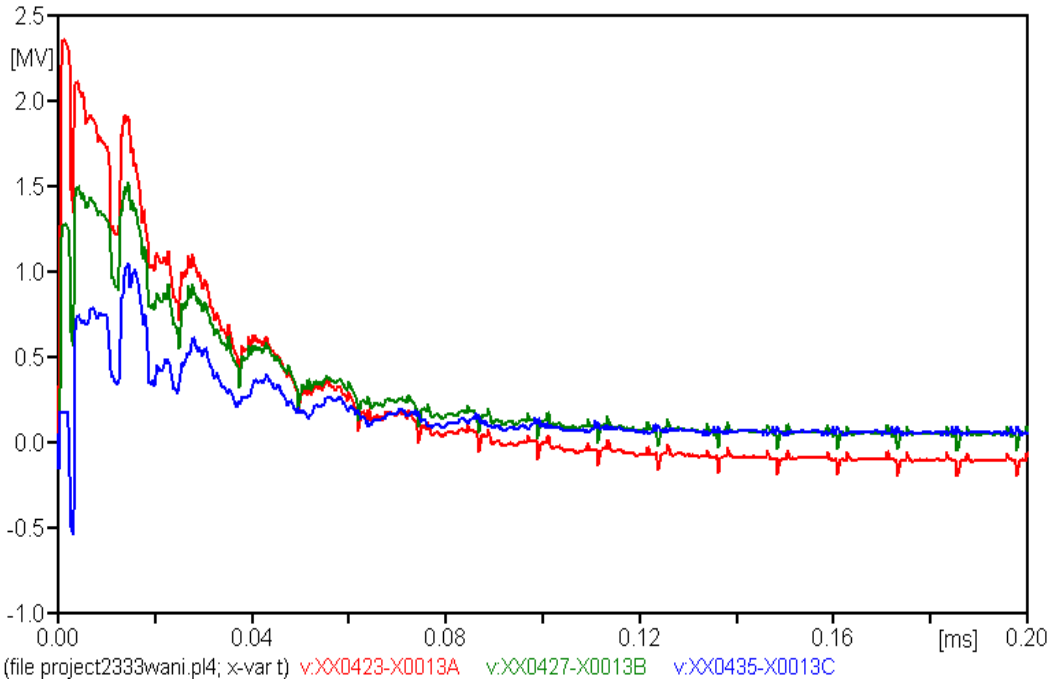
2.5
[MV]
2.0
1.5
1.0
0.5
0.0
-0.5
-1.0
0.00
0.04
0.08
0.12
0.16
[ms]
0.20
(file project2333wani.pl4; x-var t) v:XX0423-X0013A v:XX0427-X0013B v:XX0435-X0013C

(a)

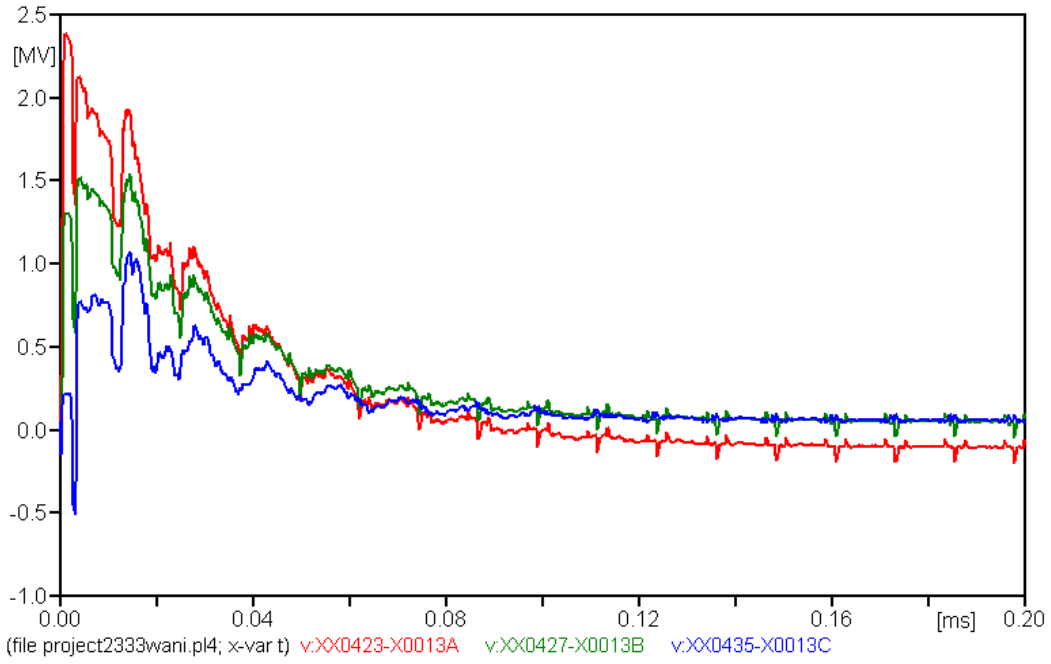
2.5
[MV]
2.0
1.5
1.0
0.5
0.0
-0.5
-1.0
0.00
0.04
0.08
0.12
0.16
[ms]
0.20
(file project2333wani.pl4; x-var t) v:XX0423-X0013A v:XX0427-X0013B v:XX0435-X0013C

(b)

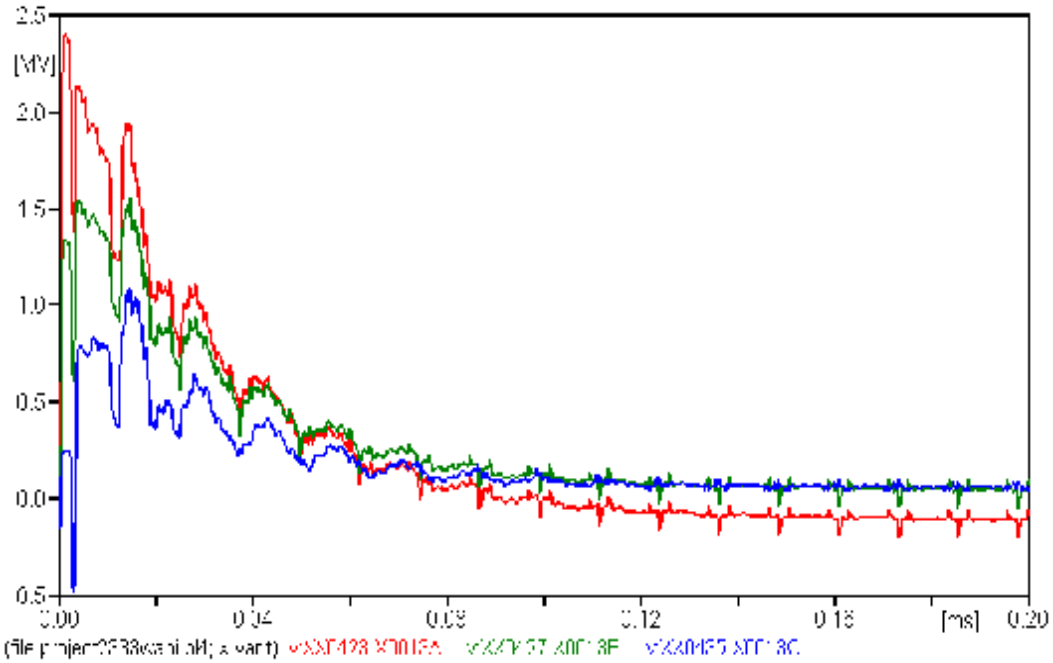
2.5
[MV]
2.0
1.5
1.0
0.5
0.0
0.5
0.00
0.04
0.08
0.12
0.16
[ms]
0.20

(c)

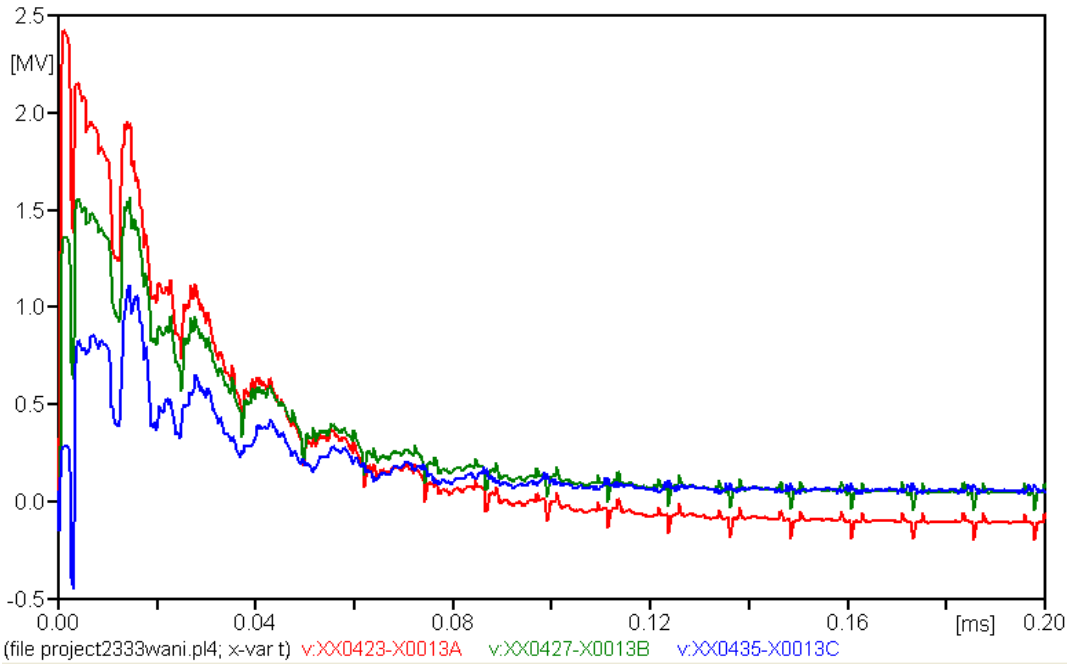
2.5
[MV]
2.0
1.5
1.0
0.5
0.0
-0.5
0.00
0.04
0.08
0.12
0.16
[ms]
0.20
(file project2333wani.pl4; x-var t) v:XX0423-X0013A v:XX0427-X0013B v:XX0435-X0013C

(d)

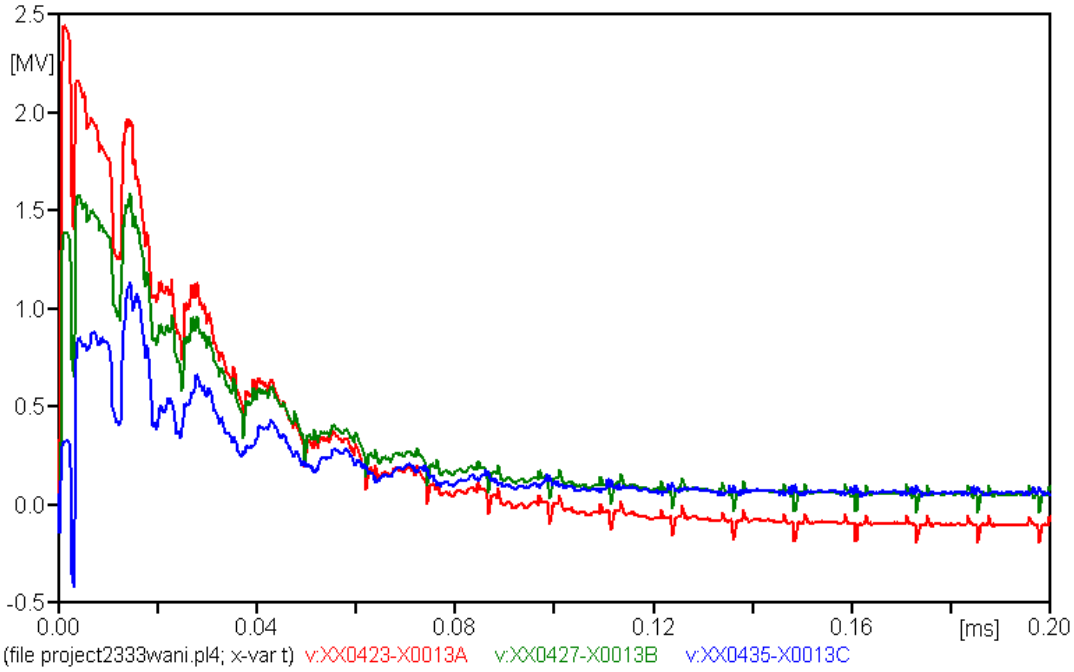
2.5
[MV]
2.0
1.5
1.0
0.5
0.0
-0.5
0.00
0.04
0.08
0.12
0.16
[ms]
0.20
(file project2333wani.pl4; x-var t) v:XX0423-X0013A v:XX0427-X0013B v:XX0435-X0013C

(e)

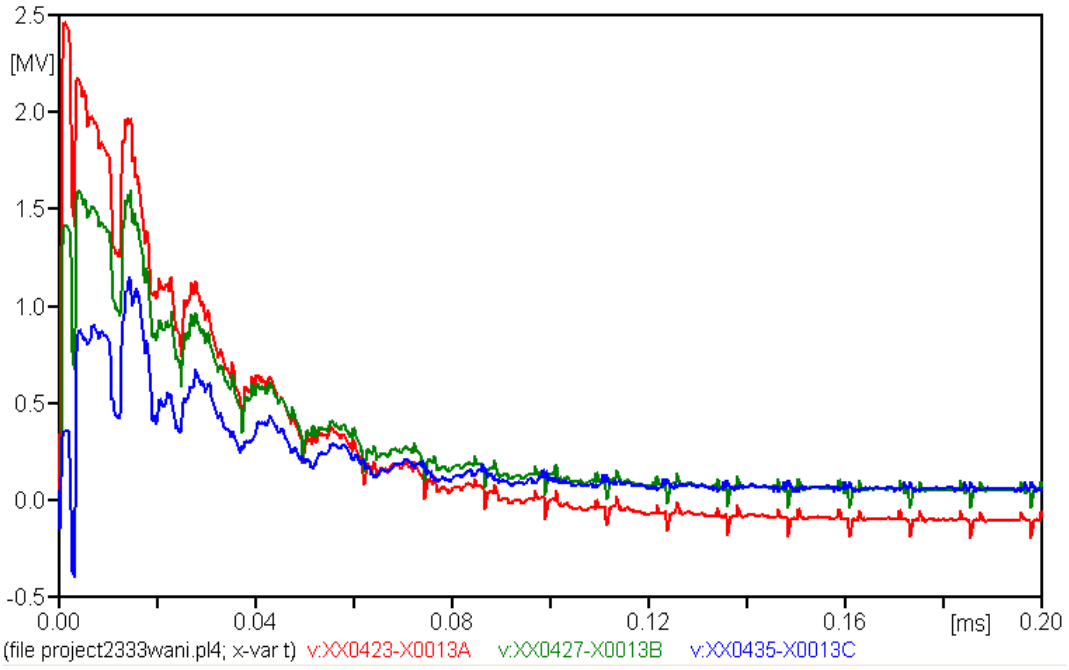
2.5
[MV]
2.0
1.5
1.0
0.5
0.0
-0.5
0.00
0.04
0.08
0.12
0.16
[ms]
0.20
(file project2333wani.pl4; x-var t) v:XX0423-X0013A v:XX0427-X0013B v:XX0435-X0013C

(f)

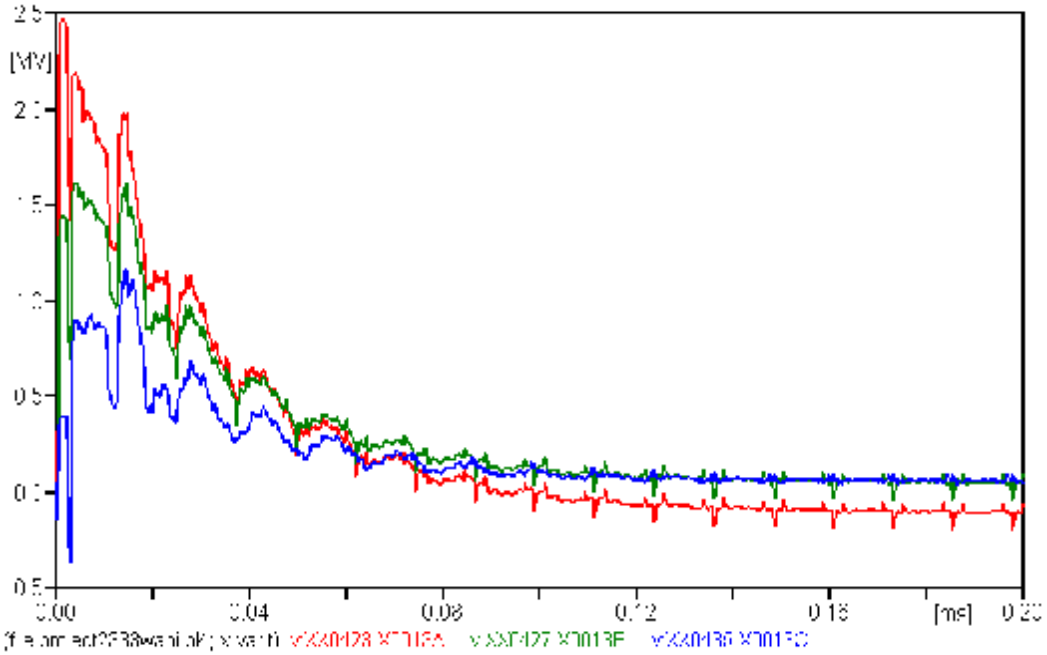
[MV]
[ms]

(g)

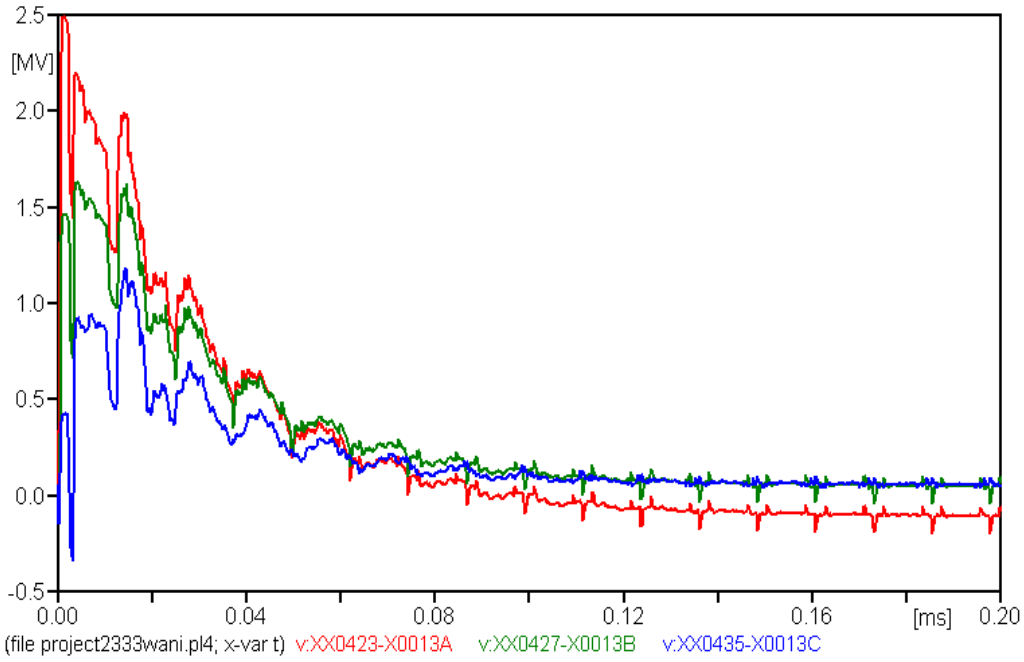
2.5
[MV]
2.0
1.5
1.0
0.5
0.0
-0.5
0.00
0.04
0.08
0.12
0.16
[ms]
0.20
(file project2333wani.pl4; x-var t) v:XX0423-X0013A v:XX0427-X0013B v:XX0435-X0013C

(h)

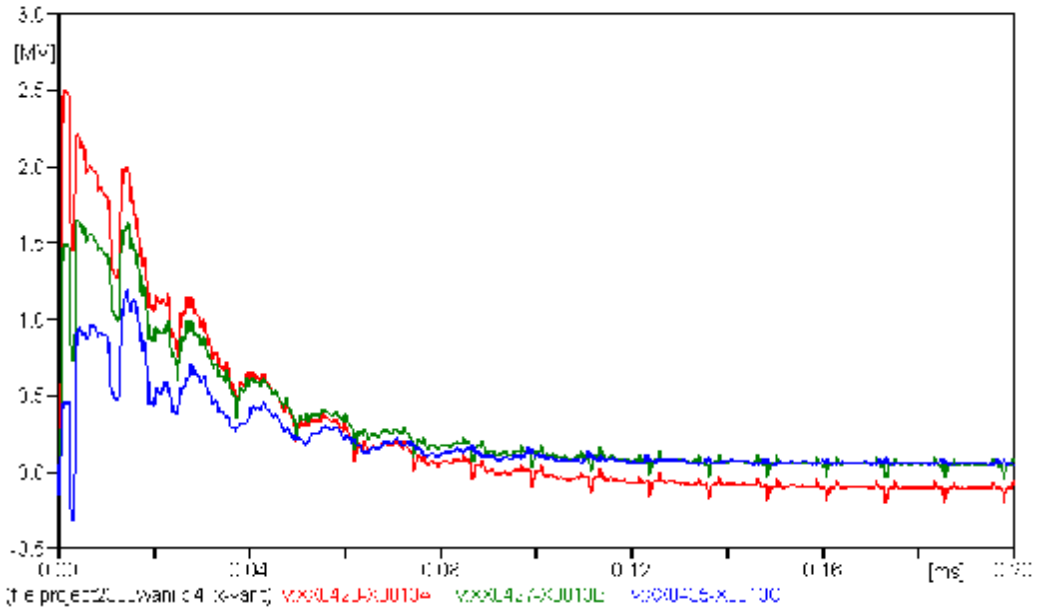

(i)

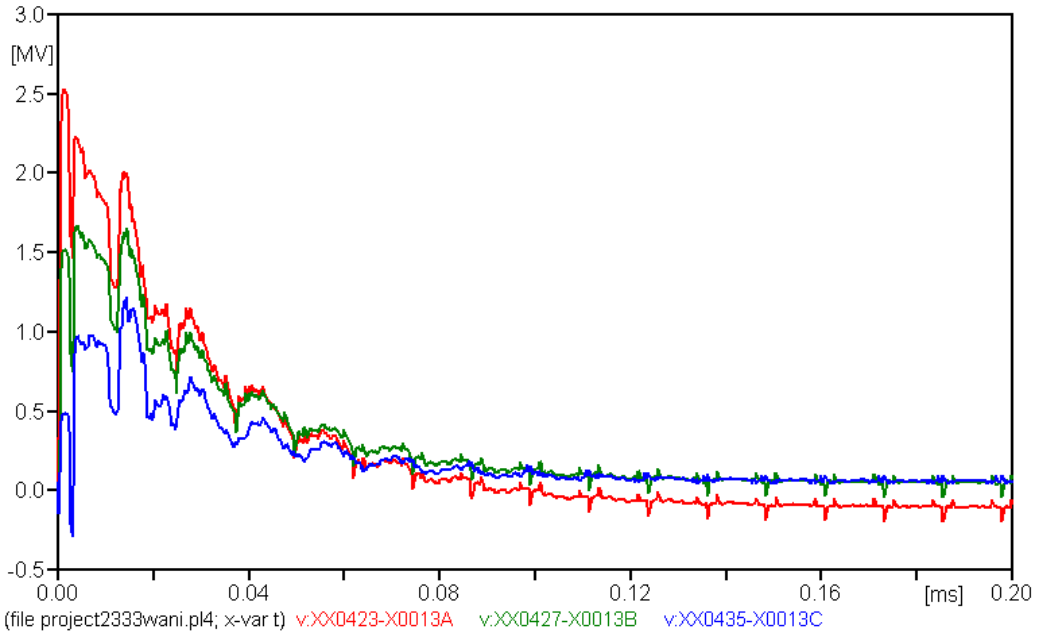

(j)

Figure 5.8: Voltage across insulator strings, for 34.5kA lightning-strike current (a) 5Ω, (b) 10Ω, (c)15Ω, (d) 20Ω, (e) 25Ω, (f) 30Ω, (g) 35Ω, (h) 40Ω, (i) 45Ω, (j) 50Ω.

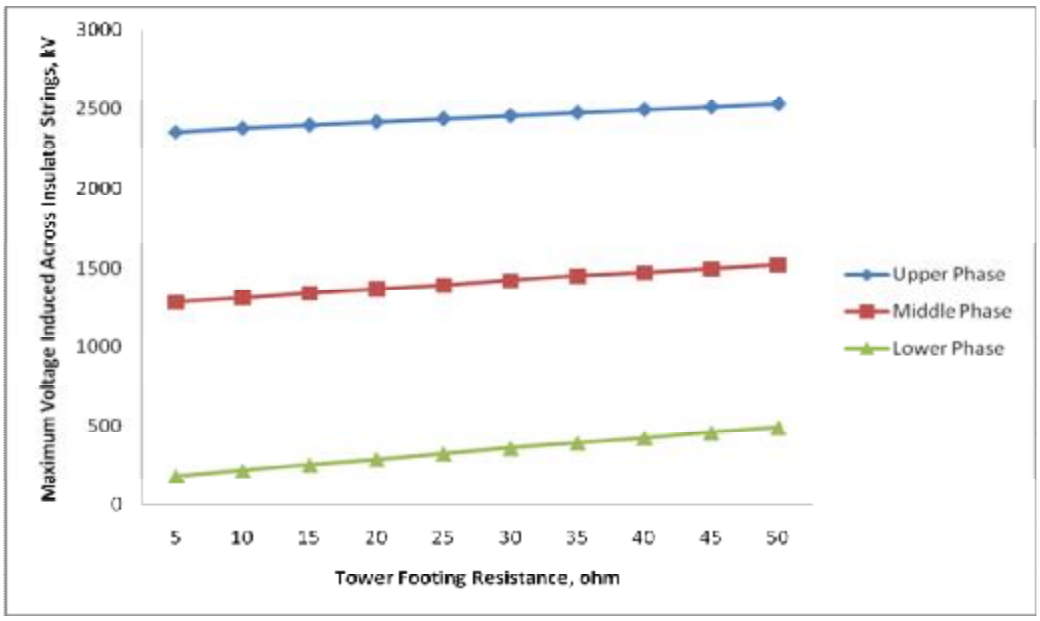

Figure 5.9: Graph of maximum voltage across insulator strings versus tower-footing resistance, for 34.5kA lightning-strike current

Table 5.3: Back flashover across insulator strings at each phase, for 34.5kA lightning-strike current

Tower Footing Resistance (Ω)	34.5kA		
	Upper	Middle	Lower
5	Y	Y	N
10	Y	Y	N
15	Y	Y	N
20	Y	Y	N
25	Y	Y	N
30	Y	Y	N
35	Y	Y	N
40	Y	Y	N
45	Y	Y	N
50	Y	Y	N

Y : Flashover
N : No Flashover

c) Lightning current = 50kA, front/tail time = 1.2/50μs

Lightning-strike current of 50kA was injected into the top tower. Figure 5.10(a) – (j) show the waveforms for voltages obtained across insulator strings at each phase when the tower-footing resistance varied from 5Ω to 50Ω. Figure 5.11 shows the graph of maximum voltage induced across insulator strings versus tower-footing resistance. Table 5.4 show phases that flashover when tower-footing resistance increases.

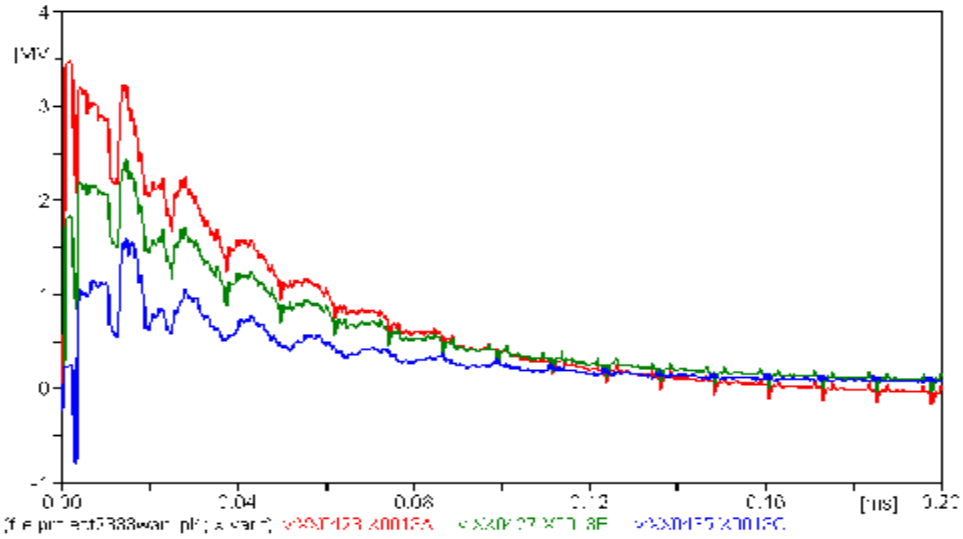

(a)

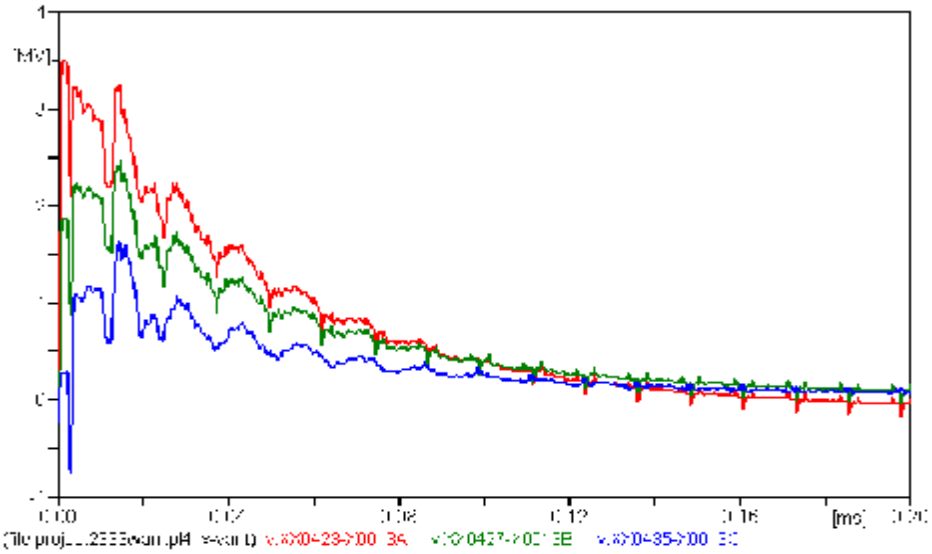

(b)

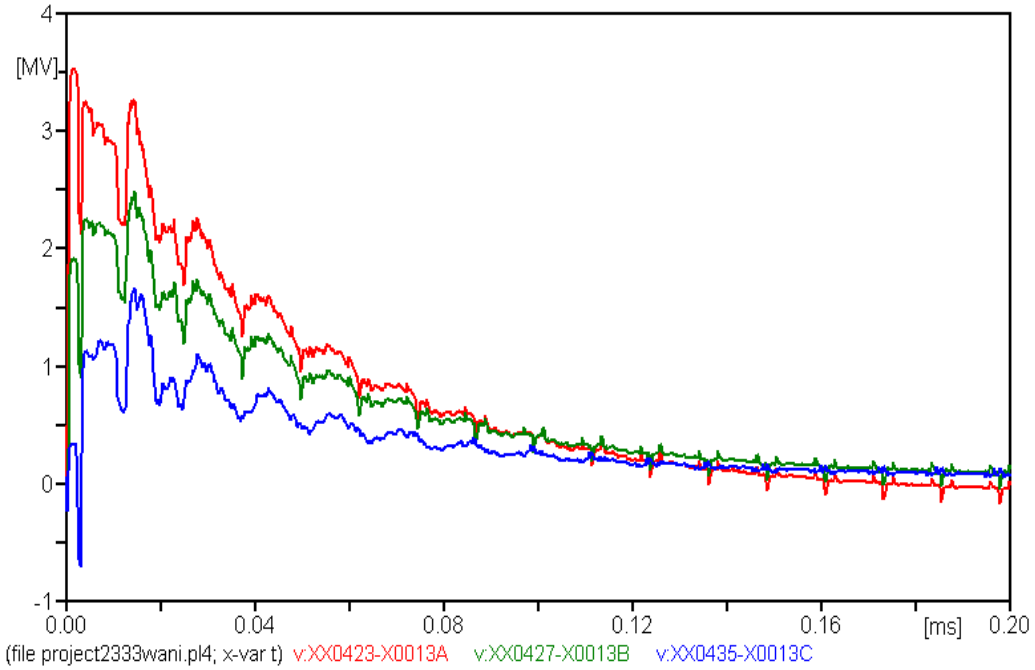
4
[MV]
3
2
1
0
-1
0.00
0.04
0.08
0.12
0.16
[ms]
0.20
(file project2333wani.pl4; x-var t) v:XX0423-X0013A v:XX0427-X0013B v:XX0435-X0013C

(c)

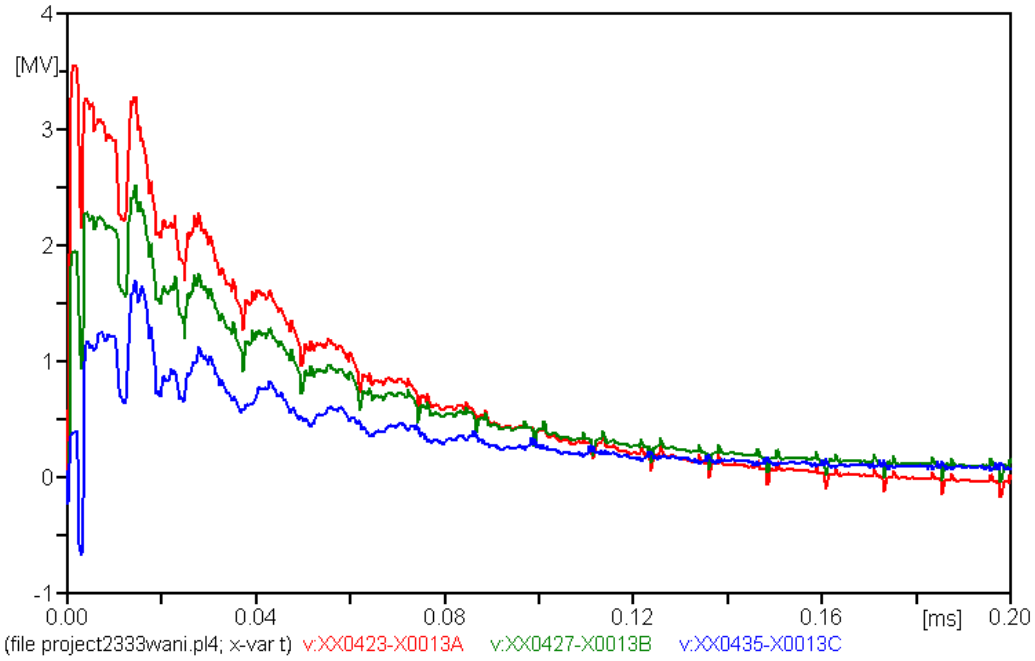
4
[MV]
3
2
1
0
-1
0.00
0.04
0.08
0.12
0.16
[ms]
0.20
(file project2333wani.pl4; x-var t) v:XX0423-X0013A v:XX0427-X0013B v:XX0435-X0013C

(d)

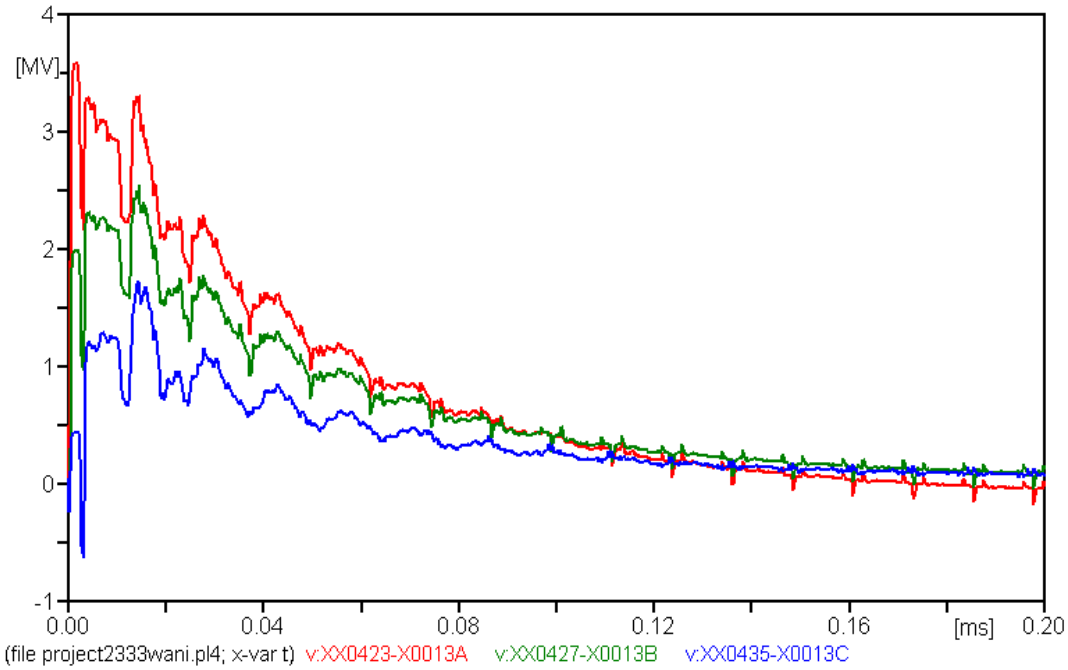
4
[MV]
3
2
1
0
-1
0.00
0.04
0.08
0.12
0.16
[ms]
0.20
(file project2333wani.pl4; x-var t) v:XX0423-X0013A v:XX0427-X0013B v:XX0435-X0013C

(e)

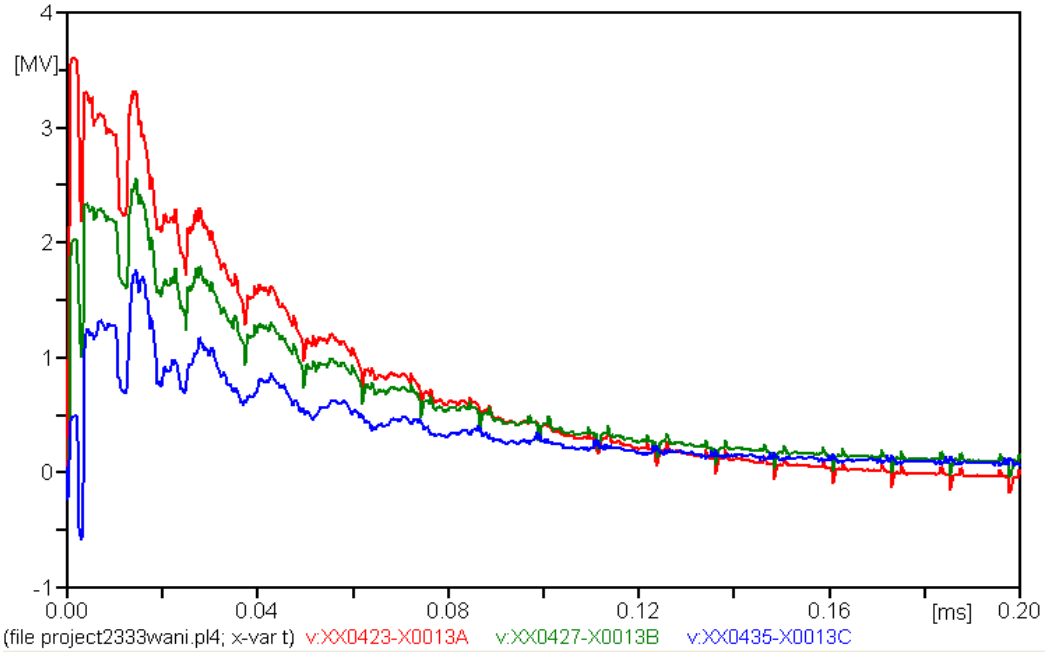
4
[MV]
3
2
1
0
-1
0.00
0.04
0.08
0.12
0.16
[ms]
0.20
(file project2333wani.pl4; x-var t) v:XX0423-X0013A v:XX0427-X0013B v:XX0435-X0013C

(f)

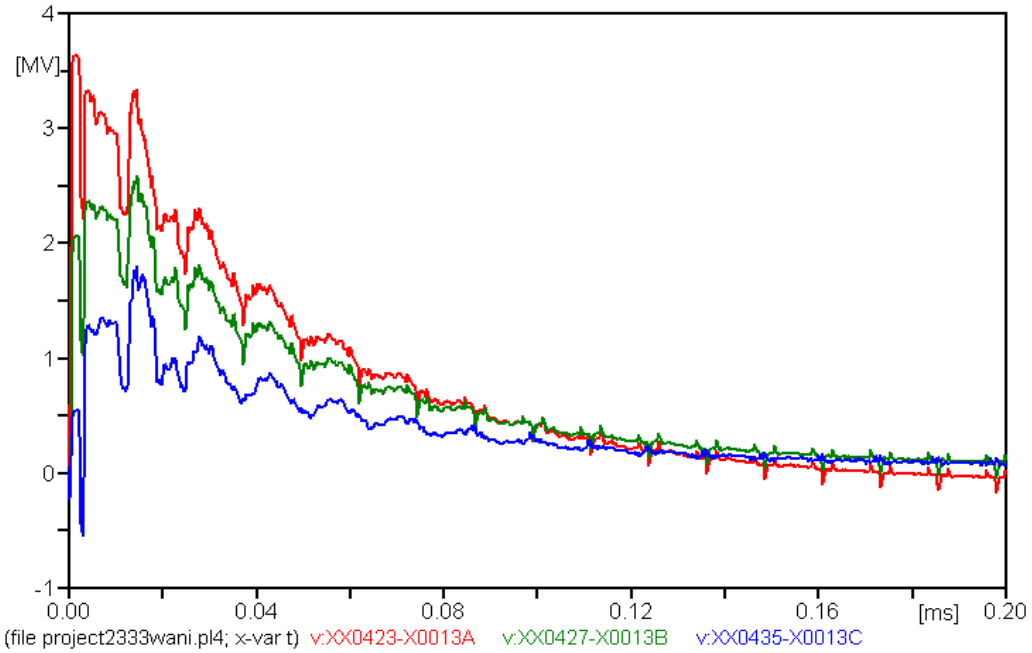
4
[MV]
3
2
1
0
-1
0.00
0.04
0.08
0.12
0.16
[ms]
0.20
(file project2333wani.pl4; x-var t) v:XX0423-X0013A v:XX0427-X0013B v:XX0435-X0013C

(g)

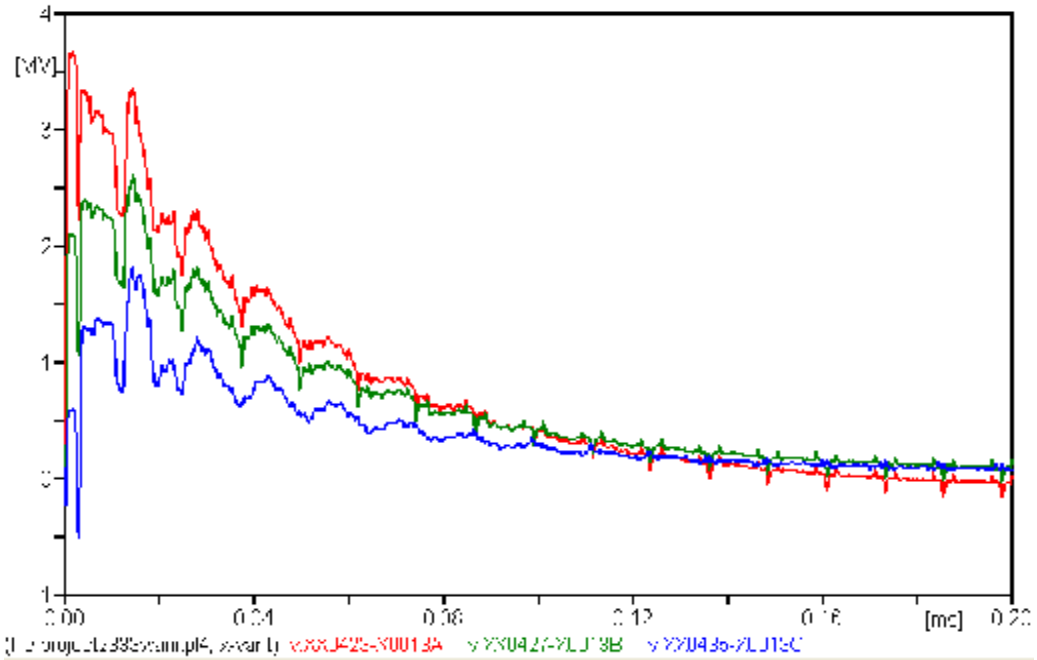
4
[MV]
1
[ms]

(h)

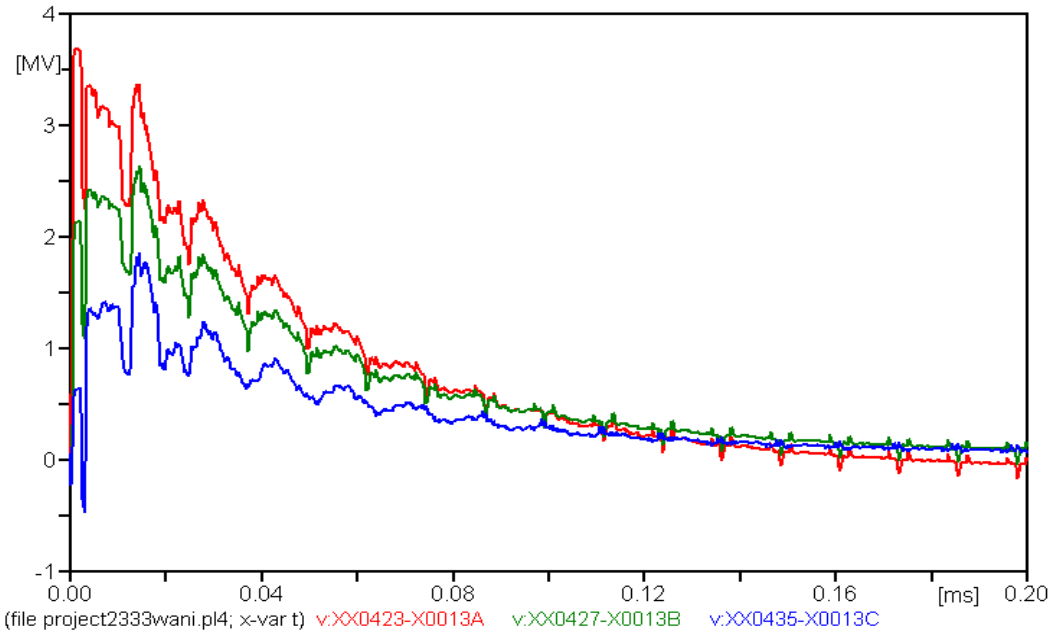

(i)

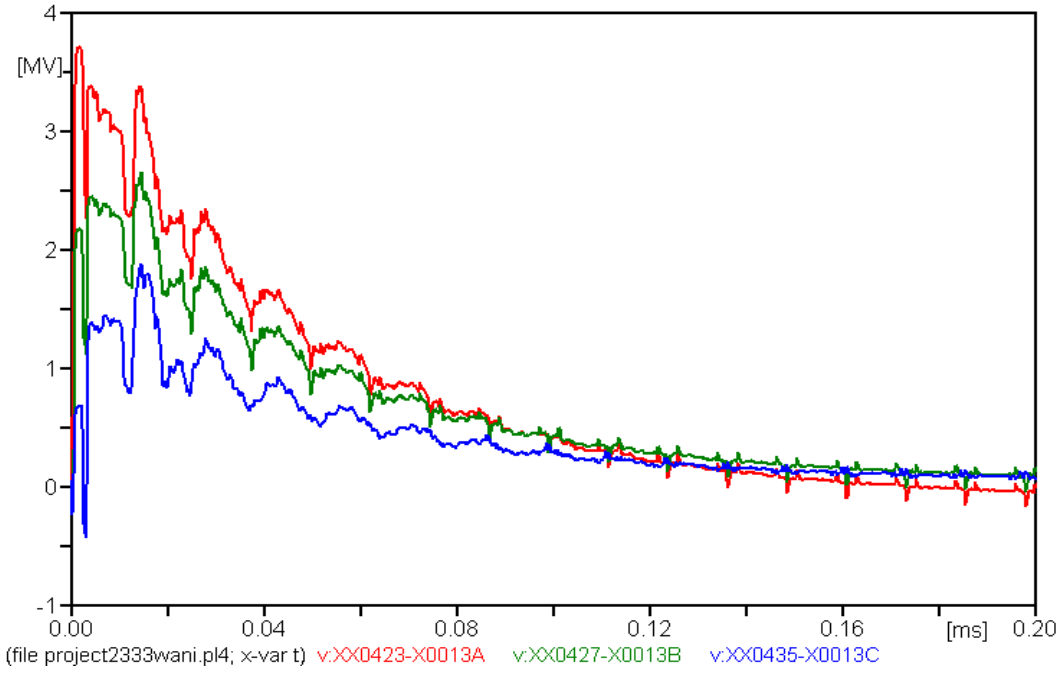

(j)

Figure 5.10: Voltage across insulator strings, for 50kA lightning-strike current (a) 5Ω, (b) 10Ω, (c)15Ω, (d) 20Ω, (e) 25Ω, (f) 30Ω, (g) 35Ω, (h) 40Ω, (i) 45Ω, (j) 50Ω.

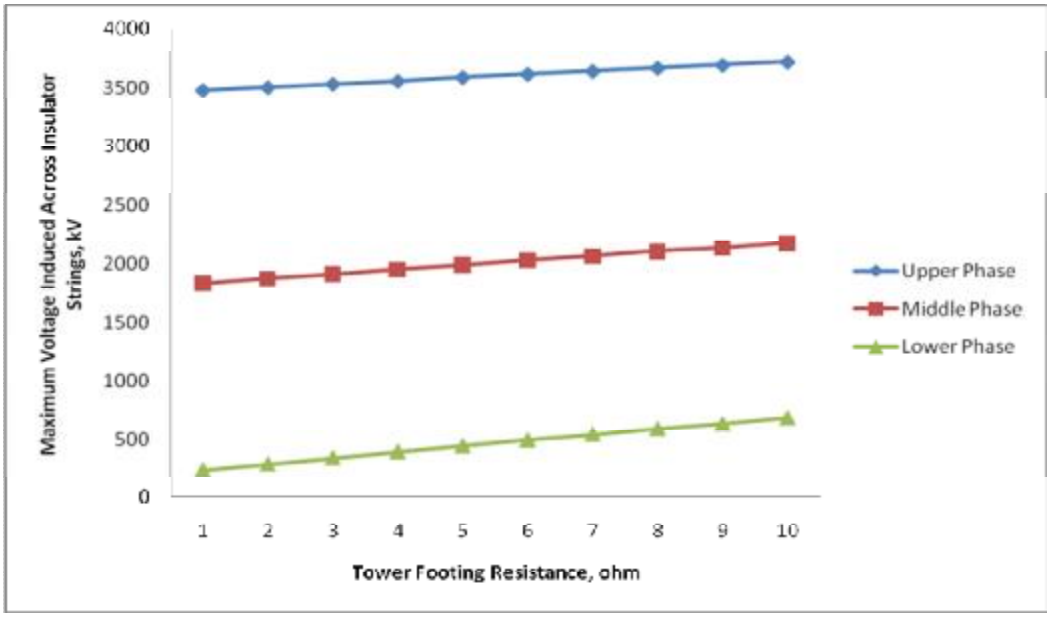

Figure 5.11: Graph of maximum voltage across insulator strings versus tower-footing resistance, for 50kA lightning-strike current

Table 5.4: Back flashover across insulator strings at each phase, for 50kA lightning-strike current

Tower Footing Resistance (Ω)	50kA		
	Upper	Middle	Lower
5	Y	Y	N
10	Y	Y	N
15	Y	Y	N
20	Y	Y	N
25	Y	Y	N
30	Y	Y	N
35	Y	Y	N
40	Y	Y	N
45	Y	Y	N
50	Y	Y	Y

Y : Flashover
N : No Flashover

d) Lightning current = 100kA, front/tail time = 2/77.5μs

Lightning-strike current of 100kA was injected into the top tower. Figure 5.12(a) – (j) show the waveforms for voltages obtained across insulator strings at each phase when the tower-footing resistance varied from 5Ω to 50Ω. Figure 5.13 shows the graph of maximum voltage induced across insulator strings versus tower-footing resistance. Table 5.5 show phases that flashover when tower-footing resistance increases.

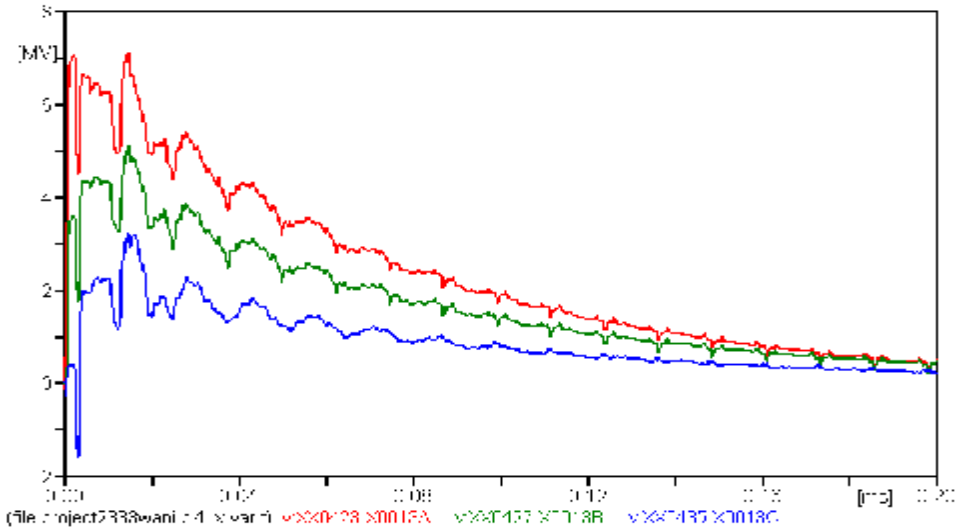

(a)

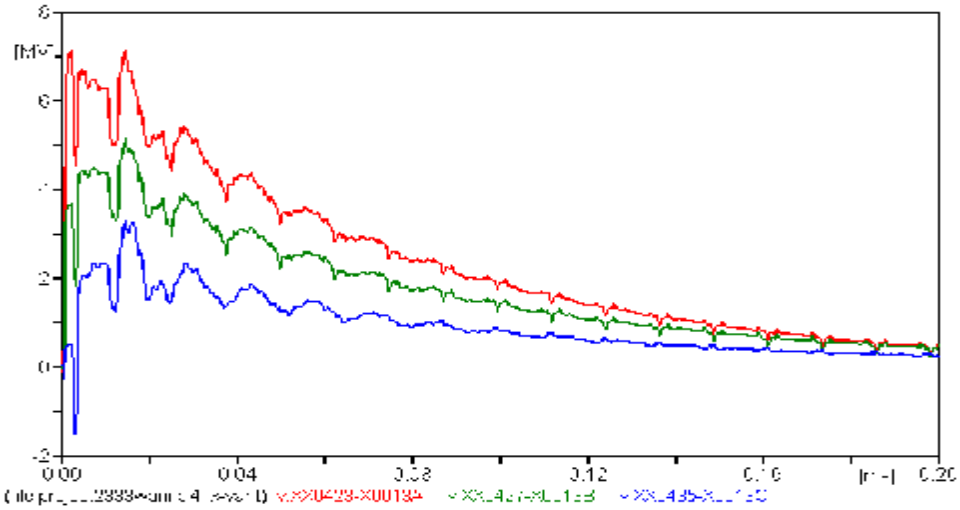

(b)

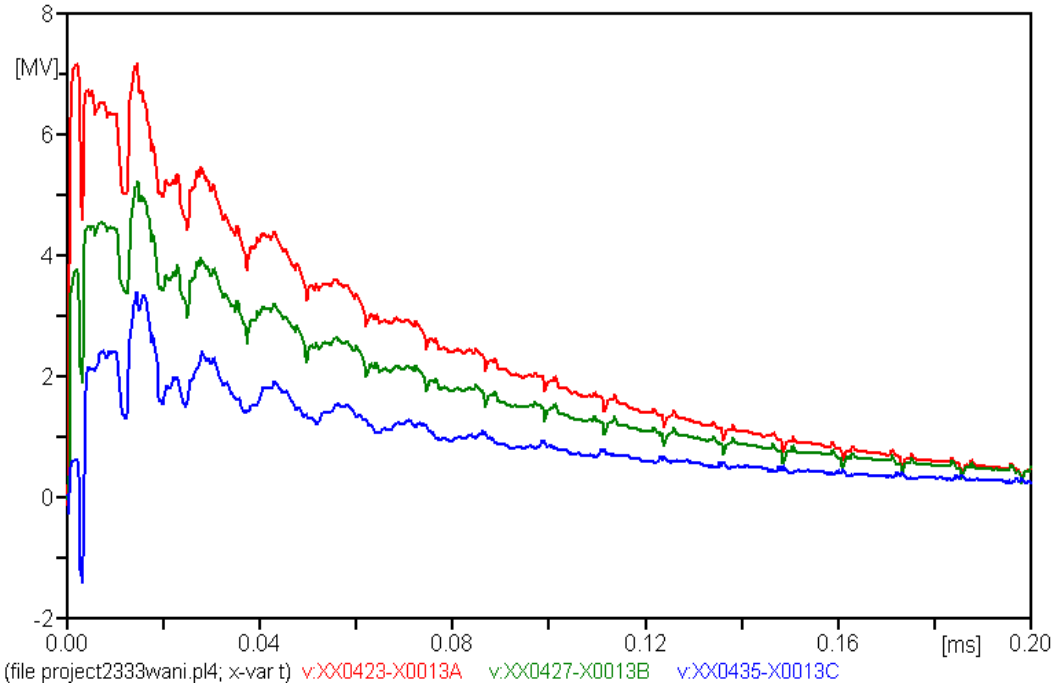
8
[MV]
6
4
2
0
-2
0.00
0.04
0.08
0.12
0.16
[ms]
0.20
(file project2333wani.pl4; x-var t) v:XX0423-X0013A v:XX0427-X0013B v:XX0435-X0013C

(c)

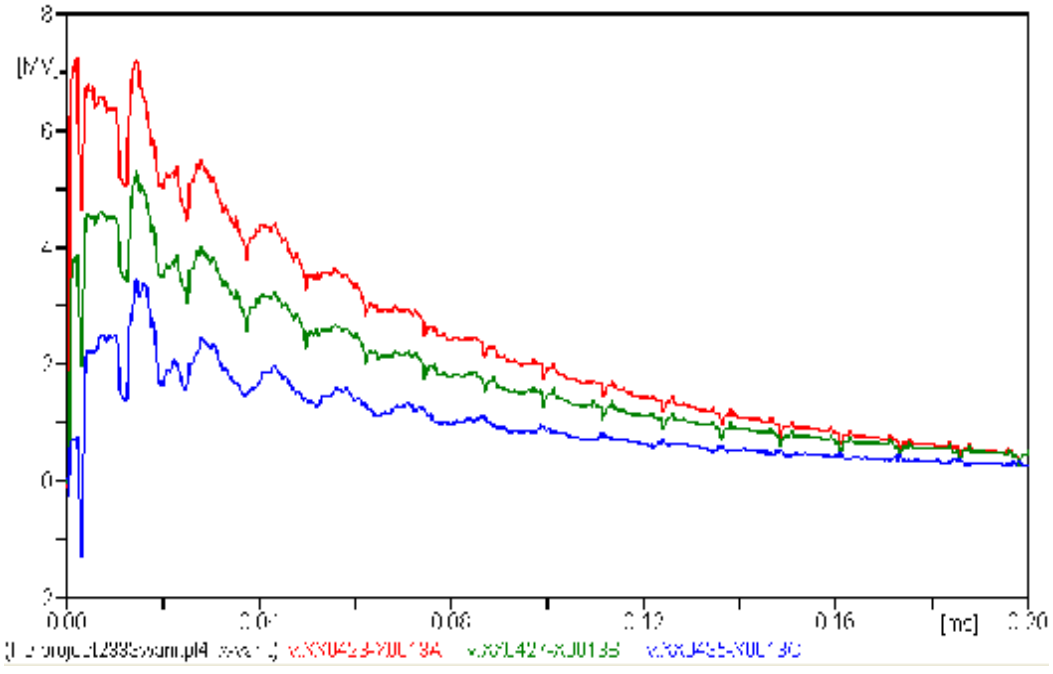
8
6
0
0.16
[ms]

(d)

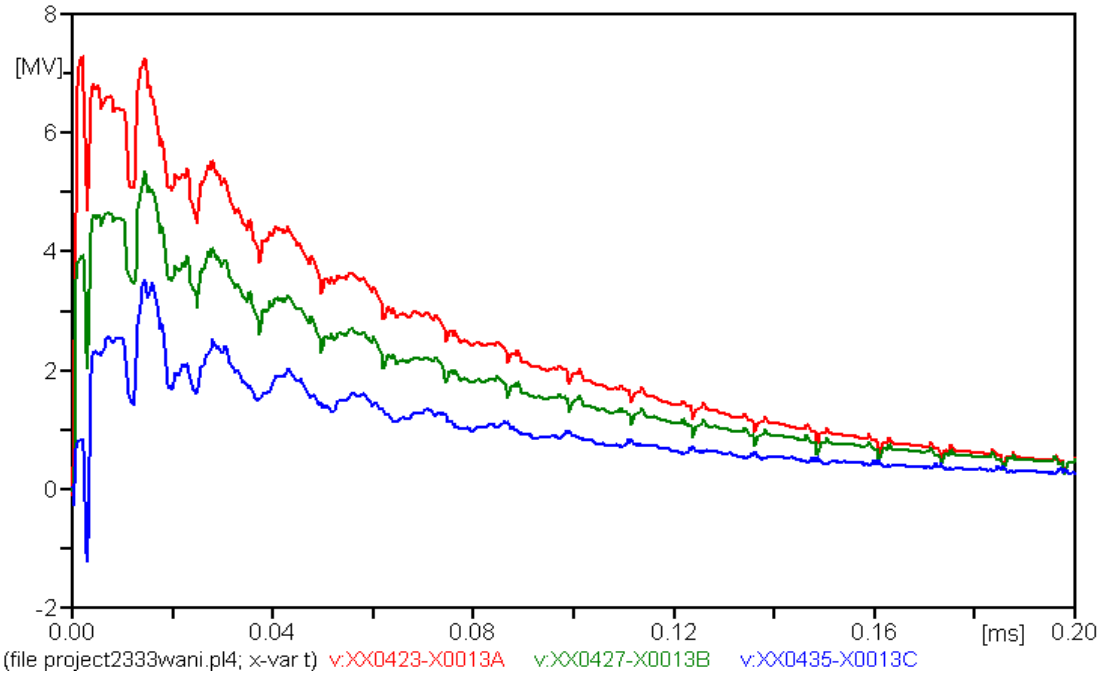
8
[MV]
6
4
2
0
-2
0.00
0.04
0.08
0.12
0.16
[ms]
0.20
(file project2333wani.pl4; x-var t) v:XX0423-X0013A v:XX0427-X0013B v:XX0435-X0013C

(e)

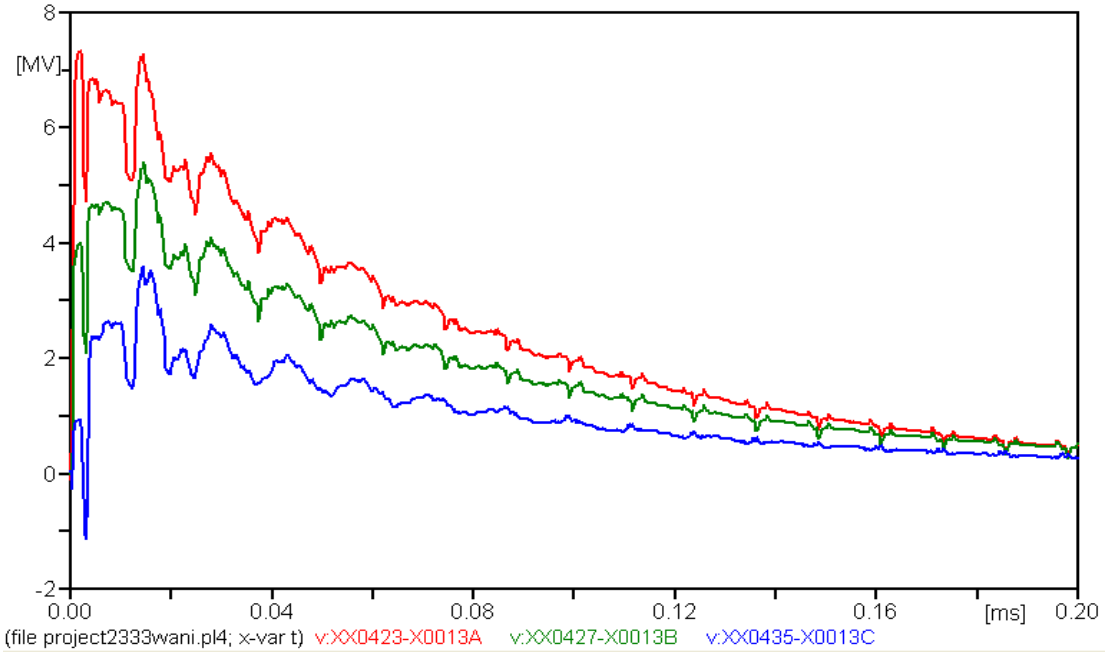
8
[MV]
6
4
2
0
-2
0.00
0.04
0.08
0.12
0.16
[ms]
0.20
(file project2333wani.pl4; x-var t) v:XX0423-X0013A v:XX0427-X0013B v:XX0435-X0013C

(f)

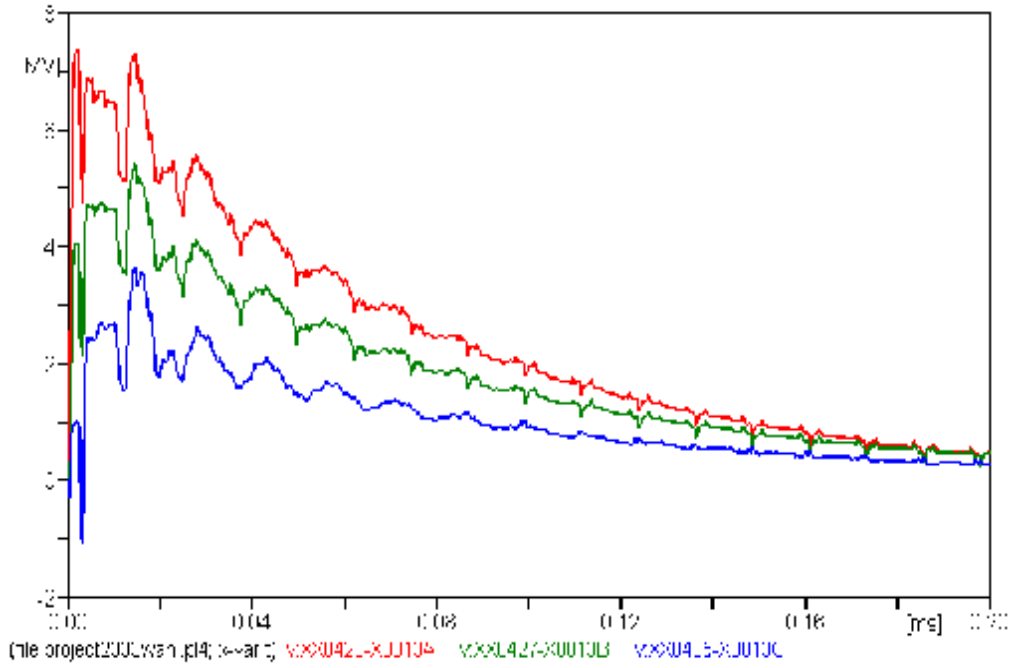

(g)

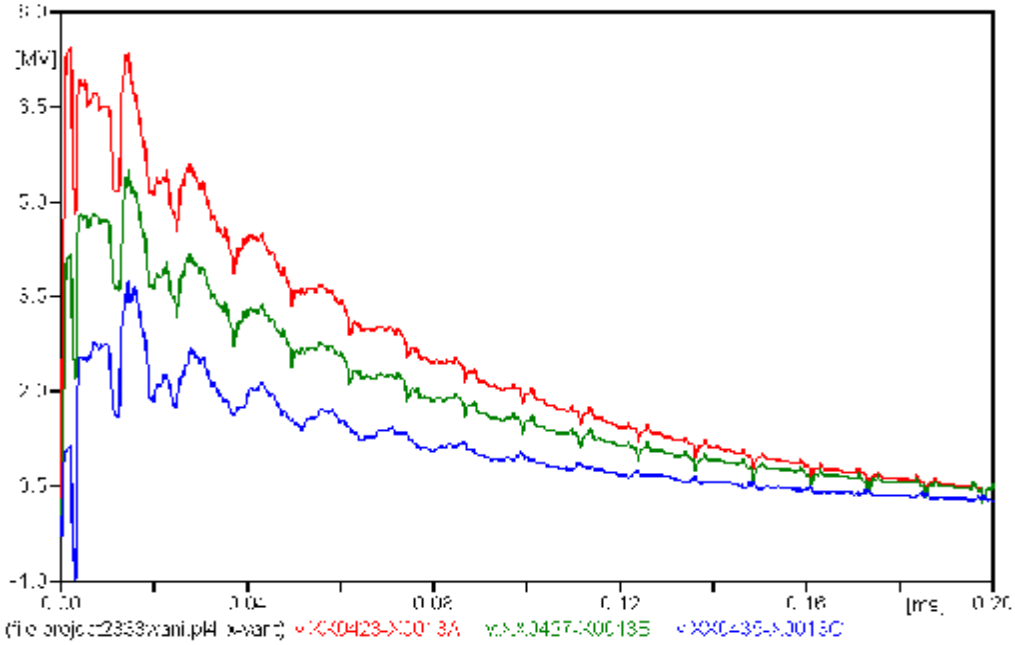

(h)

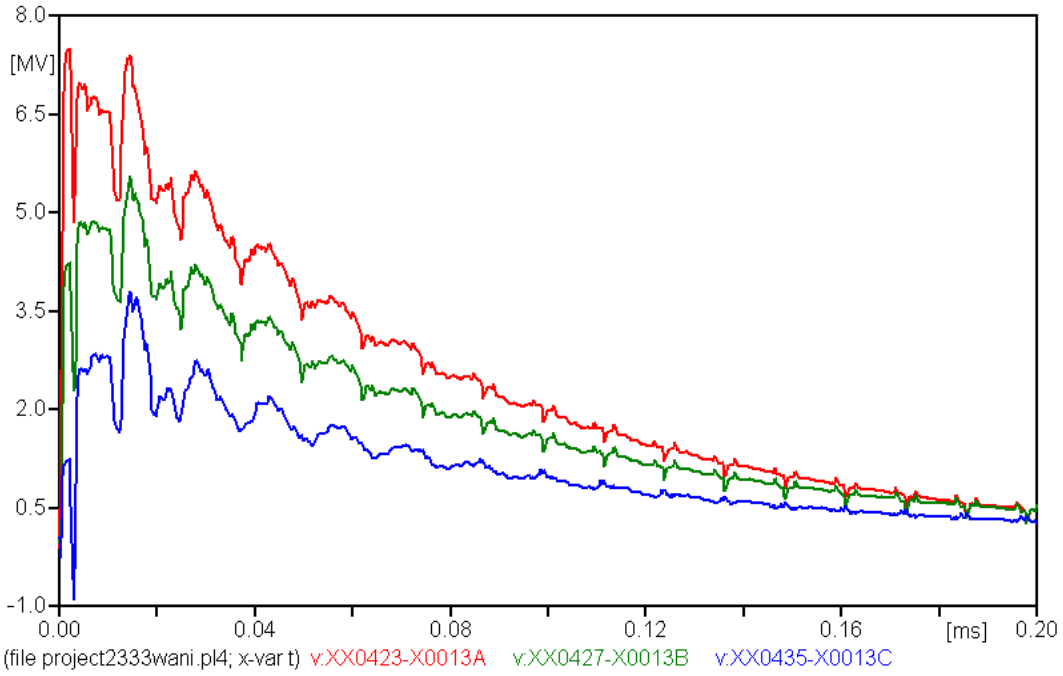

(i)

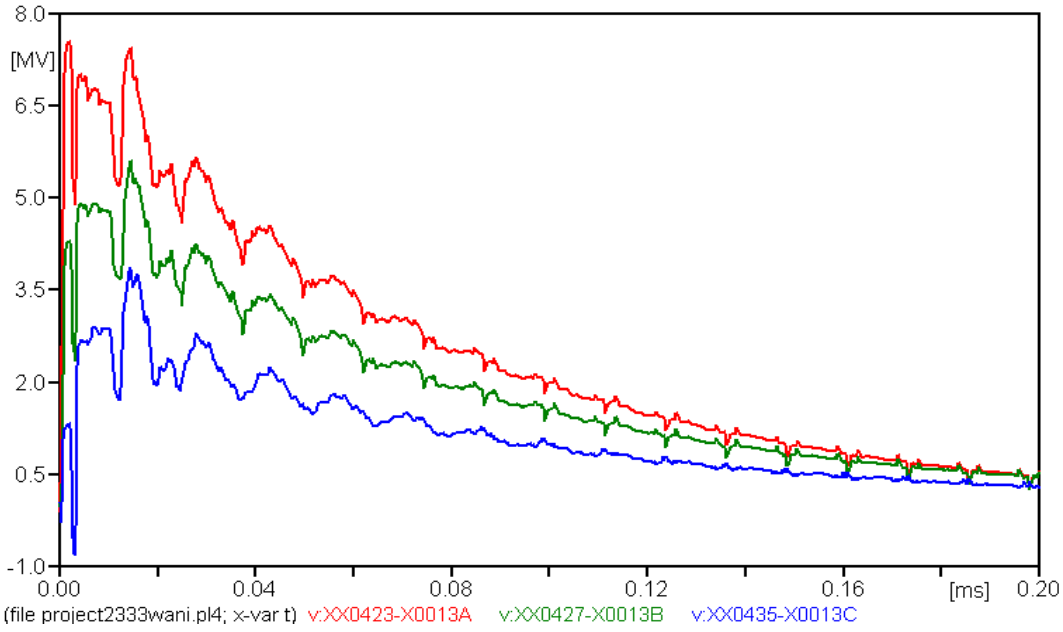

(j)

Figure 5.12: Voltage across insulator strings, for 100kA lightning-strike current (a) 5Ω, (b) 10Ω, (c)15Ω, (d) 20Ω, (e) 25Ω, (f) 30Ω, (g) 35Ω, (h) 40Ω, (i) 45Ω, (j) 50Ω.

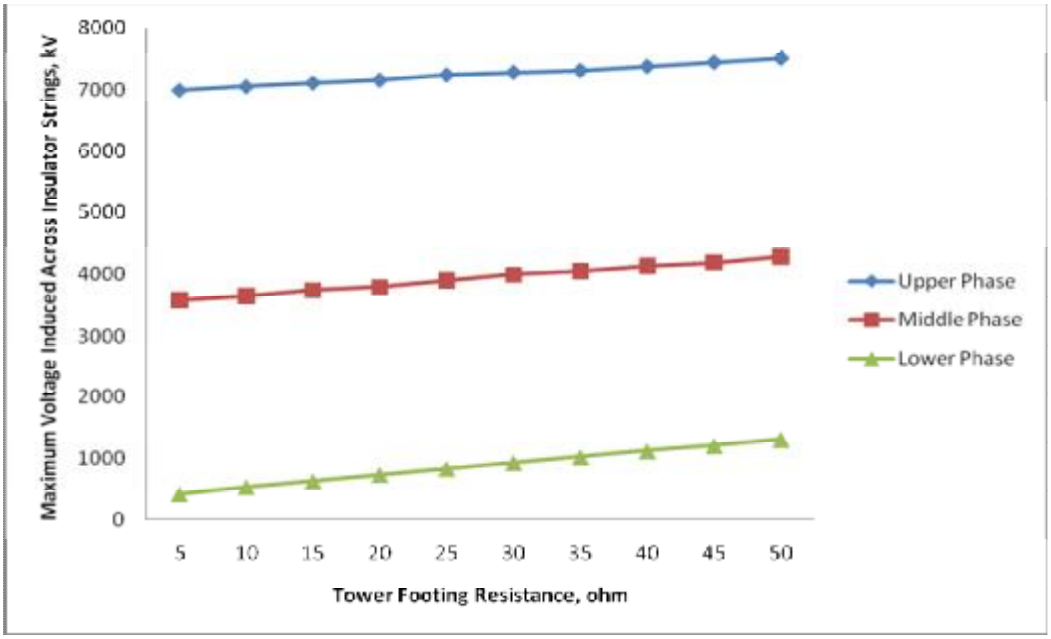

Figure 5.13: Graph of maximum voltage across insulator strings versus tower-footing resistance for 100kA lightning-strike current

Table 5.5: Back flashover across insulator strings at each phase, for 100kA lightning-strike current

Tower Footing Resistance (Ω)	100kA		
	Upper	Middle	Lower
5	Y	Y	N
10	Y	Y	N
15	Y	Y	N
20	Y	Y	Y
25	Y	Y	Y
30	Y	Y	Y
35	Y	Y	Y
40	Y	Y	Y
45	Y	Y	Y
50	Y	Y	Y

Y : Flashover
N : No Flashover

Tower-footing resistance is an important parameter considered in lightning performance of transmission lines. According to graph of maximum voltage induced across insulator strings versus tower-footing resistance (see Figures 5.7 and 5.13), increase in tower-footing resistance was observed to increase back-flashover voltage induced across insulator strings at each phase. This indicates that the higher the tower-footing resistance, the higher the possibility for damage to transmission-line equipment through induced higher back-flashover voltage across insulator strings. In this part, the maximum voltage induced across the insulator strings is recorded at 1.5μs average time.

Referring to Tables 5.2 and 5.3 for 20kA and 34.5kA lightning-strike currents, back-flashover occurs only in upper and middle phases when tower-footing resistance is varied from 5Ω to 50Ω. No back flashover occurs in lower phase here. Table 5.4 shows that when lightning-strike current is 50kA, back flashover occurs at upper and middle phases every time as tower-footing resistance increase. However, back-flashover also occurs at lower phase when tower-footing resistance is 50 Ω. On the other hand, Table 5.5 shows that back-flashover occurs at upper and middle phases every time, while for lower phase, back-flashover occurs when tower-footing resistance equals, or is greater than, 20Ω.

Tower-footing resistance is the parameter that determines peak over-voltage occurring at transmission-tower top. Voltage reflection from tower base arrives sooner at tower top than do reflections from adjacent towers past return of first reflection. The lower the tower-footing resistance, the more negative reflections produced from tower base towards tower top. Reducing peak voltage at tower top thus helps (M.Z.A. Ab Kadir et al.; European Journal of Scientific Research, 2009).

Lightning performance of a transmission line can be improved through modifications to line, such as improving tower-footing resistance. The improvement can be done by counterpoise method. Types of counterpoise are continuous and radial.

During a lightning event, a given length of counterpoise with many radial sections attached to one tower will provide a lower dynamic impedance that the same total length of continuous counterpoise (J. Sardi, M.Z.A. Ab Kadir, W.F. Wan Ahmad, H. Hizam, I. Mohamed Rawi, A. Ahmad; PECon 08, 2008).

However, this method is quite difficult and expensive, especially at hilly terrains. Line arrester installation is thus the best option in preventing insulation flashover. Transmission Line Arresters (TLAs) can be installed to limit voltages between phase conductors and tower structure, as they are properly selected and located.

Generally, there are few methods that can be used for optimizing TLA application to improve lightning performance of a transmission line in service. Double circuit outages can be eliminated by installation of line surge arresters in all conductors of all circuits, but this is uneconomical as TLAs are expensive. A better installation of TLAs is based on tower-footing resistance. The method entails selecting a high tower-footing resistance on some sections of a line. The strategy is based on the assumption that the higher the tower-footing resistance, the higher the current has to be diverted by surge arrester. Table 5.6 shows the strategy for arrester installation, while Figure 5.14 shows location of the arrester in the circuit (Siti Rugayah Bte Dugel, Master Degree Thesis, Universiti Teknologi Malaysia, 2007).

Table 5.6: Strategy for Arrester Installation

No	R_f	TLA Location
1	$R_f \leq 10$	No TLA
2	$10 \leq R_f \leq 20$	3
3	$20 \leq R_f \leq 40$	2 & 3
4	$40 \leq R_f$	1,2 & 3

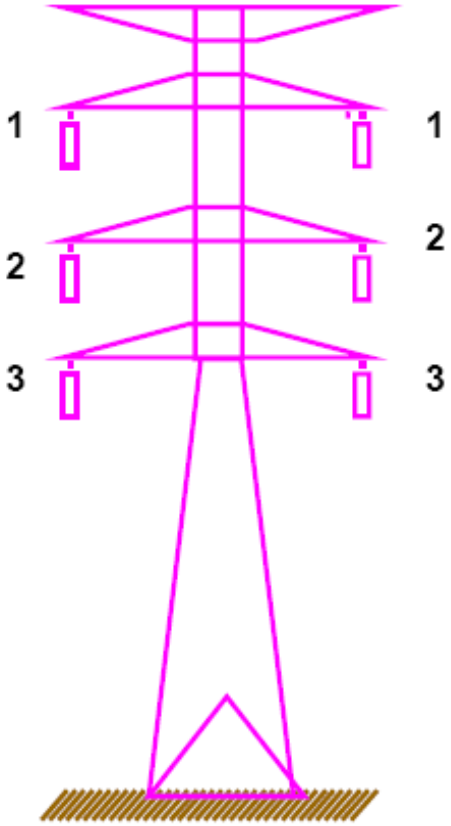

Figure 5.14: Circuit location and TLA placement for a double circuit line

5.4 Discussion

Lightning over-voltage analysis is important to reliable operation of electric power system. Observing lightning over-voltage experimentally is difficult, hence numerical simulation such as modelling the overhead transmission line by using ATP-EMTP software (as was done in this dissertation) is the best approach.

Parameters used in the modeling (transmission-line and tower models, cross-arms model, insulator-strings model, AC voltage source, tower surge impedance, tower-footing resistance, and lightning-strike current model) were based on reliable references. This was a first attempt at modeling a 132kV overhead transmission line via ATP-EMTP software; no equivalent preceding research. Simulation results showed correct modeling of the 132kV overhead transmission line.

There were, however, limitations in ATP-EMTP software use in lightning over-voltage analysis of the 132kV overhead transmission-line system modeled. In the analysis, ATP settings for time step of the simulation and end time of the simulation were 1E-9sec and 2E-4sec. Duration of the simulation was thus 2E-4sec. Use of the 300 m/μs propagation velocity for tower surge impedance and cross- arms impedance caused ATP setting for time-step of the simulation to be 1E-9 sec. If end-time of the simulation is set to 1 second, and setting for time step of the simulation maintained at 1E-9 seconds, simulation would take longer (more than one day) to finish, owing to small time-step setting. End-time of the simulation thus must be maintained at 2E-4 seconds.

This limitation caused a problem when performing point-of-wave-switching simulation for 0°-360° phase angles on the developed model. To perform point-of-wave-switching simulation, changing start-time of the lightning-strike model to the necessary value equaling 0°-360° phase angles is essential. This requires higher-value end-time simulation, which cannot be done with this software.

The problem might be solved by using other impedance model for both tower surge impedance and cross-arms impedance without using 300m/μs propagation velocity. There are, however, no other models suggested by other researchers so far for these parameters. Further research in a new model for the two parameters might solve the problem, and thus simulation of wave-switching point can be performed.

CHAPTER 6

CONCLUSIONS AND RECOMMENDATIONS

6.1 Conclusion

This dissertation developed a 132kV overhead transmission-line model via ATP-EMTP software. Steps and procedures required to design the model were studied. The model was essential to investigation of lightning over-voltage performance on overhead transmission-line system. Back-flash over-voltages obtained across insulator strings were investigated via magnitudes of lightning-strike current injected into transmission-tower top. Results obtained from simulation showed that the higher the magnitude of the lightning-strike current, the higher the back-flash over-voltage induced across the insulator strings.

Effect of tower-footing resistance on back-flash over-voltage at each phase was investigated. Tower footing resistance is a particularly important parameter in determining lightning-overvoltage performance of transmission-line system. Simulation results show that the higher the tower-footing resistance, the higher the voltage induced across the insulator strings; this can damage transmission-line equipment such as transformer. Keeping tower-footing resistance as low as possible is thus important to improving transmission-line performance. Tower footing resistance can be improved by installing either continuous, or radial, counterpoise. Transmission-line arrester (TLA), however, is the better option when a counterpoise is not possible. Installation of TLAs is the best way for eliminating double circuit outage in transmission system.

6.2 Recommendations

Simulation results on the 132kV overhead transmission-line system modeled in the dissertation work base the following suggestions for improvements and better results:

a) Find other methods of modeling tower surge impedance and cross-arms that does away with using the 300 m/μs propagation velocity as it affects setting time of simulation step time.

b) Use EMTP-RV software instead of ATP-EMTP software to simulate point-of-wave-switching simulation might produce better results. Also, lightning over-voltage analysis can use modeling methods proposed by other researchers such as the Rule method (Overvoltage Protection and Insulation Coordination of AC Power Apparatus, DL/T620-97), the Travelling Wave method (W.B. Zhang, J.L. He, Y.M. Gao, Tsinghua University Press, 2002), the Monte Carlo method (B.J. Wang, Hydraulic and Electrical Power Press, 1990), and the Fault-Tree method (Z.C. Zhang, Overvoltage Symposium, 1997).

c) Continue the work to calculate the Back Flashover Rate (BFR) of transmission line system.

d) Further extended the investigation of back-flashover voltage pattern recognition when lightning-strike current are injected into other transmission-tower top.